ABSTRACT

ANALYTICAL MODEL FOR STAGING EMERGENCY EVACUATIONS

by

Vivek V. Korikanthimath

Disaster response in areas of high population density is centered on the efficient evacuation of people and possibly goods. Developing evacuation plans suitable for different levels of urgency based on the intensity of threat is a challenging task. In case of densely populated cities (e.g., New York, Los Angeles), the level of threat is enhanced by the congestion of their transportation systems, and the decision to evacuate a region simultaneously or by dividing it into multiple stages (or zones) affects the required evacuation time and associated delays.

The evolution of the traffic conditions on the evacuation route can vary significantly based on the type of evacuation strategy employed (i.e., simultaneous or staged). In this dissertation, mathematical models are developed for estimating evacuation time and delay. Evacuation time is the time for evacuating all vehicles from a designated region, while delay includes queuing and moving delays incurred by evacuees. The base model handles a uniform demand distribution over the evacuation route and deterministic evacuees' behavior. The relationship between delay and evacuation time is investigated, and the impact of a staged versus a simultaneous evacuation is analyzed. A numerical method is adopted to determine the optimal number of staging zones. A sensitivity analysis is conducted of parameters (e.g., demand density, access flow rate, and evacuation route length) affecting evacuation time and delay.

To account for the heterogeneous demand distribution over the evacuation region and evacuees' behavioral responses to an evacuation order (e.g., fast, medium, and slow), a more realistic model is developed by enhancing the base model. Based on a numerical searching process, the enhanced model determines the optimal time windows and lengths of individual staged zones dependent on the demand distribution, behavioral response, and evolution of traffic conditions on the evacuation route. The applicability of the model is demonstrated with a numerical example. Results indicate that evacuation time and delay can be significantly reduced if a staged evacuation can be appropriately implemented.

Finally, the impact of compliance is investigated. Compliance is defined as the conformity of a staged zone to its demand loading pattern. It is found that the level of compliance and deviation from scheduled access time influence the effectiveness of staging. Further, a method to revise the optimal staging scheme to accommodate the non-compliant demand is illustrated.

The models developed in this research can serve as useful tools to provide suitable guidelines for emergency management authorities in making critical decisions during the evacuation process.

ANALYTICAL MODEL FOR STAGING EMERGENCY EVACUATIONS

by
Vivek V. Korikanthimath

A Dissertation
Submitted to the Faculty of
New Jersey Institute of Technology
in Partial Fulfillment of the Requirements for the Degree of
Doctor of Philosophy in Transportation Engineering

Interdisciplinary Program in Transportation

August 2006

APPROVAL PAGE

ANALYTICAL MODEL FOR STAGING EMERGENCY EVACUATIONS

Vivek V. Korikanthimath

Dr. Steven I-Jy Chien, Dissertation Advisor — Date
Professor of Civil and Environmental Engineering, NJIT

Dr. Athanassios K.Bladikas, Committee Member — Date
Associate Professor of Industrial and Manufacturing Engineering, NJIT

Dr. Lazar N. Spasovic, Committee Member — Date
Professor of Civil and Environmental Engineering, NJIT

Dr. Janice R. Daniel, Committee Member — Date
Associate Professor of Civil and Environmental Engineering, NJIT

Dr. Kyriacos C. Mouskos, Committee Member — Date
Research Professor, CCNY-CUNY

BIOGRAPHICAL SKETCH

Author: Vivek V. Korikanthimath

Degree: Doctor of Philosophy

Date: August 2006

Undergraduate and Graduate Education:

- Doctor of Philosophy in Transportation Engineering,
  New Jersey Institute of Technology, Newark, NJ, 2006
- Master of Science in Mechanical Engineering,
  New Jersey Institute of Technology, Newark, NJ, 2003
- Bachelor of Engineering in Mechanical Engineering,
  Karnatak University, Dharwad, India, 2000

Major: Transportation Engineering

Presentations and Publications:

Steven Chien, Lazar Spasovic, Kier Opie, Vivek Korikanthimath, Dejan Besenski, "Simulation-Based Analysis for Toll Plazas with Multiple Toll Collection Methods," The 84th TRB Annual Meeting, Washington DC, January 2005.

Steven Chien, and Vivek Korikanthimath, "Analysis and Modeling of Simultaneous and Staged Emergency Evacuations," the Journal of Transportation Engineering, ASCE, 2006 (forthcoming).

To beloved Sant.Kanwar Singh Maharaj

ACKNOWLEDGMENT

I am very thankful to my advisor Dr. Steven Chien for providing valuable insight and encouragement in my research. I would also like to thank Dr. Athanassios K. Bladikas, Dr. Lazar N. Spasovic, Dr. Janice R. Daniel, and Dr. Kyriacos C. Mouskos for serving on my dissertation committee.

I express my deepest gratitude to the National Center for Transportation and Industrial Productivity (NCTIP) for funding my research. Special thanks are given to Keir Opie and Joshua Curley for their kind support and encouragement during my research.

Finally, I'd like to thank my family for their encouragement and moral support.

TABLE OF CONTENTS

TABLE OF CONTENTS
(Continued)

Chapter **Page**

TABLE OF CONTENTS
(Continued)

TABLE OF CONTENTS
(Continued)

Chapter **Page**

LIST OF TABLES

LIST OF TABLES
(Continued)

LIST OF FIGURES

LIST OF FIGURES
(Continued)

Figure **Page**

LIST OF FIGURES
(Continued)

Figure **Page**

LIST OF FIGURES
(Continued)

Figure **Page**

LIST OF SYMBOLS

Variable	Description	Unit
Q	evacuation demand (number of vehicles to be evacuated)	vehicle
L	length of the evacuation route	mile
$\overline{Q} = Q / L$	demand density of the evacuation route	vpm
q	access flow rate per mile	vph/mile
x	length of a staged zone	mile
N	number of staged evacuation zones	-
qx	accumulated flow (demand) entering the evacuation route	vph
u_x	speed of vehicles from a zone on evacuation route	mph
c	capacity of the evacuation route	vph
k_x	density of vehicles from a zone on evacuation route	vpm
u_f	free-flow speed	mph
u_c	critical speed (speed at maximum discharge rate)	mph
k_c	critical density (density at maximum discharge rate)	vpm
k_j	jam density (maximum density at which all vehicles are stopped)	vpm
t_D	discharge time for a staged zone	hour
T_D	discharge time for N staged zones	hour
T_R	transit time for N staged zones	hour
t_S	staging time for a staged zone	hour
T_S	staging time for N staged zones	hour

T_E	total evacuation time for N staged zones	hour
t_D'	queue formation time for a staged zone	hour
n_q	number of vehicles queued from a zone at time t_D'	vehicle
d_q	queuing delay for a staged zone	veh-hour
D_Q	queuing delay for the evacuation	veh-hour
D_M	moving delay for the evacuation	veh-hour
D_T	total delay for the evacuation	veh-hour
d_S	queued shadow demand	vehicle
x_i	length of staged zone i	mile
q_L	lower acceptable flow limit	vph
q_U	upper acceptable flow limit	vph
$q_i^{(t)}$	percentage of demand accessing from zone i at t	%
$\bar{Q}_i^{(t)}$	demand to be evacuated while staging the zone i at t	vehicle
$Q_i^{(t)}$	demand loaded while staging the zone i at t	vehicle
δ_t	unit time interval	hour
Q_S	shadow evacuation demand	vehicle
$Q_E^{(t)}$	discharged volume at interval t	vehicle
$d_i^{(t)}$	number of queuing vehicles at t	vehicle
$T_i^{(t)}$	evacuation time for demand $\bar{Q}_i^{(t)}$	hour

r	zone closest to the beginning of the evacuation route from which demand accesses the evacuation route at t	-
l_r	average access distance of zone r	mile
x_r	length of zone r	mile
$u_r^{(t)}$	speed of vehicles passing from zone r over distance $x_r - l_r$	mph
$u_i^{(t)}$	speed of the evacuation route while staging zone i at t	mph
$k_i^{(t)}$	density of the evacuation route while staging zone i at t	vpm
$n_i^{(t)}$	estimated travel time of Akcelik's model	hour/mile
n_0	free-flow travel time of Akcelik's model	hour/mile
J_D	delay parameter of Akcelik's model	-
t_{c_i}	time point at which zone (i+1) is commenced	hour
t_{c_l}	time point at which the last vehicle exits the evacuation route	hour
t_s	duration of shadow evacuation time	hour
$f(x)$	demand density function	vpm
$d_{M_i}^{(t)}$	moving delay experienced by the discharged volume at t	veh-hour
P	average compliance level of an evacuation region	%
P_i	level of compliance for zone i	%
$q_{C_i}^{(t)}$	percentage of scheduled (compliance) demand accessing from zone i at interval t	%
$q_{N_i}^{(t)}$	percentage of non-compliance demand accessing from zone i at interval t	%
Q_i	evacuation demand of zone i	vehicle

T_{sim}	evacuation time of simultaneous evacuation for 90% of Q	hour
T_n	evacuation time of a staged evacuation for 90% of Q	hour
T_{opt}	evacuation time of the optimal staged evacuation for 90% of Q	hour
ΔT	reduction in evacuation time due to a staged plan	hour
ΔT_{opt}	reduction in evacuation time due to the optimal staged plan	hour
$Q_{c_i}^{(t)}$	scheduled demand of zones 1 through i accessing while staging zone i at t	vehicle
$Q_{n_i}^{(t)}$	non-compliance demand of zones 1 through N accessing while staging zone i at t	vehicle
$Q_{T_i}^{(t)}$	total demand (scheduled and non-compliance) accessing the evacuation route while staging zone i at t	vehicle
α	slope factor of logit- based function	-
β	half loading time of logit- based function	-
$P(t)$	cumulative percentage demand loaded at t	-
η	effectiveness of a staged evacuation plan considering compliance levels	%
$t_{D_i}^{(t)}$	discharge time of vehicles traveling from zone r while staging zone i at t	hour
$t_{R_i}^{(t)}$	travel time of vehicles from zone r while staging zone i at t	hour

CHAPTER 1

INTRODUCTION

1.1 Background

Emergency evacuation can be defined as the exodus of people and goods from a place or an area under threat. Emergency evacuation is carried out in response to disasters including but not limited to earthquakes, hurricanes, nuclear plant catastrophes, chemical plant leaks, and terrorist attacks. Due to the unexpected occurrence of the above-mentioned events, it is challenging to counteract them and execute a suitable plan to mitigate their effects. Disaster response in populous areas is centered on evacuating people and/or goods in a fast and safe manner. To accomplish this task, the development of a sound approach for planning emergency evacuations is necessary.

Evacuation planning is a critical constituent of emergency planning and is highly location and event dependent. For instance, in case of densely populated cities (e.g., New York, Los Angeles), the level of threat is enhanced by the congestion of their transportation systems. In general, evacuation can be classified into simultaneous evacuation and staged evacuation. A simultaneous evacuation is one in which all the residents are evacuated concurrently, whereas in staged evacuation, people are evacuated by locations or zones in a particular time frame and sequence. Strategies employed in evacuation vary over circumstantial and environmental conditions. A strategy suitable for hurricane evacuation would differ from that of an evacuation corresponding to a nuclear plant disaster. Further, the decision to evacuate a region simultaneously or in multiple stages affects the required evacuation time and associated delays.

Employing either simultaneous or staged evacuation calls for good professional judgment due to the urgency of the situation. In this regard, existing evacuation plans have exposed strategic and procedural limitations as they are based on conventional standards and limited prior evacuation experience (Smith, 2000). The evolution of the traffic conditions on the evacuation routes can vary significantly based on the type of evacuation strategy employed (i.e., simultaneous or staged). The fundamental speed-density relations can differ depending on the chosen method and affect evacuation time and delay for a region. Previous simulation models used in modeling evacuation were location specific and some of them failed to consider behavioral aspects of evacuees (i.e., compliance to evacuation orders, network loading rates). The absence of behavioral analysis in evacuation modeling results in inaccurate estimation of the total evacuation time and delays. Therefore, an efficient model that can assist in decision making to implement staged evacuation would prove invaluable.

This research aims at developing analytical models that optimize evacuation staging by minimizing evacuation time and the associated delay. While the base model discussed in Chapter 3 handles deterministic evacuees' behavior and a uniform demand distribution along the evacuation route, the enhanced model discussed in Chapter 4 will incorporate behavioral aspects related to loading rates, and non-uniform demand distribution and provide a rational approach to evacuation modeling. In addition, the practicability of staged evacuation due to the impact of compliance will be investigated. The results of the research can provide appropriate guidelines for emergency management authorities in making critical decisions during the evacuation process.

1.2 Problem Statement

Previous studies on emergency evacuation have been inclined to maximize the vehicle throughput and/or minimize evacuation time; however the discussion of the associated delay was limited. Delay consideration in evacuation modeling is particularly important because high delays infuse uncertainty and anxiety amongst evacuees resulting in incidents, and jeopardize safety. This reduces the overall efficiency of the evacuation. Staging of evacuation reduces congestion and helps in minimizing evacuation time (Chen and Zhan, 2004). While reviewing literature on emergency evacuation, it was found that information on impact analysis of simultaneous and staged evacuation is still limited. Further, some evacuation models were developed without considering the behavioral aspects of evacuees, which resulted in misrepresentation of the models' performance. Therefore, it is desirable to develop a sound model to optimize evacuation staging by minimizing evacuation time and delay. The new model should also be capable of dealing with critical parameters (e.g., demand distribution along the evacuation route, and loading patterns) and realistically model evacuation behavior. While staged evacuation is known to reduce evacuation time as compared to simultaneous evacuation, the practicability of staged evacuation has not yet been investigated. For instance, non-compliance behavior of evacuees to evacuation order can further increase the complexity for estimating the demand accessing the evacuation route over time and the evacuation time and delays may be underestimated. Thus, an investigation of the effectiveness of staged evacuation under varying levels of compliance is imperative.

1.3 Objectives

The primary objective of this research is to develop analytical models to minimize evacuation time and the associated delays. This research presents the development of a base model that handles uniform demand distribution over the evacuation route and deterministic evacuees' behavior, and an enhanced model that incorporates stochastic evacuees' behavior and demand heterogeneity. The objectives are outlined as follows:

1. Develop a base model to optimize evacuation staging by minimizing both evacuation time and the associated delays.

2. Enhance the base model to incorporate stochastic behavior of evacuees and heterogeneous demand distribution.

3. Investigate the practicability of staged evacuation by considering the impact of compliance.

1.4 Scope of Work

The base model handles deterministic behavior of evacuees and homogeneous demand distribution over the evacuation route. Sensitivity analysis of critical parameters (e.g., evacuation route length, demand density, access flow rate) affecting evacuation time and delay is conducted. This analysis is helpful in determining the most suitable conditions under which, staged evacuation can be employed.

Behavioral response of evacuees to evacuation orders and demand distribution over the evacuation route affect the evacuation time and delay. Therefore, the base model is enhanced to incorporate behavioral aspects including network loading profiles (fast, medium, and slow), and variation in demand distribution. A model that generates the

optimal staging scheme is developed. Sensitivity analysis of demand and capacity on evacuation time and delay is also conducted.

Since the level of compliance of staged zones affects the effectiveness of staging, the practicability of staged evacuation under various levels of compliance is analyzed. Further, a method to revise the optimal staging scheme to accommodate the non-compliance demand is illustrated.

1.5 Dissertation Organization

This dissertation is organized into six chapters. Chapter 1 introduces the research problem to be tackled and the research objectives to be achieved. Chapter 2 discusses the results of literature review on various models and techniques employed in past evacuation studies to maximize vehicular throughput and/or reduce evacuation time. It also discusses staging of evacuation, use of contraflow (reverse lane operations), speed-flow-density models, and application of behavioral modeling in evacuation. Chapter 3 describes the methodology and the development of the base model to optimize evacuation staging for deterministic evacuee behavior and homogeneous demand distribution. Chapter 4 illustrates the enhancement of the analytical model to incorporate stochastic behavior of evacuees and heterogeneous demand distribution. Chapter 5 investigates the practicability of staged evacuation by considering the impact of compliance, and finally, Chapter 6 presents the conclusions of this research with recommendations for future work.

CHAPTER 2

LITERATURE REVIEW

The purpose of this literature review is to summarize previous and state-of-the-art evacuation related practices, and to seek ways to utilize pertinent fundamental concepts to develop a sound/modeling approach for evacuation. This chapter is organized into six sections: Section 2.1 reviews methodologies related to minimization of evacuation time and delays; Section 2.2 discusses the techniques used to maximize roadway capacity during evacuation; Section 2.3 explains the concept of Evacuation Staging and discusses its importance and necessity; Section 2.4 reviews the application of various existing traffic models (e.g., microscopic, macroscopic) in modeling evacuation; Section 2.5 compares the various speed-density models to select suitable models for determining the discharge rate of the evacuation route under various demand to capacity ratios; Section 2.5 elucidates the significance of evacuees' behavioral analysis and investigates existing approaches in modeling behavior; and finally, Section 2.6 summarizes the review of literature and establishes the rationale for the model proposed in this research.

2.1 Estimation of Evacuation Time and Delay

Evacuation decision-making is a persistent problem for emergency management agencies due to the involvement of critical parameters such as intensity of threat, evacuees' behavior, demand, etc (Whitehead, 2000). The ability of emergency managers to accurately and efficiently issue evacuation orders has become a major source of concern among analysts, households, and the emergency management community. To this end,

implementing inappropriate evacuation plans results in increase in evacuation time and delays causing uncertainty and anxiety amongst evacuees.

Research in modeling emergency evacuation began to grow in the 1970's in the area of hurricane evacuation (Urbanik, 1978; U.S. Army Corps of Engineers, 1979). The Three Mile Island nuclear accident in 1979 shifted the attention to modeling of evacuation of nuclear sites. Some of the earlier studies provided evacuation time estimates for nuclear plant evacuations (HMM Associates, 1980; Urbanik and Desrosler, 1981). The occurrence of Hurricane Andrew in 1992 proved very expensive in terms of damage, and Hurricane Floyd in 1999 led to one of the greatest evacuations in the U.S. history. These events moved the attention back to hurricane evacuation. Recent studies have focused on evacuations relating to suburban fire and terrorist attacks, where models were developed to minimize the evacuation time (Cova and Church, 1997; Cova and Johnson 2002; Hamza-Lup et al., 2005).

Sinuany-Stern and Stern (1993) developed a behavioral-based microscopic simulation model with SLAM II (Simulation Language for Alternative Modeling) to conduct sensitivity analysis of the evacuation time for a radiological emergency situation. Results of the study revealed that the major traffic parameters that influenced the evacuation time were interaction with pedestrians, intersection traversing time, and car ownership. The route choice mechanisms affecting evacuation time were probability of evacuees to choose the shortest distant path and myopic behavior of evacuees that overlooked roadway congestion. They also found that the estimated evacuation time is closer to real world situations when interaction with pedestrians and a uniform distribution of intersection traversing time are assumed.

Hobeika and Kim (1998) conducted a study that compared the traffic assignment results (evacuation time estimates and number of congested links) of Dial's algorithm and a User Equilibrium (UE) algorithm. Overall, it was found that the UE algorithm was more efficient and closer to real world behavior than Dial's algorithm. While Dial's assignment considered the effects of trip volume on travel time and the trip-maker's stochastic choice function for route selection, the probability of choosing one route was treated independent of the probability of selecting another alternative route, regardless of the overlap of the link volumes between the other routes, thus ignoring traffic-congestion. On the other hand, the UE algorithm was based on the concept that for each O-D pair, the travel times on all used paths were equal and was less than the travel times that would be experienced by vehicles on any unused paths.

Urbanik (2000) investigated the effectiveness of conducting Evacuation Time Estimate (ETE) analyses for nuclear power plants. The study affirmed that five factors govern the traffic flow during evacuation, namely the number and distribution of evacuating vehicles, the loading rate at which the evacuating vehicles enter the roadway system, the capacity of the roadway system, any unforeseen degradation to roadway capacity caused by uncontrollable events such as flooding or traffic accidents, and any planned enhancements to evacuation performance caused by special traffic management actions that decrease demand (e.g., evacuation routing) or increasing capacity (e.g., lane reversals) .

Malone et al. (2001) developed a steady state car following evacuation model for traffic flow based on empirically estimated driving parameters (car length, reaction time and the deceleration parameter). The total evacuation time was formulated as a function

of number of vehicles to be evacuated, the discharge rate, and length and velocity of the evacuation route. Further, in order to account for randomness or variance in vehicle velocities, a cellular automata model was developed and the results were validated using simulation. Results of the study showed that placing limitations on the number and types of vehicles that can slow down traffic during evacuation could minimize evacuation time. The use of buses was recommended during evacuation as buses reduce the total number of passenger cars to be evacuated. It was also suggested that vehicles with lower speeds always travel in the right lane.

Cova and Johnson (2003) developed a network flow model to optimize lane-based evacuation routing plans for a complex road network. A mixed-integer programming model was used to generate routing plans that traded total vehicle travel distance against merging, which reduced the traffic crossing-conflicts at intersections. PARAMICS was used to compare the routing plans to the no routing plan (i.e., random destination choice). The results of the study showed that channeling flows at intersections to remove crossing conflicts can significantly decrease evacuation time over no routing plans.

With agent based modeling approach, Church and Sexton (2002) investigated how evacuation time can be affected under different settings such as opening alternative exits, varying number of vehicles leaving a household, and applying different traffic control methods. Batty et al. (2003) also used agent based simulation approach to analyze route-changing patterns for a carnival event. Results of the studies showed that evacuation time can be significantly decreased by increasing vehicle occupancy, using traffic control at critical intersections, and providing additional access or exits along the evacuation route.

Cova and Johnson (2002) developed a method to test neighborhood evacuation plans for an urban- wildland interface, which allows an analyst to map travel time variation based on vehicles used per household and departure times. This was achieved by augmenting PARAMICS with an off-the-shelf microsimulation software used to manage household trip generation, departure timing, and destination choice. A case study for a fire-prone community was presented where GIS was used to determine the spatial effects of a second access road on evacuation times. Results of the study indicated that the second access road would reduce the travel times for some households based on their proximity and access to exit, but evacuation travel times at all locations could become more consistent (i.e., have a lower standard of deviation as compared to the one road alternative).

Murray-Tuite and Mahmassani (2004) studied the effects of household interactions (e.g., trip chains) on evacuation time. Integer linear programming approach was applied to determine where household members are to meet in an evacuation event. A micro-assignment simulation approach was used to capture the resulting traffic interactions in the network. Based on the comparison of evacuation times for different network loading strategies (that were based on wait time at locations, e.g., school and other meeting points), it was found that a minimum of 150% of the original demand should be used for planning evacuation if trip chains are not considered. This demand consideration helps to avoid underestimation of evacuation times and achieve realistic results.

Pal et al. (2004) used Oak Ridge Evacuation Modeling System 2.5 (OREMS), a traffic modeling software package and ArcView 3.2, a GIS software package to develop

evacuation models for Baldwin and Mobile counties along the Alabama Gulf Coast. ArcView 3.2 was used to define the road network, population, and area being evacuated, and OREMS was used to model the effect of evacuation on the traffic network. The results from the developed GIS/traffic simulation models showed that the estimated evacuation times of the two counties were consistent with the actual evacuation times during a hurricane evacuation event. It was also found that the least traffic congestion occurred when speeds were limited to 60 mph on interstates and 40 mph on other roads.

Han and Yuan (2005) used VISSIM, a microscopic, behavior-based simulation software, to mimic traffic operations under a hypothetical event of a nuclear plant accident by applying Dynamic Traffic Assignment (DTA) and most desirable destinations (MDD) methods. DTA was used to route the evacuees according to network conditions at the time of departure, and the MDD choice for the evacuees was modeled by considering the shortest travel time to destination according to the departure time. The implementation of the two strategies led to significant improvement in overall evacuation time compared to static destination selection and traffic assignment. Results also showed that applying either of the strategies: (1) Police officers controlling traffic at key intersections, and (2) Reversing lanes on congested road sections, can lead to reduction in delay and evacuation time.

Liu et al. (2005) developed a two-level integrated model for optimizing evacuation plans (to yield the range of most viable parameters for target control strategies such as the percentage of demands diverted to each evacuation route, turning percentage at critical locations, merging ratios at ramps and signal timings) that serve as the input for a simulation-based analysis. The model employed the cell transmission concept

(Daganzo, 1994), but with a revised formulation for large-scale network applications. The high level optimization maximized the throughput during specified evacuation duration, and the low level one minimized the total travel time and wait time. A set of optimal evacuation plans was generated for the available resources and specified evacuation time window. The applicability and reliability of model were evaluated with microscopic software, named Ocean City Evacuation Network.

2.2 Evacuation Staging

Staging of evacuation can alleviate congestion and hence reduce evacuation time (Chen and Zhan, 2004). The necessity for staging can also arise due to various critical factors that ought to be considered during the evacuation decision-making process, such as the type of incident, the urgency level, etc. Staging can be most suitably employed for evacuating substantially large or populous areas. The level of urgency depends on the type of the evacuation event (e.g., hurricanes, earthquakes, nuclear power plant disaster, terrorist attacks, etc). For instance, in case of a nuclear plant disaster, the primary goal would be to evacuate residents instantaneously, while on the other hand, a hurricane evacuation can be planned to minimize delays. In this regard, employing appropriate staging can achieve significant benefits.

Church and Cova (2000) developed a network partitioning optimization model to determine the vulnerability of a neighborhood during evacuation based on the levels of bulk lane demand. Bulk lane demand was defined as the ratio of evacuation demand to exit capacity. The higher the value of bulk lane demand, the longer time it would take to clear the demand. The model delineated a neighborhood into small contiguous areas

about a point (e.g., an intersection) that maximized bulk lane demand and defined the neighborhood as having the greatest risk in evacuating in a timely manner. By applying this model for selected intersections across a road network, street segments can be classified in terms of worst-case or high bulk lane demand values. With this, a map depicting the difficulty in evacuation across the network could be developed.

Malone et al. (2001) evaluated a proposal for staging of evacuation of different coastal counties in Charleston, SC, to reduce evacuation time. It was found that staggering the evacuation over some time period for the counties, consistent with how hurricanes affect the coast, instead of evacuating all at once, reduces the size of the bottleneck. This increases the average traffic speed without significantly increasing traffic density that can cause traffic jams. Thus, it was recommended that staggering of evacuation decreases the evacuation time.

Chen and Zhan (2004) used agent based simulation modeling approach (utilizing PARAMICS software) to analyze the effectiveness of simultaneous and staged evacuations (e.g., 24 scenarios for four evacuation zones). Results revealed that the performance of staged evacuation was highly related to network structure and distribution of population density. Also, when the roads were at capacity, staged evacuation can reduce the total evacuation time, for a grid roadway structure. However, there was no significant benefit to use staged evacuation strategy in terms of evacuation time, for a ring road network, even if the population density was high due to the limited number of radial outlets from the evacuation zone.

Wilmot and Meduri (2005) developed a criteria-based methodology to delineate hurricane evacuation zones depending on their elevations. The procedure was initiated by

creating a layer in GIS based on the Maximum of the Maximum Envelope of Water, (MOM) for the endangered region. Portions of ZIP code areas were divided into subareas based on highway locations and elevation point file data were overlaid on the subareas to calculate the mean and standard deviation of the elevation of each subarea. The authors opined that hurricane evacuation zones can be delineated by overlaying zones of homogeneous elevation on a surge map to identify those that will be flooded in each scenario.

Sbyati and Mahmmasani (2006) developed an evacuation scheduling model based on system-optimal assignment method where trips are scheduled between a selected set of origin nodes and destinations with the objective of minimizing the network clearance time. An iterative bi-level formulation method was used and the dynamic network assignment problem was solved in the upper level to determine the time-dependent route assignments, and a dynamic loading problem was solved in the lower level to determine the corresponding route travel times. Results show that scheduling evacuation reduces network clearance time, total trip time, and average trip time.

Liu et al. (2006) developed a cell-based network optimization model for planning staged evacuation. This model computes the optimal starting time and routes for each evacuation zone based on incident impacts, and demand generation patterns of evacuees using the S-shaped logit-based function. The applicability of the model was demonstrated with an example network with evacuation zones that are based on the level of threat. Preliminary numerical results show that evacuation time, average travel time and wait time can be reduced with staging.

2.3 Flow Maximization

One of the most significant issues associated with evacuation is managing demand. Most emergency management officials agree that the roadway capacity is insufficient to completely evacuate people from large cities (e.g., New Orleans and Miami) in a short time period in the event of a hurricane (Wolshon, 2004). Evacuation demand has a major effect on the speed and efficiency of evacuations. Demand can be minimized by providing better public information by working with the news media to give more accurate descriptions of congestion levels on evacuation routes and the intensity of threat at specific areas. However, practitioners employ contraflow, or reverse lane operations, to maximize roadway capacity to accommodate higher demands during evacuation.

2.3.1 Contraflow Operations

Contraflow is the reversal in the direction of traffic in one or more inbound lanes to increase outbound capacity in order to accommodate the traffic in the outbound direction. Contraflow plans were developed after Hurricane Hugo, which devastated Charleston in 1989 (Munday, 1999). They were also used to accommodate unbalanced traffic during peak hours or special events. For example, in New Hampshire, contraflow operation is used twice a year to lessen congestion on the New Hampshire International Speedway (NHIS) during Winston Cup NASCAR races. During hurricane George in 1998, only the Florida and Georgia DOTs had contraflow plans in place to evacuate traffic on their interstate freeways. According to a recent study, 11 of the 18 coastal states threatened by hurricanes have developed contraflow plans (Wolshon et al., 2001). As shown in Figure 2.1, various alternatives ranging from normal operation to a complete reversal of both

inbound lanes exist. Four types of contraflow operations have been in practice for two-lane two-way highways.

1. Two lanes reversed;
2. One lane reversed, one lane normal for emergency/service vehicle access;
3. One lane reversed, one lane normal for inbound traffic entry; and
4. One lane reversed and use of outbound right shoulder

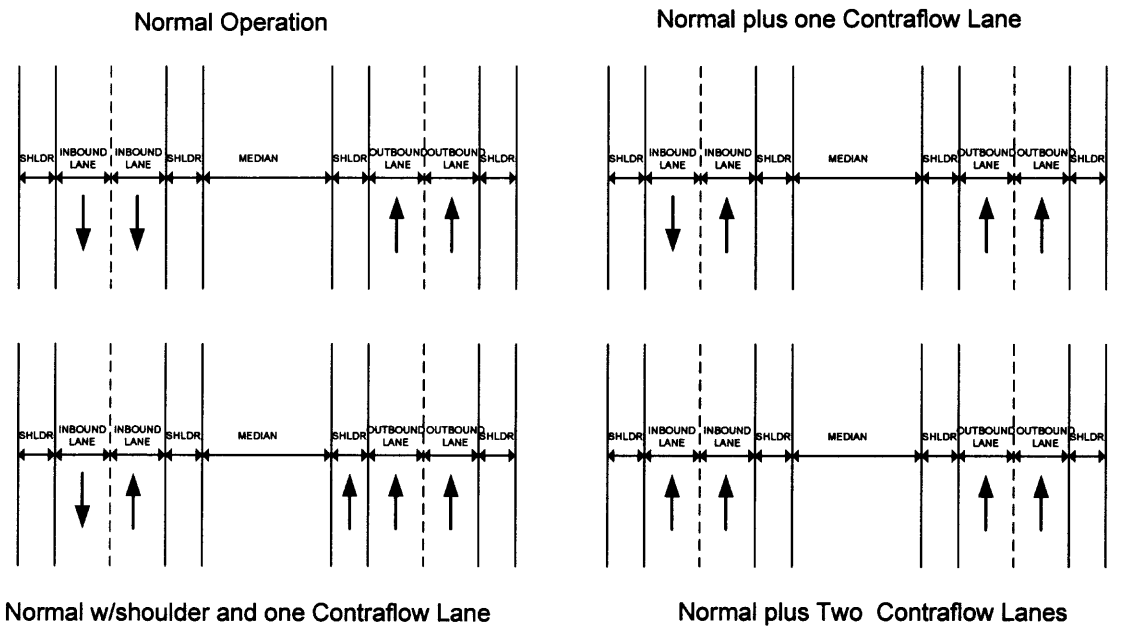

Figure 2.1 Freeway contraflow lane use configurations.
Source: (Wolshon et al. 2001)

Each of the alternative strategies provides 30% to 67% capacity increase over normal two-way operation. According to a study by FEMA (2000), a full reversal would provide a near 70% capacity increase over conventional two outbound lane configurations. Single inbound lane reversals are helpful in maintaining a lane for inbound law enforcement personnel and emergency service vehicles for managing incidents. It can also permit access for people who want to travel against the evacuation traffic. However, this strategy also raises the potential for head-on accidents. Another strategy to improve capacity is to use the outbound left shoulder as an additional outbound lane. This has been estimated to

increase capacity by about only eight percent (FEMA, 2000). The increase in capacity depends on the width and condition of the shoulder, since flow rates are decreased because drivers tend to reduce speeds when they are laterally constrained. Table 2.1 illustrates the estimated average total outbound capacity (vph) in one direction (PBS&J, 2000).

Table 2.1 Interstate Contraflow Flow Rates for Four-Lane Freeways

Contraflow Strategies	Estimated Capacity (vph)
Normal Two-Way Operation	3,000
Three Lane (one contraflow lane)	3,900
Three Lane (using outside shoulder)	4,200
All- lane Reversed (no shoulder lanes)	5,000

Source: (PBS&J, 2000)

2.3.2 Current Practices

Lim (2003) used the microscopic traffic simulation tool, CORSIM 5.0, to evaluate the effectiveness of contraflow termination points. A contraflow section is terminated by using a median crossover that redirects or splits a portion of the traffic on the contraflow lane. Ten scenarios, which were designed based on the number of lanes at the median crossover and the percentage of exiting traffic at the previous interchange were simulated and the resulting performance of each scenario was ranked by the total number of vehicles that traveled, traffic flow, speed, density, and delay. It was found that maintaining a substantial number of exit opportunities along the intermediate segments of the evacuation section can increase the overall efficiency of evacuation.

Kwon and Pitt (2005) studied the feasibility of applying the mesoscopic dynamic traffic assignment (DTA) model, Dynasmart-P, for evacuating traffic in downtown Minneapolis, Minnesota. The contraflow operations were found to be very effective when

the capacities of the key entrance ramps were increased. Simulation results revealed potential gains in flow and hence a reduction in travel time due to increase in capacities of outbound ramps from the evacuation region

Tuydes and Ziliaskopoulos (2004) modified the cell transmission model (CTM) for better utilization of the available network capacity by allowing reversibility on some or all road segments when a drastic demand pattern shift is experienced during a disaster. The model calculated the system optimal solution of a dynamic traffic assignment problem and optimal capacity reallocation (also known as contraflow optimization). Comparisons of the base case with no reversibility and the re-designed one considering contraflow were tested on an example network. Results showed significant reduction in evacuation time when contraflow or reverse lane operations were used.

2.4 Traffic Flow Theory Applied to Modeling Evacuation

Since the purpose of this research is to develop an analytical model that determines the optimal staging to minimize evacuation time and delay, a review of the existing traffic flow models used in evacuation will provide vital inputs for achieving this objective. The following section presents a general classification and a brief discussion on the type of traffic flow models employed in evacuation modeling.

2.4.1 Model Classification

Various methods have been adopted in categorizing traffic flow models in the past. Classifying models as macroscopic vs. microsimulation, deterministic vs. microsimulation, empirical vs. theoretical, empirical vs. analytical are not valid ways of

qualifying models. This is because, models never fall into clear-cut categories, but there is a spectrum of models (Akcelik, 2004).

The U.S Highway Capacity Manual (HCM, 2000) defines an analytical model as "A model that relates system components using theoretical considerations that are tempered, validated, and calibrated by field data.", whereas it defines a simulation model as "A computer program that uses mathematical models to conduct experiments with traffic events on a transportation facility or system over extended periods of time". Analytical models use direct mathematical computations to determine system states, and simulation models use various rules (mostly in the form of mathematical equations) for movement of vehicles (individually or in platoons). Therefore, fundamentally both analytical and simulation models are mathematical derivatives of their forms. In general, models used for evacuation planning are classified into two groups namely, microscopic and macroscopic (Fujishige et al., 2002). Another class of models called mesoscopic models that trade the accuracy of microscopic models and the computational efficiency of macroscopic models has also been employed.

Prior to 1990, evacuation simulation studies were scarce due the lack of adequate computing resources. Due to the advancement in computer technology, simulation has become popular in recent years. The following sections discuss evacuation models that employ several techniques to minimize evacuation time or delay and/or maximize vehicle throughput or roadway capacity.

2.4.2 Microscopic Models

Microscopic models have been used for experimental analyses by simulation of behavior of individual evacuees. These models are typically based on car-following and lane-changing theories that can represent traffic operations and driver behavior. Microscopic modeling also incorporates analytical techniques such as queuing analysis, shock-wave analysis. Most microscopic models employ the Monte Carlo process to generate random numbers for representing driver/vehicle behavior in real traffic conditions. Examples of microscopic models applied in evacuation include Car Following Models, Agent Based Models (Distributed Artificial Intelligence-Based Models), and Cellular Automata Models.

(1) Car Following Models

Car following models represent individual vehicle following behavior in a single stream of traffic. They state rules for maintaining a safety distance between vehicles and use realistic driver behavior and detailed vehicle characteristics to model various traffic flows, which are observed in real traffic such as soliton wave, shock wave, and kink wave, etc. Car Following Models assume feasible values of car length, driver reaction time and deceleration parameters to obtain optimal values of flow rate, density, and velocity. Application of car following models in evacuation modeling includes studies conducted by Lim (2003) and Malone et al. (2001).

Malone et al. (2001) developed an evacuation model based on car following distance to derive traffic flow rate in terms of empirically estimated driving parameters (car length, reaction time and the deceleration parameter). The evacuation time M, is defined as a function of discharge and travel time as formulated in Equation 2.1:

$$M = W\frac{N}{lq} + \frac{(1-W)D}{u} \tag{2.1}$$

where W is weight factor for maximizing either discharge rate or velocity, N is total demand, l is number of lanes, q is discharge rate, D is distance to be traveled, and u is speed of the evacuation route. The density k was obtained from the reciprocal of the vehicle spacing denoted as S, which was obtained from data compiled in a series of 23 observational studies of highway capacity using empirical parameters:

$$S = \alpha + \beta u + \gamma u^2 \tag{2.2}$$

where α is the effective vehicle length (L), β is reaction time, and γ is reciprocal of twice the maximum average deceleration of a following vehicle. Using Equation 2.2 and the fundamental flow-density relationship $q = uk$, the optimal speed, u^* and optimal density, k^* were derived as $u^* = \sqrt{\frac{L}{\gamma}}$ and, $k^* = \frac{\beta\sqrt{\frac{\gamma}{L}} - 2\gamma}{\beta^2 - 4\gamma L}$ respectively. The optimal discharge rate during evacuation was determined as a product u^* and k^*.

(2) Cellular Automata Models

Cellular automata was introduced by von Neumann and Ulam in the 1960s for modeling biological self-reproduction (Nagel and Schreckenberg, 1992). Creamer and Ludwig (1986) used a cellular automata model in the form of a Boolean simulation of traffic flow where vehicles were represented by 1-bit variables that are placed in computer memory locations corresponding to the locations of vehicles on the roadway. Based on the occupancies of cells at a discrete time instant, the pattern of cars within a lane of a roadway is represented by corresponding set of 0's or 1's. Malone et al. (2001)

developed a Cellular Automata evacuation model to account for the variance in the traveling speeds of vehicles on the evacuation route. By doing so, the model takes in to account the random behavior of drivers and avoids over prediction of speed.

(3) Agent Based Models

Agent-based modeling approach, also known as individual-oriented or distributed artificial intelligence-based modeling approach, is an important tool for simulating individual and collective behaviors in a dynamic system (e.g., transportation system) where the future conditions are unpredictable. The basic components of an agent-based system include a model of the agents and a model of their environment. Individual vehicles are treated as autonomous decision-making agents. Each agent makes decisions and acts based on the interactions with other agents and information provided by the environment. A set of rules (e.g., vehicle acceleration, deceleration, lane changing, etc) is employed to govern the behavior of the agents. The collective behavior resulting from the interactions among individual vehicles during evacuation can be captured for measuring the evacuation time. Agent based models have been applied in previous studies conducted by Church and Sexton (2002), Batty et al. (2003), and Chen and Zhan (2004) as discussed in Sections 2.1 and 2.2.

(4) Simulation Models

Microscopic traffic simulation models, designed for modeling normal traffic operations could be applied to model traffic situations during evacuations. Prior to 1990 the number of studies that employed microsimulation for evacuation modeling was limited due to

inadequate computational capabilities. However, due to advancement in computer technology, the number of studies employing microsimulation has increased.

The earliest application of microsimulation in evacuation modeling required customizing the general-purpose microsimulator NETSIM2 to manage an evacuation (Rathi and Santiago, 1990). Stern and Sinuany-Stern (1989) presented a behavioral-based microsimulation model, based on the SLAM II simulation language for small-city evacuations that included pedestrian flows. Cova and Johnson (2002) developed a network flow model to optimize lane-based evacuation routing plans in a complex road network using the microsimulation model PARAMICS. In another study, Cova and Johnson (2002) developed a method to test neighborhood evacuation plans for an urban-wildland interface using PARAMICS. Lim (2003) used the microscopic traffic simulation tool, CORSIM to evaluate the effectiveness of contraflow termination points in evacuation. A comparison of prominent microsimulation software packages employed in evacuation modeling is presented in Table 2.2.

Table 2.2 Comparison of Microscopic Simulation Models Used in Evacuation Modeling

Criteria	INTEGRATION	MITSIM	VISSIM	CORSIM	PARAMICS
Developer	FHWA	Massachusetts Institute of Technology	PTV System Software and Consulting GMBH	FHWA	The Edinburgh Parallel Computing Centre and Quadstone Ltd
User Interface	Text-based and graphical user interface	Text-based and graphical user interface	Graphical user interface	ASCII text files	Text-based and graphical user interface
Control Strategies and Algorithms	Car following model. Internal strategies	Car following model External.	Driver-vehicle-element (DVE) model and signal control model.	Car following model Pre-timed and actuated signal control	Car following model Internal.
Automated Highway System					x
Dynamic Traffic Assignment		x			x
Modeling Transit			x	x	x
Dynamic Route Guidance	x	x			x
Variable Message Signs	x	x			x
Incident Management	x	x		x	x

2.4.3 Macroscopic Models

Macroscopic models used in evacuation do not track behavior of individual vehicles but regard them as a section or homogeneous group. Continuum models, either simple or high order are usually employed in these models. These models treat traffic as an aggregate fluid flow that uses the law of conservation of mass. According to the continuum theory, flow is a function of density at any point on the road. The simple continuum model comprises of a continuity equation (Equation 2.3) representing the relationship among speed u, density k, and flow rate q at location x and time t. The continuity equation indicates that vehicles are neither created nor lost along the road.

$$\frac{\partial k}{\partial t} + \frac{\partial q}{\partial x} = 0 \tag{2.3}$$

The use of the variables u, k and q reduces the computation requirements for macroscopic modeling, making real-time calculation quite feasible. This is because aggregate behavioral data is easier to obtain and validate. The simple continuum model does not consider vehicle acceleration and inertia effects and thus cannot describe non-equilibrium traffic flow dynamics (e.g., breakdown of traffic, stopping and going) with precision. A high-order continuum model takes into account acceleration and inertia effects by using a momentum equation in addition to the continuity equation. This momentum equation accounts for the dynamic speed-density relationship observed in real traffic flow. Macroscopic models applied in evacuation planning include static network models and dynamic network models, which are discussed below.

(1) Static Network Evacuation Models

In case of static network evacuation models, the varying behavior of evacuees is not considered and hence flows during evacuation are independent of time. Static network models include shortest path, minimum cost network flow (Yamsda, 1996), and quickest path (Chen and Chin, 1990; Chen and Hung, 1993) models. A quickest path problem is one in which, for a given fixed flow and entrance and exit nodes in a network, the quickest path is found in order to send the flow as quickly as possible.

(2) Dynamic Network Evacuation Models

Unlike the static network models, dynamic network models treat traffic flow as time-varying function to represent movements of evacuees. Dynamic network models can be classified into (a) discrete-time dynamic network models and (b) continuous -time dynamic network models, which are discussed next.

2(a) Discrete-Time Dynamic Network Models

Discrete-time dynamic network could be modeled as a maximum flow or quickest flow. In the maximum flow model, the objective is to find a dynamic flow rate that maximizes the total flow between a pair of entrance and exit nodes within a given time. A polynomial approximation algorithm for this was developed by Hoppe and Tardos (1994). However, in the quickest flow model, the objective is to find a dynamic flow rate to send a given flow amount between a pair of entrance and exit nodes in the shortest possible time. Burkard et al. (1993) obtained a polynomial-time algorithm for the quickest flow problem by reducing it to a maximum dynamic flow problem.

2(b) Continuous Time Dynamic Flow Models

Continuous time dynamic flow models consider the quickest flow with constant capacity and travel time, and a maximum flow with zero travel time. The Quickest flow model determines the shortest time of sending a flow in a network in which demand exceeds capacity. Burkard et al. (1993) gave polynomial algorithms to reduce the quickest flow problem to the maximum dynamic flow problem by binary search. On the other hand, the objective of the maximum flow model is to send as much flow as possible from the source to the sink within a specified time bound, when capacities are less than the entering flows.

(3) Simulation Models

Several macroscopic evacuation models have been developed from the trip-based four-step model with slightly different functional requirements to match evacuation modeling. They have similar databases integrating data on population, socioeconomic characteristics, route network, and other analysis elements. Also, the models use similar algorithms of trip generation, distribution and assignment. Table 2.3 presents a review of various macroscopic simulation models. Most of the computer simulation models are proprietary and the developers are reluctant to release their models for investigation. The optimization algorithms used in the models vary at different levels of their application.

Table 2.3 A Review of Macroscopic Evacuation Simulation Models

#	Model	Developer/ Year	Features
1	Calculated Logical Evacuation and Response (CLEAR)	Pacific Northwest Laboratories, 1981	• Developed for the Nuclear Regulatory Commission • Simulates vehicle movement only along the main routes, which reduces the computational load.
2	MASS Evacuation (MASSVAC)	Hobieka et al., 1985	• Models nuclear power plant evacuations, operational strategies for hurricane evacuations • Estimates the maximum time to evacuate the network given various disaster intensity levels and identifies potential areas where heavy congestion is likely to occur. • Dynamic traffic assignment
3	Sea, Lake and Overland Surges from Hurricanes (SLOSH)	National Weather Service (NWS), 1984	• Used to plan evacuation routes and locate emergency shelters
4	Hurricane and Evacuation Program (HURREVAC)	FEMA, USACE, and NWS, 1988	• Used to track hurricanes to assist in evacuation decision making • Uses Geographic Information System (GIS) information to correlate demographic data with shelter locations and their proximity to evacuation routes to estimate the effect of strategic-level evacuation decisions.
5	NETVAC	MIT, 1982	• Requires time-varying O-D tables as input • Outputs of the model are lengths of queues, speeds and measures of level of service and flow pattern throughout the evacuation process for each link at each specified interval • Dynamic traffic assignment

Table 2.3 A Review of Macroscopic Evacuation Simulation Models (continued).

6	DYNamic EVacuation model (DYNEV)	KLD Associates, 1984	• Requires traffic volume entering each link as input. • Output of the model gives detailed information about the operational performance of each link, including vehicle speed, traffic density, and volume. • Static traffic assignment
7	Oak Ridge Evacuation Modeling System (OREMS)	Oak Ridge National Laboratory (ORNL), 1995	• Developed using CORSIM • Combines the trip distribution and traffic assignment submodel with a detailed traffic flow simulation submodel • Simulates traffic flow during various defense oriented emergency evacuations. Can be used to estimate evacuation times, identify operational traffic characteristics • Allows users to experiment with alternate routes, destinations, traffic control and management strategies, and evacuee response rates. • Dynamic traffic assignment
8	Evacuation Travel Demand Forecasting System (ETIS)	PBSJ, 2000	• Forecasts evacuation traffic volumes and congestion through a web based travel demand forecast system 1. Static traffic assignment

2.4.4 Mesoscopic Models

Mesoscopic models unite the properties of both microscopic and macroscopic simulation models. Similar to microscopic models, mesoscopic models track the behavior of individual vehicles, but vehicle movement follows the approach of macroscopic models, which is controlled by the average speed. Thus, mesoscopic models trade the accuracy of microscopic models and the computational efficiency of macroscopic models. These models are employed when a high level of detail is desired with real-time simulation.

The cell transmission model (CTM) initially developed by Daganzo (1994) is a mesoscopic model, where a highway is segmented into small cells and the contents of the cells (i.e., number of vehicles) are tracked over time In a cell-transmission scheme the cell data is updated at closely spaced time intervals by calculating the number of vehicles that cross the boundary separating each pair of adjoining cells during the corresponding clock interval. This flow is based on a comparison between the maximum number of vehicles that can be sent by the cell directly upstream of the boundary and those that can be received by the downstream cell. Application of CTM in evacuation includes the models developed by Tuydes and Ziliaskopoulos (2004), and Liu et al. (2005).

Mesoscopic simulation models used in evacuation include NETCELL and Dynasmart-P. NETCELL is a freeway network simulation program by Daganzo (1994), which captures the dynamic evolution of traffic over a freeway network with three-legged junctions (Cayford et al., 1997). Dynasmart-P was developed by FHWA and the University of Maryland (Dynasmart-P, 2001). The most significant feature of Dynasmart-P is its dynamic traffic assignment capability.

2.5 Speed-Flow-Density Relationships

Understanding the relationship among different traffic parameters (e.g., Speed, Density, Flow, etc) is important for developing the evacuation model proposed in this research to determine discharge rate of an evacuation route under varying traffic conditions. The total demand to be evacuated and maximum discharge rate influence the estimation of evacuation time and delay considerably.

2.5.1 Speed- Density Models

The calibration of speed vs. density has been focused upon in modeling traffic stream characteristics mainly due to two reasons (Roess et al., 1998):

1. Speed-density curves are monotonically decreasing and can be expressed in simple mathematical equations as compared to flow vs. speed and flow vs. density curves.
2. Speed-density curves represent the most basic interaction of drivers on roadways as drivers perceive density, or the proximity of other vehicles, and adjust their speeds accordingly. Drivers cannot sense flow, which is a point measure and does not have an impact on their behavior.

Seven models were proposed to represent the speed-density relationship (Hall, 1994) as discussed below.

Greenshield (1935) developed the following linear speed-density model (Equation 2.4) by conducting several field studies:

$$u = u_f \left(1 - \frac{k}{k_j} \right) \tag{2.4}$$

where u_f is free flow speed (speed achieved under very low density), and k_j is jam density (maximum density at which all vehicles are stopped). While results of this linear speed-density model have continued to be widely accepted, Drake et al. (1967) indicated that the speed-density forms should not be perfectly linear.

In order to develop a model that could reasonably represent real world data, Ellis (1964) fitted data (free flow, impeded flow, congested flow, etc) in various flow ranges for different linear models. The advantage of this piecewise modeling approach is that non-linear relationships can be approximated by linear equations.

Greenberg (1959) developed a logarithmic speed-density model (Equation 2.5),

$$u = u_c \ln\left(\frac{k_j}{k}\right) \tag{2.5}$$

where u_c is critical speed (speed at maximum discharge rate). Since this model fails at low values of density, a maximum free flow speed must be assumed for estimating actual speed based on jammed and observed densities.

Underwood (1961) developed an exponential model for representing the relationship between speed and density, which is given by

$$u = u_f e^{\left(\frac{-k}{k_c}\right)} \tag{2.6}$$

where k_c is critical density (density at maximum discharge rate). Although the Underwood model is practicably suitable for low density conditions, it is unreliable at higher values.

Edie (1961) developed a discontinuous, exponential model, which employed the Greenberg model (Equation 2.5) and the Underwood model (Equation 2.6) for high and low density conditions, respectively. This model reasonably describes the entire range of

speeds and densities. Figure 2.2 shows a discontinuity in the flow-density curve at the point of critical density.

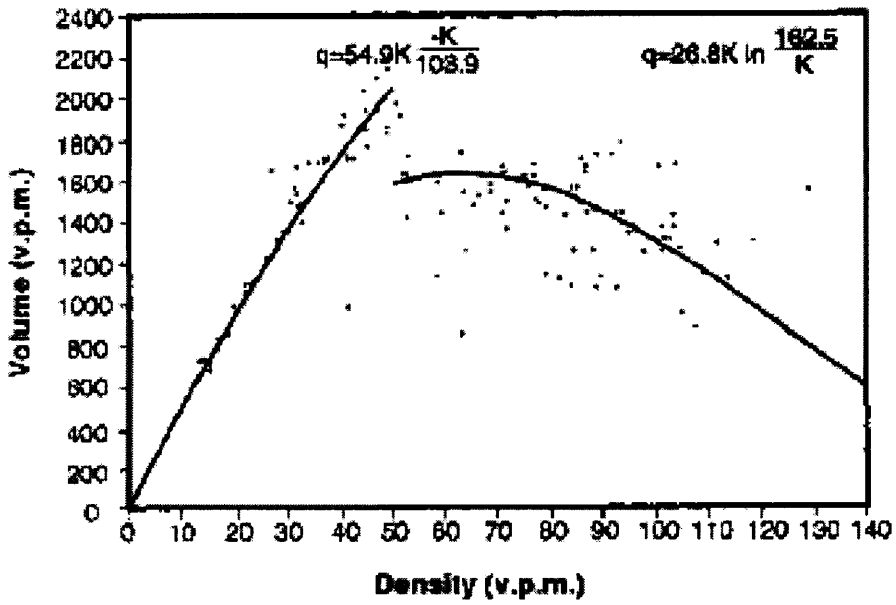

Figure 2.2 Edie's model fitted to Eisenhower Expressway, Chicago data.
Source: (Drake et al. 1967)

May (1967) developed a bell shaped curve (Equation 2.7) with field data to model speed-density relationship.

$$u = u_f e^{\left(-0.5\left(\frac{k}{k_c}\right)^2\right)} \tag{2.7}$$

Similar to Underwood's model, this model is unsuitable under high density conditions.

Drake et al. (1967) conducted empirical tests to statistically compare the speed-density models discussed above. The data collected from the middle lane of the Eisenhower Expressway in Chicago that comprised of a series of 1224 1-minute observations were used. The measured information consisted of volume, time mean speed, and occupancy. Density was calculated by dividing the volume by time mean

speed. Edie's model seemed to provide the best estimates of the fundamental parameters (speed, density, flow) at the least standard error (Hall, 1994). However, the other models tended to underestimate the maximum flows. Thus, Edie's model is applied here to determine the speed-density relationship of an evacuation route.

2.5.2 Speed-Flow Models

Under uncongested conditions, for a given demand of the evacuation route, density is first determined using Undewood's model and then the corresponding speed is obtained. This procedure will be discussed in section 3.3. On the other hand, under congested flow conditions, the practicable flow is determined first using a suitable model that provides feasible values of speed and density. The selection of the model for congested condition is discussed as below.

Several models have been proposed to approximate speeds for flows near and above the roadway capacity. The BPR function (Equation 2.8) used in planning models is developed based on the HCM (1965) and has speeds sensitive to increasing flows.

$$u = \frac{u_f}{\left(1 + 0.15\left(\frac{v}{c}\right)^4\right)} \tag{2.8}$$

where $\frac{v}{c}$ is the volume to capacity ratio. However, the BPR curve seems to overestimate speed as the volume-to-capacity ratios exceeds 1.0 and underestimates speeds if volume-to-capacity ratio is less than 1.0.

The Metropolitan Transportation Commission (MTC) function (Equation 2.9) was developed as a modification of the BPR function by changing the coefficient in the BPR function from 0.15 to 0.20 and the exponent from 4.0 to 10 (Singh, 1995).

$$u = \frac{u_f}{\left(1+0.2\left(\frac{v}{c}\right)^{10}\right)} \tag{2.9}$$

This function followed the 1995 HCM speed-flow relationship very closely by having reduction in speed of 10 mph instead of 5 mph from the free-flow speed at $\frac{v}{c}$ ratio equal to 1.0.

Davidson (1966) developed a model for travel time estimation (Equation 2.10) using the concepts of queuing theory. The speed is obtained from the reciprocal of travel time, T, from Equation 2.10.

$$T = T_0\left(1+\frac{J_D\left(\frac{v}{c}\right)}{1-\frac{v}{c}}\right) \tag{2.10}$$

where:
T : Estimated travel time (hours/mile)
T_0 : Free-flow travel time (hours/mile)
J_D : Delay parameter (calibrated based on type of roadway)

Akçelik (1991) proposed a modified time dependent form of the Davidson's function to model travel times while volumes are near or above the capacity (Equation 2.11). Akçelik's equation was derived as a modification to Davidson's equation for predicting the travel time on any road facility (Dowling and Alexiadis, 1997).

$$T = T_0 + \left[0.25p \left(\left(\frac{v}{c} - 1\right) + \sqrt{\left(\frac{v}{c} - 1\right)^2 + \frac{8J_D\left(\frac{v}{c}\right)}{cp}} \right) \right] \tag{2.11}$$

where p is the time period during which an average demand is assumed to persist (e.g., 1 hour). The Akçelik's function can deal with varying traffic flow for better link travel times estimation for congested conditions (i.e. $\frac{v}{c} > 1.0$).Similar to Equation 2.10, the speed for Akçelik's model is obtained from the reciprocal of T.

The performance of the models discussed above for varying demand to capacity ratio is shown in Figure 2.3.

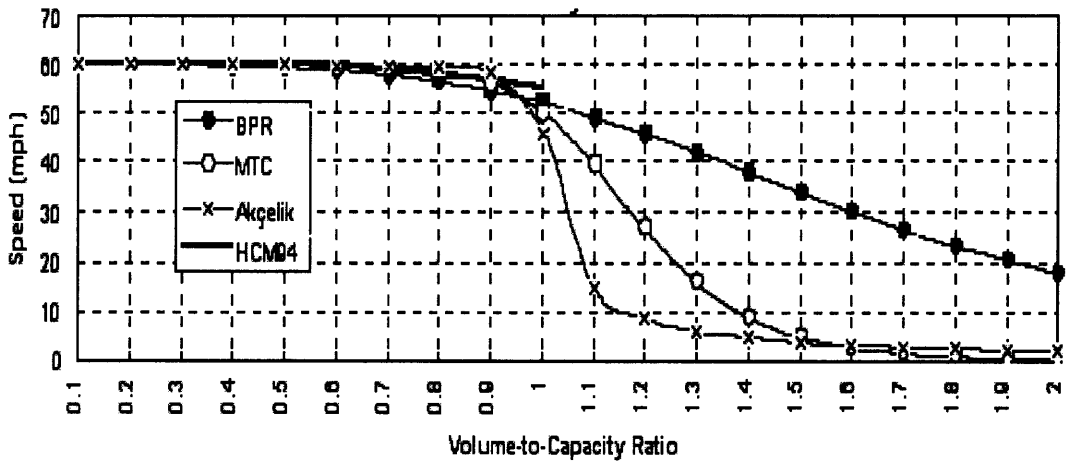

Figure 2.3 Comparison of models for congested conditions.
Source: (Singh, 1999)

A comparison of the models for estimating speeds for flows near and above capacity based on the root-mean square error (RMS) of observed speeds (using floating car runs) for 119 selected freeway segments over the San Francisco Bay area yielded the following results (Singh, 1999): The RMS error for the MTC curve was 10.1, compared to BPR, which was 10.8, Updated BPR was 10.4, and Akçelik was 9.83.

Also, research by Dowling et al. (1998) that used the Akçelik speed-flow model to refine the speed estimates of network assignment model, demonstrated that Akçelik's model produces significantly improved traffic assignment run times and provides more accurate speed estimates.

Thus, this research will also employ the Akçelik's model to estimate speeds under congested conditions (i.e. $\frac{v}{c} > 1.0$). The speed obtained from Akçelik's model is then used to compute the density through Edie's model, and the corresponding practicable discharge rate. The application of Akçelik's model will be discussed in section 4.3.

2.6 Modeling Evacuees' Behavior

The performance of behavioral models is different from that of non-behavioral based models (Stern and Stern, 1989) because behavioral models account for information diffusion and decision making time. Integrating behavioral aspects in evacuation modeling yields more realistic estimation of evacuation times. The state-of-practice in evacuation travel demand modeling has two main steps namely, travel demand forecasting and the estimation of departure times of evacuees (Fu, 2004). Travel demand forecasting helps in estimating evacuation time and delay. Departure times, which depend on the behavioral response of evacuees (network loading rates, e.g., fast, medium, slow) to evacuation orders has a significant effect on the traffic conditions of the evacuation route and affect the evacuation time and delay.

2.6.1 Travel Demand Forecasting

Lewis (1985) first developed a general travel demand forecasting process for hurricane evacuation, which is analogous to the four-step urban travel demand-forecasting model. The problems that were discussed included transportation planning, evacuation travel pattern, estimation of travel demand, calculation of clearance time, and the development of traffic control measures. Barrett et al. (2000) proposed a modeling framework for developing dynamic hurricane evacuation models for long term and short term planning purposes as well as for real-time operational purposes. They proposed functional requirements for dynamic hurricane evacuation modeling. The system provides evacuation time, evacuation routes and departure times that drivers can be predicted to choose and maximize the system performance.

The data availability on evacuation behavior increased the development of trip generation models for hurricane evacuation. Most of the post hurricane surveys and behavioral studies were conducted after the late 1980s (Baker, 1991; PBS&J, 1993; Irwin et al., 1995; U.S. Army Corps of Engineers, 1997, 1999, and 2001) The collected survey data included information pertaining to percentage of people who evacuated, factors affecting people's decision to evacuate, destination choice, departure time, number of vehicles used for evacuation, socioeconomic and demographic profiles of evacuees. Analysis of the surveyed data to understand the behavior of people in hurricane risk conditions revealed information on evacuation participation rates, reasons for evacuating or not evacuating, distribution of departure times etc. The results of the analysis have been used in developing models for evacuation.

2.6.2 Behavioral Models

Behavioral models used in modeling evacuation can be categorized into: Empirical models, Behavioral response curves, Regression models, and Sequential logit model.

(1) Empirical Models

Empirical models use the planner's knowledge and judgment, based on the collected data to produce general functions for departure time estimation. Tweedie et al. (1986) developed a loading function that approximates the Rayleigh probability distribution function as follows:

$$F(t) = 1 - e^{-t^2/1800} \tag{2.12}$$

where *F(t)* is the percentage of the population mobilized by time *t*; and *t* is the mobilization time in minutes. Mobilization time is defined as the time from issuing of an evacuation order to the time of departure of evacuees. The specific amounts of time at which given percentages of the evacuees could be expected to be mobilized as shown in Figure 2.4 was obtained by interviewing key experts with the Civil Defense Office of Oklahoma. According to this model, 1800 minutes is the maximum time at which all evacuees are assumed to have mobilized, for a hurricane evacuation.

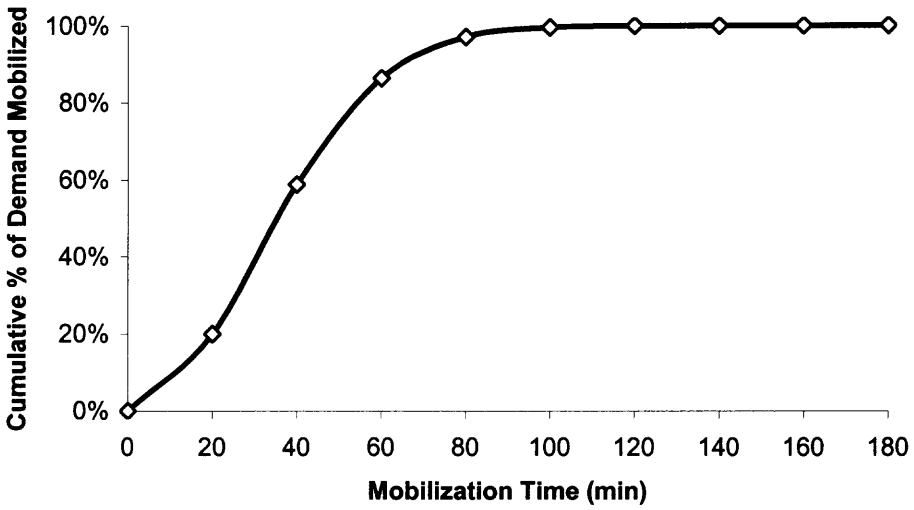

Figure 2.4 Cumulative percentage of demand mobilized vs. time.
Source: (Tweedie. 1986)

(2) Behavioral Response Curves

A response curve or loading curve portrays the assumed departure time distribution of evacuees and represents the cumulative percentage of demand evacuating with time. It is a sigmoid or "S" shaped curve. Network loading during evacuation starts at a lower rate in the beginning when evacuation orders are given and increases in course of time until it reaches a maximum, approximately halfway through the total loading period. Based on the classification of the U.S. Army Corps of Engineers (USACE), loading curves could be classified into "quick", "medium", and "slow" depending on how readily the evacuees respond to an evacuation order (U.S Army Corps of Engineers, 2000). The curves are based on historic data obtained from previous hurricane evacuations. In general, a quicker response, leads to a steeper curve. As illustrated in Figure 2.5, the time point of 0 is when the evacuation order is given.

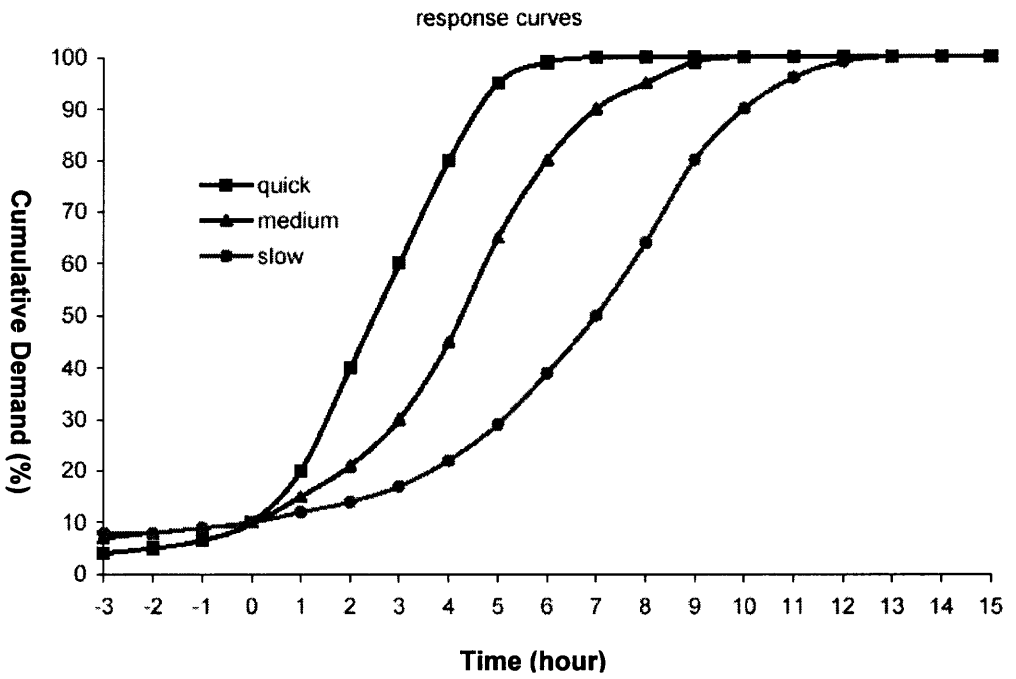

Figure 2.5 Evacuation demand loading curves.
Source: (U.S Army Corps of Engineers. 2000)

A certain proportion of demand (e.g., 10%) also known as Shadow demand leaves before time 0. The curves represent an average response to evacuation orders and do not reflect the impact of varying traffic conditions during the evacuation. The loading curve could be described by the following equation (Jamei, 1984).

$$P(t) = \frac{1}{1+e^{-\alpha(t-\beta)}} \tag{2.13}$$

where $P\ (t)$ is the cumulative percentage of demand being loaded onto the network at time t; α is the curve slope factor, which represents the response of evacuees to the disaster.; and β represents the half loading time (the time point at which half of the total volume is loaded onto the network). Evacuation time is more sensitive to changes in α than β (Radwan et al., 1985). Radwan et al. (1985) and Hobeika et al. (1998) adopted Equation 2.13 in evacuation software packages (e.g.,MASSVAC).

(3) Regression Models

Irwin et al. (1995) developed a logistic regression model to estimate the probability of an individual evacuating by utilizing data obtained from surveys following hurricane Andrew. Based on the estimated model, the independent variables that significantly affected the probability of evacuating included perception of risk, type of dwelling, gender, and age.

Mei (2002) used logistic regression approach to develop trip generation models with household survey data obtained after Hurricane Andrew in Southwest Louisiana. The probability of a household evacuating was modeled as the dependent variable. The independent variables which were found to be significant were housing type, whether the household received a mandatory evacuation order or not, age of the respondent, distance of the household from the nearest water body, and marital status. Variables that were found to be insignificant included residence ownership, prior hurricane experience, race, education level, and household size. The performance of the models was compared with other existing evacuation model, (e.g., the PBS&J model, developed for the same area). The results showed that the models developed in this study performed better than the existing PBS&J model in predicting household evacuation trip generation for southwestern Louisiana.

(4) Sequential Logit Model

Fu and Wilmot (2004) developed a sequential logit model for estimating dynamic travel demand during hurricane evacuation. The model considered the decision to evacuate as a series of binary choices over time. The probability that the utility of a household to evacuate is greater than the utility of the household to not evacuate at time i, given that it

did not evacuate earlier denoted as $P(i)_{S/C}$ is modeled as a function of the household's socio-economic characteristics, the characteristics of the hurricane, and policy decisions made by authorities as the storm approaches.

$$P(i)_{S/C} = \frac{e^{V_i^S}}{e^{V_i^S} + e^{V_i^C}} \qquad i = 1, 2, \ldots. I \tag{2.14}$$

where I is the total number of time intervals. U_i^S and U_i^C are the random utilities of a household choosing to evacuate or not to evacuate in time interval i, respectively. Each of the random utilities comprises of a systematic component V_i and an error term ε_i.

Generally,

$$U_i = V_i + \varepsilon_i \tag{2.15}$$

By assuming that the error term ε_i is independent among the alternatives (i.e., whether to evacuate or not) at any one time period, the probability of the household evacuating in time interval i, $P(i)$ is given by

$$P(i) = \Pr(U_1^C \geq U_1^S \cap U_2^C \geq U_2^S \cap \ldots. U_{i-1}^C \geq U_{i-1}^S \cap U_i^S \geq U_i^C) \tag{2.16}$$

$$= P(1)_{C/S} P(2)_{C/S} \ldots\ldots P(i-1)_{C/S} P(i)_{S/C} = P(i)_{S/C} \prod_{j=1}^{i-1} [1 - P(j)_{S/C}]$$

The sequential logit model captures the five main parameters that affect evacuation behavior as stated by Baker (Baker, 1991), namely the flood risk level (hazardousness) of the area, action by public authorities, type of housing, prior perception of personal risk, storm-specific threat factors. Using data collected after Hurricane Andrew in Southwestern Louisiana, the model was estimated on 85% of the data and then tested on the remaining 15% of the data. When the model was used to predict evacuation behavior on the 15% testing data set, it reproduced observed evacuation behavior with an

RMSE of 3.09 evacuations. Based on the results, it was concluded that a sequential logit model is capable of modeling dynamic evacuation demand satisfactorily.

While the above discussed behavioral models have their advantages, they also have limitations in terms in their applicability. Rayleigh distribution approach (Tweedie et al., 1986) only depends on the maximum mobilization time. With Tweedie's approach, the majority of the evacuation demand is mobilized during the first two hours of the total evacuation period which, is not a very realistic assumption given the empirical evidence obtained from various past-hurricane studies.

The sequential logit model (Fu and Wilmot, 2004) is constructed to impersonate a 3-day long evacuation, and detailed analysis show that the sequential model does not yield promising results for short time evacuations (e.g., 24 hours) (Ozbay et al., 2006). The model also needs detailed household specific data, like flood risk, being mobile or not etc., because the evacuation decision for each individual household is treated separately according to the housing characteristics which makes its implementation difficult for a large population since a separate Monte Carlo simulation is needed to generate evacuation probabilities for each household.

On the other hand Behavioral response curves (Sigmoid or S-Curves) have a longer history than the sequential logit model and require considerably less site-specific data compared to sequential logit model (e.g., need only two parameters namely, half loading time and response rate which, could be obtained from past evacuation data).As a result, this research will employ the behavioral response curves to model evacuee behavior.

2.7 Summary

Although some previous studies provided the groundwork for the investigation of staged evacuation (Chen and Zhan, 2004; Sbyati and Mahmmasani, 2006; Liu et al., 2006), it was found that information on impact analysis of simultaneous and staged evacuation is still limited. This research will incorporate some of the important issues that have not been thoroughly focused in past studies including the role of critical parameters (speed, density, access flow) on evacuation time, reduction in capacity of evacuation routes due to congestion, demand loading patterns, variation in demand distributions, capacity utilization of evacuation route, etc. The impact of availability of excess capacity (e.g., contraflow) on staged evacuation will also be examined.

After a comprehensive review of existing speed-flow-density models, the Edie's model was chosen to determine the speed-density relationship of an evacuation route in the proposed model. Also, this research will employ the Akçelik's model to estimate speeds under congested conditions.

A review of various existing behavioral models was conducted and the Behavioral response curves (Sigmoid or S-Curves) model was selected to model evacuees' behavior. The Behavioral response curves model has a longer history than the sequential logit model and requires considerably less site-specific data compared to other models. The model developed in this dissertation will determine the optimal staging scheme based on demand distribution, behavioral response, and predicted evolution of traffic conditions on the evacuation routes.

CHAPTER 3

DEVELOPMENT OF BASE MODELS FOR EVACUATION TIME AND DELAY

The model developed in this chapter will help to determine the time and delay for both simultaneous and multi-staged evacuation. The models formulated here, called base models, are evacuation time and delay, which will be minimized numerically by optimizing the decision variables including the number and sizes of staged zones. The analysis of evacuation time and delay discussed here, under a general and simplified setting, provides an approach for developing guidelines for decision making during the evacuation process.

3.1 Model Formulation

This section focuses on formulating evacuation time and delay for a region with one evacuation route under a general and simplified setting. The following assumptions are made to formulate the problem:

1. The number of vehicles to be evacuated denoted as Q, in the studied region shown in Figure 3.1 is uniformly distributed over the evacuation route. Demand density, denoted as $\overline{Q}$, is Q divided by evacuation route length, denoted as L, from S to E.

2. The number of staged zones is denoted as N, whose lengths (x) are assumed to be identical and equal to $\frac{L}{N}$. The accumulated flow increases as distance increases, before reaching the maximum discharge rate, i.e., the accumulated flow at the end of a staged zone of length x is qx, where q is the access flow rate per mile. See Figure 3.2.

3. Full compliance of residents to evacuation orders is assumed (deterministic behavior).

x = Length of a staged zone (miles)
u_x = Speed of vehicles from staged zone on evacuation route (mph)
k_x = Density of vehicles from staged zone on evacuation route (vpm)

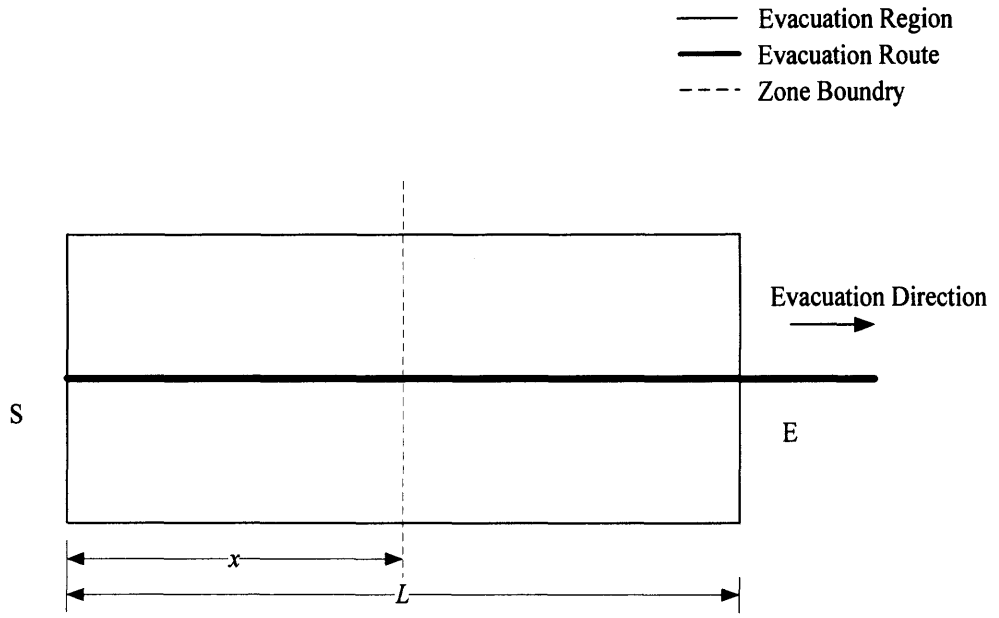

Figure 3.1 Configuration of the studied area.

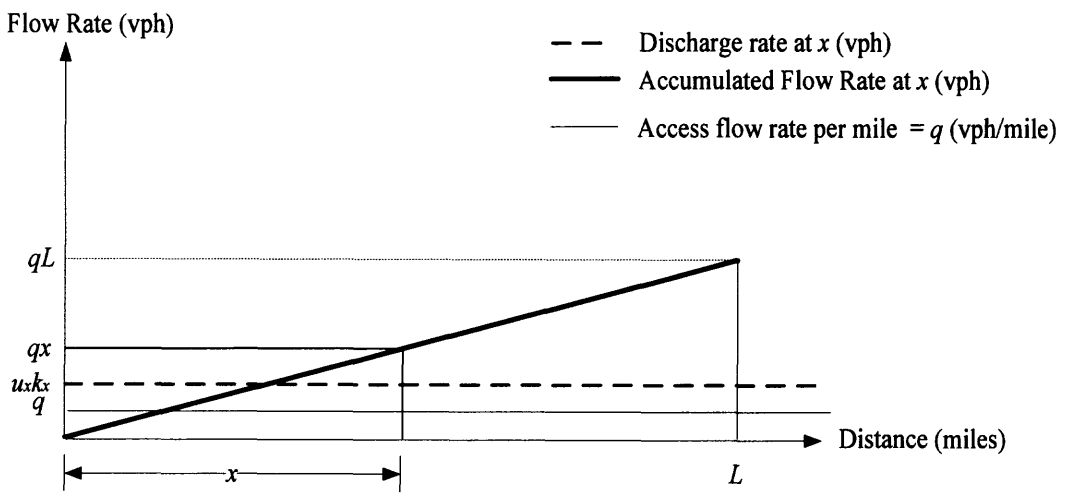

Figure 3.2 Flow rate vs. location of the evacuation route.

All the above assumptions can be relaxed to enhance the developed model to be applicable in a more realistic setting. For instance, the demand distribution discussed in assumption 1 may be replaced by actual one if data are available. Assumption 2 might be adapted to have staged zones with different lengths based on the relaxation of assumption 1. Assumption 3 will not hold in most of the cases as evacuee behavior is difficult to predict, which would certainly impact the results of analysis. However, assumption 3 can be relaxed by approximating an actual demand-loading function derived from field data.

The objective is to optimize the number of staged zones that minimizes evacuation time and the associated delay. The evacuation time is defined as the sum of three components: (1) discharge time at an achievable rate, (2) the average transit time for vehicles traveling on the evacuation route, and (3) staging time, also called preparatory time, between subsequent zones. Evacuation delay comprises of two components: (1) queuing delay incurred by evacuees accessing the evacuation route and (2) moving delay while traversing the evacuation route.

3.2 Evacuation Time Estimation

Figure 3.3 shows staged evacuation zones of the studied area with uniform demand distribution. The total evacuation time denoted as T_E is

$$T_E = T_D + T_R + T_S \tag{3.1}$$

where T_D, T_R, and T_S represent discharge time, the transit time, and staging time respectively.

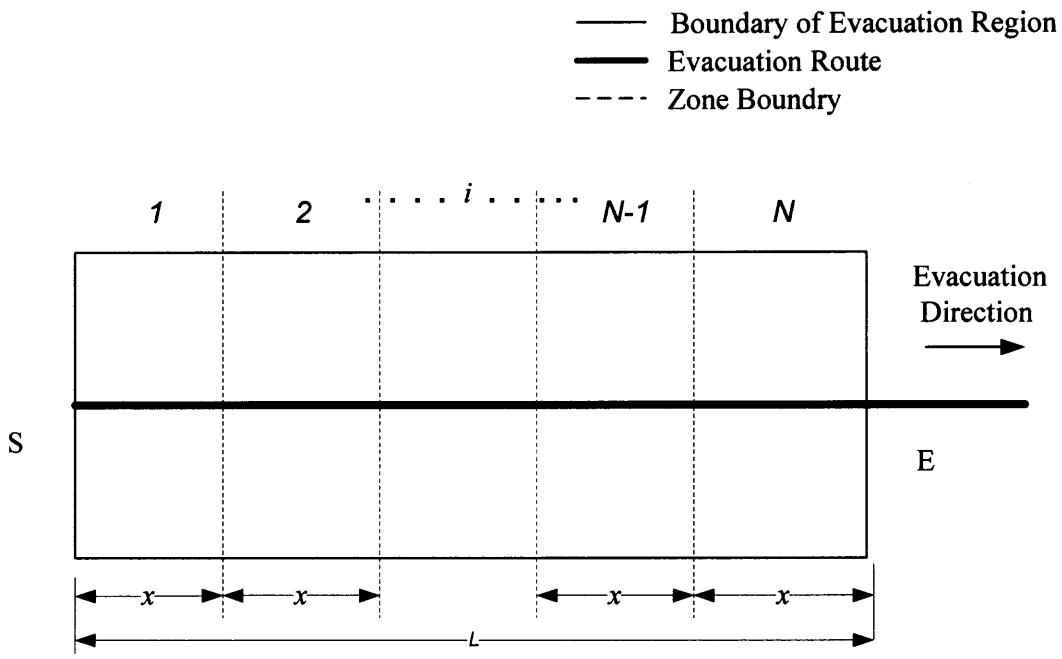

Figure 3.3 Configuration of staged evacuation.

3.2.1 Discharge Time (T_D)

Discharge rate of an evacuation route is determined by the speed-density relationship of the Edie's discontinuous exponential model, which applies the Greenberg's model for congested regime, for example $k_x > 50$ vehicles per mile, (vpm), such that

$$u_x = u_c \ln\left(\frac{k_j}{k_x}\right) \tag{3.2}$$

and the Underwood's model for uncongested regime, for example $k_x \leq 50\text{vpm}$, expressed as

$$u_x = u_f e^{\left(\frac{-k_x}{k_c}\right)} \tag{3.3}$$

for vehicles originating from a staged zone where

u_x = average travel speed

k_x = average density

u_c = critical speed (speed at maximum discharge rate)

k_c = critical density (density at maximum discharge rate)

u_f = free-flow speed (speed achieved under very low density)

k_j = jam density (maximum density at which all vehicles are stopped)

The Edie's model describes the entire range of speeds and densities. A congested flow condition occurs when the accumulated flow from a staged zone (qx) exceeds capacity, c and the corresponding density reaches 80-100 vpm (HCM, 2000). While, it is best to work with sets of roadway data in which all three variables have been measured and no estimation is needed, the Edie's model is used as an alternative here to determine the speed-density relationship and the corresponding discharge rate of the evacuation route due to the absence of evacuation traffic data (speed, density and flow). Thus, a density of 100 vpm is assumed for congested conditions in the numerical example discussed later. Note that, data obtained during evacuations could be used to calibrate the flow-density relationships under congested flow conditions in order to achieve more accurate estimation of discharge rates.

Capacity is defined as the maximum discharge rate that can be achieved under prevailing roadway conditions (Roess et al., 1998). The discharge rate for each staged zone with a length of x is the product of flow density k_x and its corresponding speed u_x. Thus,

$$qx = u_x k_x, \text{ if } qx \leq c \tag{3.4}$$

According to the Underwood's model

$$qx = u_f e^{\left(\frac{-k_x}{k_c}\right)} k_x \tag{3.5}$$

k_x can be obtained from Equation 3.5 and u_x can then be obtained by substituting k_x into Equation 3.3. The maximum discharge rate, c is formulated as

$$c = \frac{k_c u_f}{e} \tag{3.6}$$

The required discharge time for vehicles in a staged zone is

$$t_D = \frac{\bar{Q}x}{u_x k_x} \tag{3.7}$$

where $\bar{Q}x$ represents the number of vehicles to be evacuated per zone. Thus, the discharge time for an N-stage evacuation is

$$T_D = \frac{N\bar{Q}x}{u_x k_x} \tag{3.8}$$

Since $xN = L$ and $\bar{Q} = \frac{Q}{L}$, T_D can be derived as

$$T_D = \frac{Q}{u_x k_x} \tag{3.9}$$

3.2.2 Transit time (T_R)

The transit time for a staged zone denoted as t_R is the average vehicle travel time from the zone to the end of the evacuation route shown in Figure 3.3. t_R can be formulated as

$$t_R = \frac{\left(N - i + \frac{1}{2}\right)x}{u_x} \tag{3.10}$$

where $\left(N - i + \frac{1}{2}\right)x$ is the average distance traversed by vehicles from zone i on the evacuation route. u_x can be obtained from Equation 3.3. Note that the average distance traveled considered in Equation 3.10 is based on assumption 1, and can vary depending of the demand distribution of the evacuation region. Thus, the average transit time for an N-stage evacuation is

$$T_R = \frac{\sum_{i=1}^{N}\left(N - i + \frac{1}{2}\right)x}{N}\left(\frac{1}{u_x}\right) \tag{3.11}$$

3.2.3 Staging time (T_S)

Staging time is the preparatory time required between subsequent evacuation stages to clear barricades or initiate appropriate traffic flow. It is assumed to increase linearly with the number of zones

$$T_S = (N-1)t_s \tag{3.12}$$

where t_s is the staging time per staged zone.

According to the discharge time, transit time, and staging time derived in Equations. 3.9, 3.11 and 3.12, evacuation time denoted as T_E is

$$T_E = \frac{Q}{u_x k_x} + \frac{\sum_{i=1}^{N}\left(N - i + \frac{1}{2}\right)x}{N}\left(\frac{1}{u_x}\right) + (N-1)t_s \tag{3.13}$$

Since $xN = L$

$$T_E = \frac{Q}{u_x k_x} + \frac{\sum_{i=1}^{N}\left(N - i + \frac{1}{2}\right)L}{u_x N^2} + (N-1)t_s \tag{3.14}$$

By substituting for u_x from Equations 3.3 and 3.2, respectively into Equation 3.14, the required evacuation times under free-flow and congested regimes can be approximated using Equations. 3.15 and 3.16, respectively.

$$T_E = \frac{Q}{u_f e^{\left(\frac{-k_x}{k_c}\right)} k_x} + \frac{\sum_{i=1}^{N}\left(N - i + \frac{1}{2}\right)L}{u_f e^{\left(\frac{-k_x}{k_c}\right)} N^2} + (N-1)t_s \quad \text{if } qx \le c \tag{3.15}$$

$$T_E = \frac{Q}{u_c \ln\left(\frac{k_j}{k_x}\right) k_x} + \frac{\sum_{i=1}^{N}\left(N - i + \frac{1}{2}\right)L}{u_c \ln\left(\frac{k_j}{k_x}\right) N^2} + (N-1)t_s \quad \text{if } qx > c \tag{3.16}$$

3.3 Delay Estimation

Delay discussed here consists of queuing delay incurred by vehicles accessing the evacuation route and moving delay as vehicles transit the route. The queuing delay is computed based on queue length in each staged zone and the accumulated flow rate, while the moving delay is based on the difference of vehicle travel times under free-flow and congested conditions.

3.3.1 Queuing Delay (D_Q)

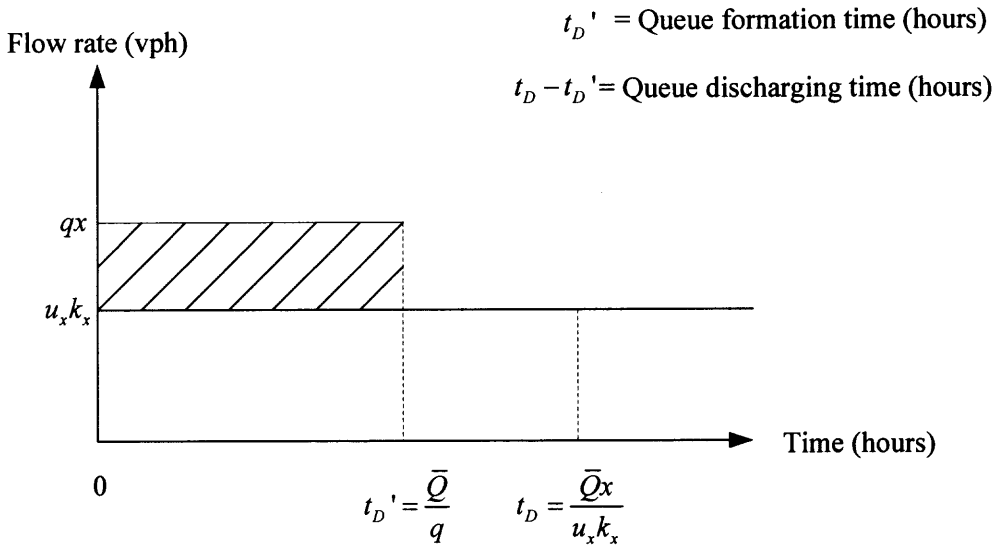

Figure 3.4 Flow rate vs. time.

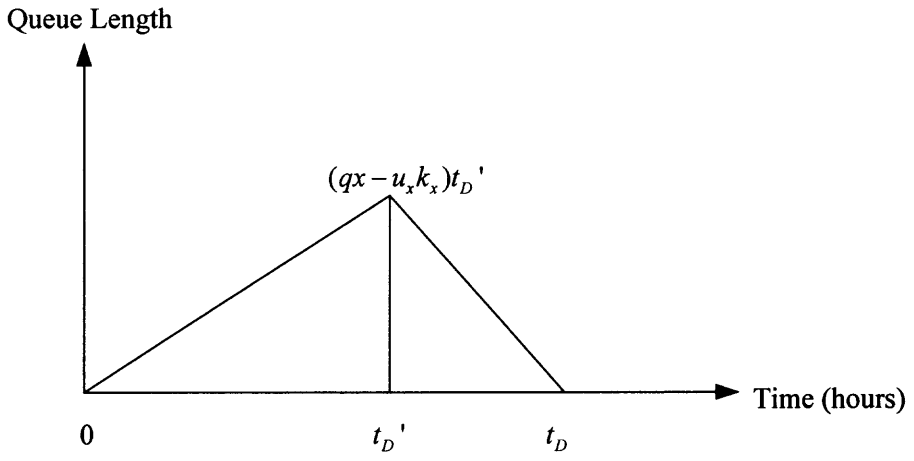

Figure 3.5 Queue length vs. time.

According to assumption 2, the accumulated flow rate at the end of a staged zone is qx. Queuing delay occurs when qx is greater than the discharge rate $u_x k_x$. Figure 3.4 shows that the discharge time is determined by the accumulated flow rate and discharge rate,

where the queue formation time t_D' is $\bar{Q}x$ divided by qx. Thus,

$$t_D' = \frac{\bar{Q}x}{qx} \tag{3.17}$$

However, if t_D' is not realized (i.e., if all vehicles in the staged zone are not discharged in t_D') owing to $u_x k_x < qx$, a queue is formed. Consequently, the queue length n_q at time t_D' is

$$n_q = (qx - u_x k_x) t_D' \tag{3.18}$$

As shown in Figure 3.5, the queue is fully discharged at time t_D, and the queuing delay denoted as d_q for a staged zone is

$$d_q = \frac{1}{2} t_D n_q \tag{3.19}$$

By substituting for t_D, t_D' and n_q, from Equations. 3.7, 3.17 and 3.18, respectively in Equation 3.19, the queuing delay for an *N*- stage evacuation

$$D_Q = \frac{N\bar{Q}^2 x}{2qu_x k_x}(qx - u_x k_x) \tag{3.20}$$

Since $xN = L$, and $\bar{Q} = \frac{Q}{L}$, D_Q is derived as

$$D_Q = \frac{Q^2}{2Lqu_x k_x}\left[\frac{qL}{N} - u_x k_x\right] \tag{3.21}$$

3.3.2 Moving Delay (D_M)

The moving delay is defined as the difference between average travel times at the operating speed u_x and the free-flow speed u_f.For instance, the moving delay for vehicles originating from a staged zone i is given by d_{mi} (See Figure 3.3), such that

$$d_{mi} = \left(\frac{\left(N - i + \frac{1}{2}\right)x}{u_x} - \frac{\left(N - i + \frac{1}{2}\right)x}{u_f} \right) \bar{Q}x \qquad \forall i \in N \tag{3.22}$$

where $\left(N - i + \frac{1}{2}\right)x$ is the average distance traversed by vehicles from zone i on the evacuation route. Thus, the moving delay for an N-stage evacuation is

$$D_M = \sum_{i=1}^{N} \left(N - i + \frac{1}{2}\right) \bar{Q}x^2 \left(\frac{1}{u_x} - \frac{1}{u_f} \right) \tag{3.23}$$

Since $xN = L$ and $\bar{Q} = \frac{Q}{L}$, D_M is

$$D_M = \sum_{i=1}^{N} \left(N - i + \frac{1}{2}\right) \frac{QL}{N^2} \left(\frac{1}{u_x} - \frac{1}{u_f} \right) \tag{3.24}$$

The total delay, D_T defined here is the sum of D_Q and D_M. Thus,

$$D_T = \frac{Q^2}{2Lqu_xk_x} \left[\frac{qL}{N} - u_xk_x \right] + \sum_{i=1}^{N} \left(N - i + \frac{1}{2}\right) \frac{QL}{N^2} \left(\frac{1}{u_x} - \frac{1}{u_f} \right) \tag{3.25}$$

By substituting for u_x from Equation 3.3 and 3.2, respectively into Equation 3.25, the total delays under free-flow and congested regimes are derived as Equations. 3.26 and 3.27, respectively.

$$D_T = \frac{Q^2\left[\frac{qL}{N} - u_f k_x e^{\left(\frac{-k_x}{k_c}\right)}\right]}{2Lu_f q k_x e^{\left(\frac{-k_x}{k_c}\right)}} + \sum_{i=1}^{N}\left(N - i + \frac{1}{2}\right)\frac{QL}{N^2}\left(\frac{1}{u_f e^{\left(\frac{-k_x}{k_c}\right)}} - \frac{1}{u_f}\right) \text{ if } qx \le c \qquad (3.26)$$

$$D_T = \frac{Q^2\left[\frac{qL}{N} - u_c k_x \ln\left(\frac{k_j}{k_x}\right)\right]}{2Lqu_c k_x \ln\left(\frac{k_j}{k_x}\right)} + \sum_{i=1}^{N}\left(N - i + \frac{1}{2}\right)\frac{QL}{N^2}\left(\frac{1}{u_c \ln\left(\frac{k_j}{k_x}\right)} - \frac{1}{u_f}\right) \text{ if } qx > c \qquad (3.27)$$

3.4 Numerical Example

The objective of this example is to demonstrate the applicability of the model developed in this chapter in determining the optimal number of staged zones that minimizes evacuation time and delay. The tradeoffs between the evacuation time and delay for both simultaneous and staged evacuations are investigated. The length of each staged zone is determined by dividing the length of the evacuation region by the number of stages. Equations 3.15, 3.16, and 3.26, 3.27 are applied to compute the evacuation time and associated delays of the studied evacuation region for both free-flow and congested regimes.

In this numerical example, the optimal staging for of a given evacuation region with a length of 15 miles, similar to Figure 3.3 is analyzed. The evacuation demand is assumed to be 20,000 vehicles and is uniformly distributed over the studied route. The access flow rate, q is assumed to be 350 vph per mile. The maximum discharge rate on

the evacuation route, c is 2,000 vph. These values are intended to demonstrate the application of this model rather than to represent any specific case.

3.4.1 Results and Discussion

Figure 3.6 shows the estimated evacuation time at various number of staged zones for the base case (L = 15 miles, q = 350 vph, Q = 20,000 vehicles) without considering staging time between zones. The evacuation time is a convex curve, and yields a minimum solution at N=3.

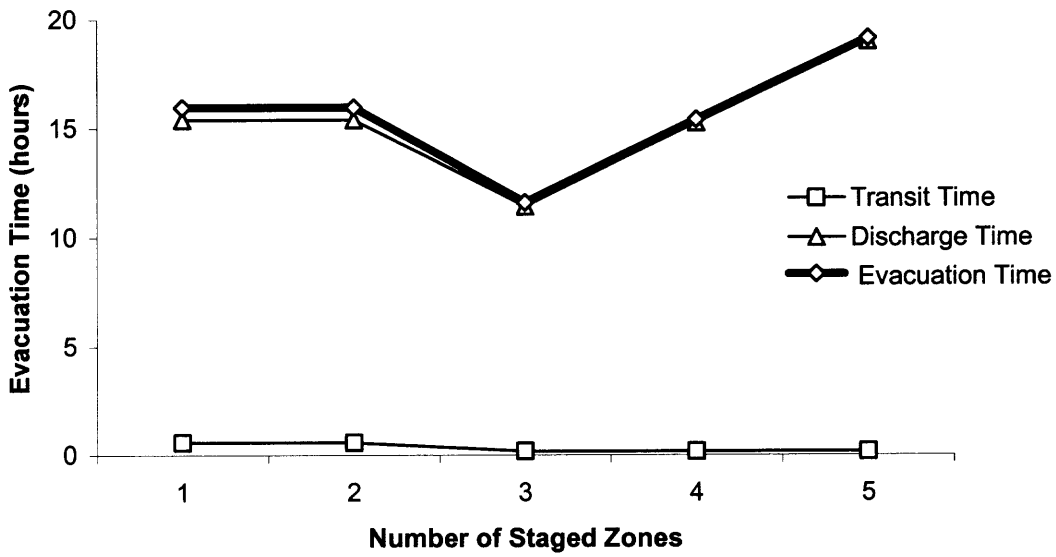

Figure 3.6 Evacuation time vs. number of staged zones (without staging time).

The evacuation time is primarily influenced by the discharge time depending on the flow rate on the evacuation route. Either simultaneous evacuation (N = 1) or a 2-stage evacuation (N = 2) causes congestion on the evacuation route due to the accumulated flow rate rising beyond the available capacity. This results in jam densities and considerably reduces the speed on the route. Thus, the discharge rate obtained under these conditions (N = 1 or 2) is less than the discharge rate for N = 3 (1,750 vph).

However if $N > 3$, evacuation time increases because of reduced discharge rates (at lower densities with higher speeds). Although, transit time decreases as the number of staged zones increases due to higher speeds (45 to 50 mph), it is less than the increase in discharge time and does not significantly help to reduce the evacuation time.

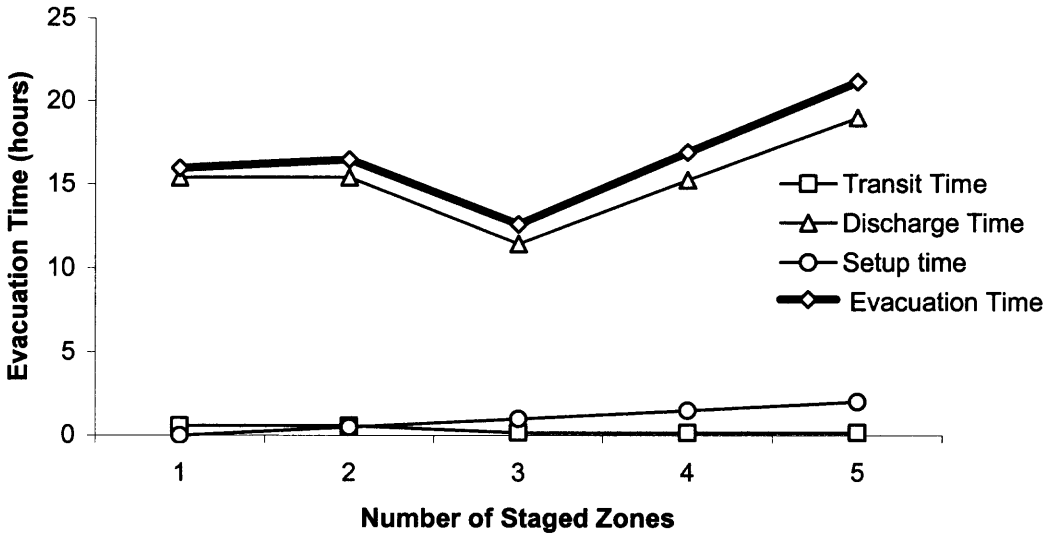

Figure 3.7 Evacuation time vs. number of staged zones (with staging time).

Figure 3.7 shows the estimated evacuation time at various number of staged zones for the base case (L = 15 miles, q = 350 vph, Q = 20,000 vehicles) by considering staging time between stages (t_s = 0.5 hour). Although the evacuation time increases for zones 2 to 5, when compared with the previous case (Figure 3.6), the evacuation time is still minimum at N=3.

Figure 3.8 shows delays at various values of N. The moving delay on the evacuation route primarily depends on the speed of the evacuating vehicles. This speed is 13 mph when $N \leq 2$ is employed. Consequently, the time taken for vehicles traversing

the evacuation route increases as N decreases. Queuing delay is mainly influenced by the queue length over time (from 0 to t_D' as shown in Figure 3.5).

The queue length for simultaneous evacuation is significantly higher than that of a multi-staged evacuation, due to a greater difference between the access and discharge rates. As a result, the queuing delay is the highest under simultaneous evacuation, and it decreases as N increases. The queuing delay is zero if qx is less than $u_x k_x$.

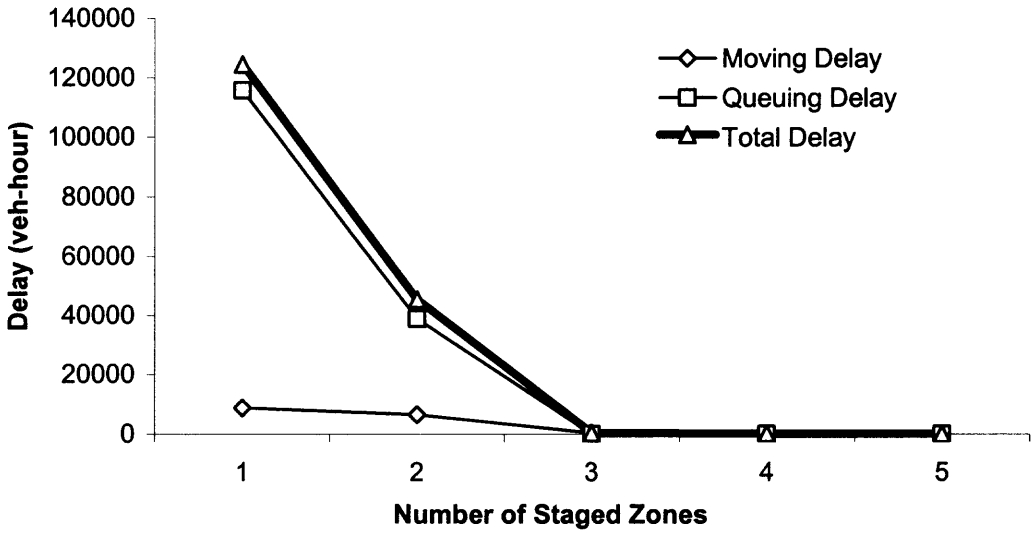

Figure 3.8 Delay vs. number of staged zones.

In this regard, based on the urgency of the evacuation, the decision of a simultaneous or multi-staged evacuation could be undertaken. For instance, evacuations for predictable events (e.g., hurricanes) allow a relatively longer preparatory time to evacuate people and goods from the areas under threat. Therefore, using multi-staged evacuation reduces delay but at increased evacuation time. In contrast to this, for evacuations that do not allow much flexibility in time (e.g., terrorist attacks, and nuclear

plant disasters) the evacuation strategy that yields the minimum evacuation time is recommended.

3.4.2 Sensitivity Analysis

Results of sensitivity analysis are discussed here to illustrate the relations among variables and identify the relative importance of factors that contribute to them. The parameters that are considered to be most sensitive to the evacuation time and delay are access flow rate q, demand Q, and the evacuation route length L.

Figure 3.9 illustrates the variation in T_E at varying q (L =15 miles, Q = 20,000 vehicles). The number of staged zones at which, the total evacuation time is minimum, increases while q increases.

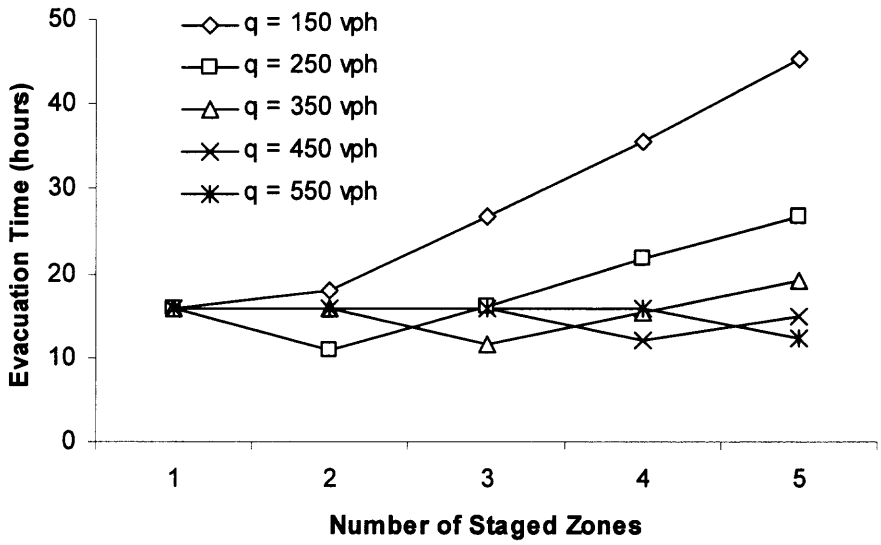

Figure 3.9 Evacuation time vs. number of staged zones for various flow rates (L =15 miles, Q = 20,000 vehicles).

As access rate reduces (e.g., q = 150 vph), simultaneous evacuation is preferred as it yields the minimum evacuation time although congested conditions prevail $(qx > c)$. This is because, the achievable discharge rate for simultaneous evacuation at q = 150 ($u_x k_x$=1,300 vph) is greater than the discharge rates attained for non-congested conditions at higher values of N. But, as q increases, (e.g., q = 450 vph), higher discharge rates are attained at higher values of N, thereby increasing the number of staged zones at which evacuation time is minimum (e.g., N = 4 gives least T_E for q = 450 vph).

Figure 3.10 demonstrates the variation in total delay D_T, with variation in q (L =15 miles, Q = 20,000 vehicles).

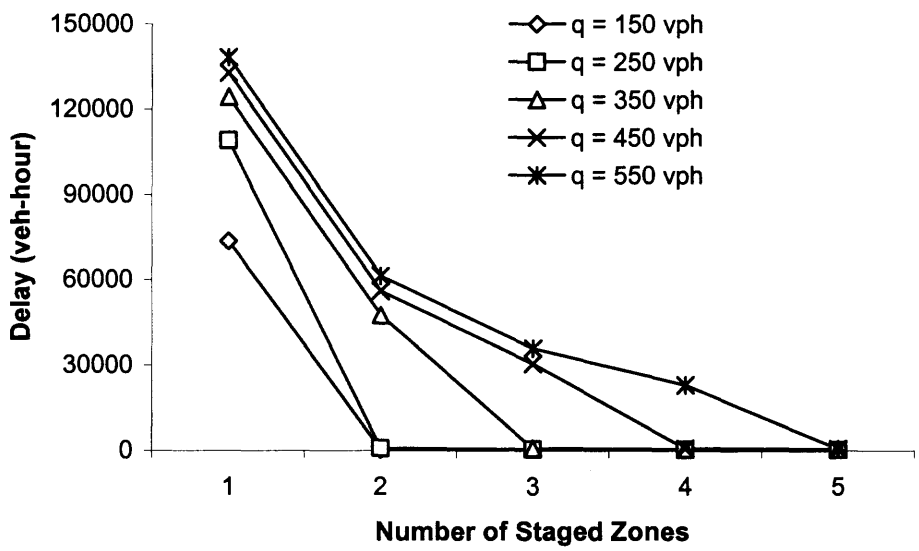

Figure 3.10 Total delay vs. number of staged zones for various flow rates (L =15 miles, Q = 20,000 vehicles).

D_T decreases as N increases at all values of q. For a particular N, D_T increases while q increases, primarily due to an increase in the queuing delay caused by a large difference between the access flow rate and discharge rates on the evacuation route. The

moving delay of the evacuation route also increases with increase in q for any N due to reduction in average speed.

Figure 3.11 shows the variation in T_E for varying Q (L =15 miles, q = 350 vph). The variation in demand is an indicative of variation in demand density for a given region. Although, the evacuation time increases with increase in demand for any N, the minimum evacuation time is yielded by N =3 for all values of Q under the current setup. Since the discharge flow rate on the evacuation route does not change at varying demand for any N, the only factor causing increase in evacuation time is demand (Q) itself. This suggests that staging of evacuation could be applied to areas of both low and high densities, but the time savings are more pronounced at higher densities.

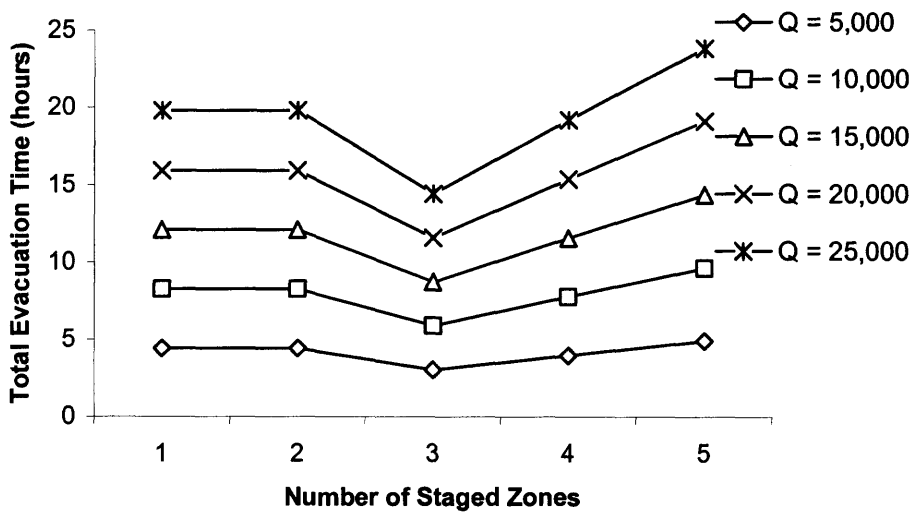

Figure 3.11 Evacuation time vs. number of staged zones for various demands (L =15 miles, q = 350 vph).

Figure 3.12 shows the total delay D_T with variation in Q (L =15 miles, q = 350 vph). D_T decreases as N increases at all values of Q. Also, D_T increases as Q increases for any value of N, due to an increase in volume entering the route from the staged zones.

However, increase in delay at higher values of N (e.g., N = 5) is only due to the occurrence of moving delay as discharge rates attained are less than capacity $(qx < c)$, which results in no queues.

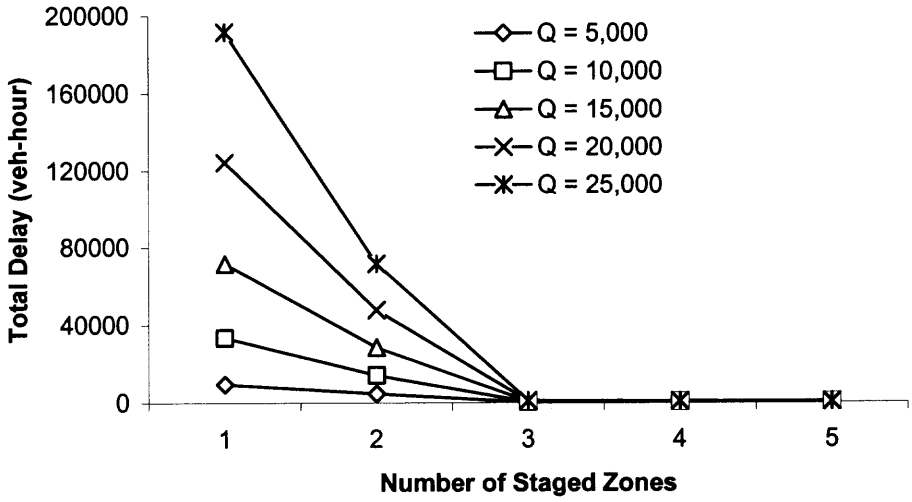

Figure 3.12 Total delay vs. number of staged zones for various demands (L =15 miles, q = 350 vph).

Figure 3.13 shows variation of T_E with L (q = 350 vph, Q = 20,000 vehicles). Here, demand of the evacuation region is assumed to vary proportionally with the length of the evacuation route at a constant demand density of $\bar{Q}$. This analysis helps in determining evacuation scenarios for affected areas of various sizes. The optimal number of stages at which, the evacuation time is minimum, increases as L increases. For a short L (e.g., L =5 miles), the minimum evacuation time is when N =1 (simultaneous evacuation), and staging does not further reduce evacuation time. However, as L increases, congested conditions prevail at lower values of N, thereby reducing the discharge rates, which increases evacuation time. Thus, the minimum evacuation time is achieved by increasing N for higher L. Figure 3.14 illustrates the variation of total

delay D_T with variation in L (q = 350 vph, Q = 20,000 vehicles). D_T decreases as N increases at all values of L. Both queuing and moving delays increase while L increases.

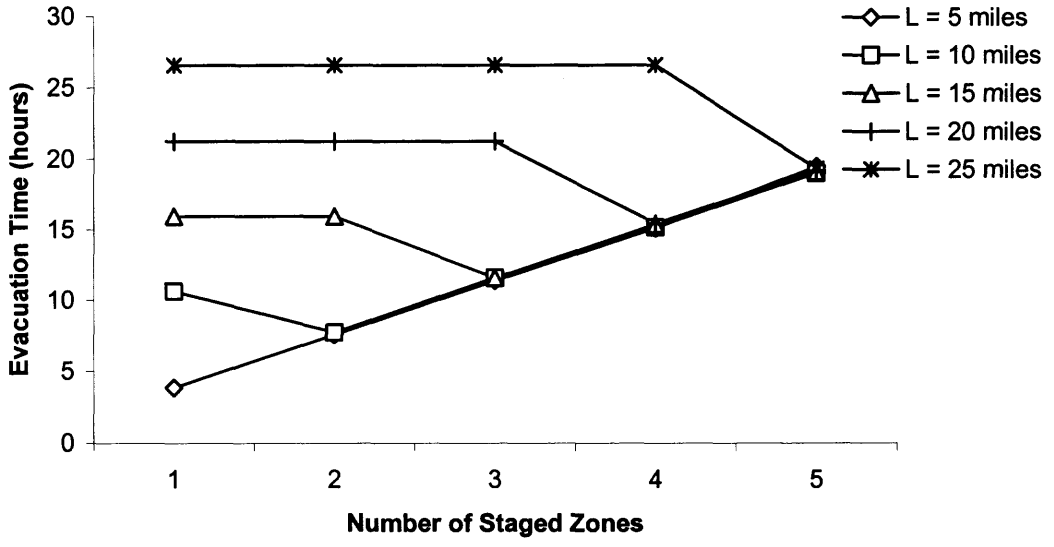

Figure 3.13 Evacuation time vs. number of staged zones for various lengths of evacuation route (q = 350 vph, Q = 20,000 vehicles).

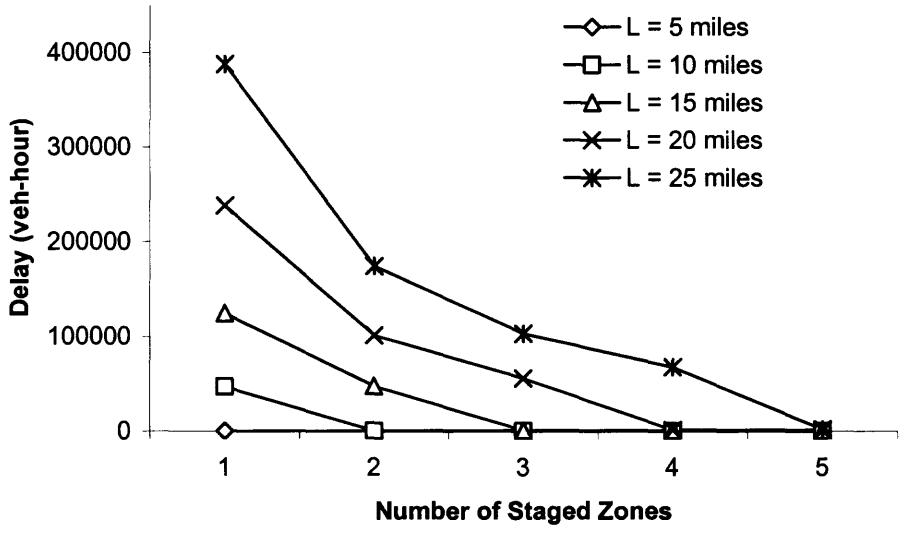

Figure 3.14 Total delay vs. number of staged zones for various lengths of evacuation route (q = 350 vph, Q = 20,000 vehicles).

3.5 Summary

In this chapter base models were developed for estimation of evacuation time and delays. Two strategies namely, simultaneous and staged evacuations were tested. Evacuation time is the duration required for evacuating all vehicles from a designated region, while delay includes queuing and moving delays. The relationship between delay and evacuation time is investigated, and the impact of staged evacuation against simultaneous evacuation is analyzed. An example is provided to demonstrate the applicability of the developed model. A numerical method is adopted to determine the optimal number of staged zones. Sensitivity analysis of parameters (e.g., demand density, access flow rate, and evacuation route length) affecting evacuation time and delay is conducted. Results indicate that evacuation time and delay can be significantly reduced if staged evacuation is appropriately implemented. The base model is limited in functionality and follows the assumptions discussed in section 3.1. However, in Chapter 4 the model is enhanced to incorporate behavioral response of evacuees' to evacuation order, and variation in demand distribution pattern.

CHAPTER 4

STAGING MODEL FOR STOCHASTIC AND HETEROGENEOUS DEMAND

By considering heterogeneous demand distribution over an evacuation region and behavioral responses of evacuees to evacuation orders (e.g., fast, medium, and slow), a more realistic model called Enhanced Model I is developed here by enhancing the base model discussed in Chapter 3, where uniform demand distribution and deterministic evacuee behavior were assumed. The optimal staging scheme that minimizes evacuation time and the associated delay is determined through a numerical search. This chapter is organized into the following sections: Section 4.1 discusses the formulation of temporal demand distribution due to various behavioral response curves, and spatial demand distribution along the evacuation route; Section 4.2 elaborates the development of the staging model that can handle the demand distributions formulated in Section 4.1; Section 4.3 presents a numerical example which demonstrates the applicability of the model developed in Section 4.2; Section 4.4 investigates the sensitivity of demand and capacity on evacuation time and delay; and finally, Section 4.4 presents a summary of Chapter 4.

4.1 Demand Distribution

The temporal and spatial demand distributions over the evacuation route play a critical role in the determination of the lengths of staged zones. In this section, the impacts of both demand distributions on evacuation time and delay are discussed.

4.1.1 Temporal Demand Distribution

The behavioral response of evacuees in complying with evacuation orders and network loading rates significantly affects evacuation time (Stern and Stern, 1989). Thus, a realistic model for evacuation time estimation should consider behavioral aspects such as responses to evacuation orders (e.g., slow, medium, or fast). Unlike the deterministic cases discussed in Chapter 3 where the demand was uniform and the access flow rate was constant during evacuation, the behavioral model developed here employs the S-shaped logit-based function formulated in Equation 4.1, which has been applied in previous studies (Hobeika and Jamei, 1985, U.S. Army Corps of Engineers, 1997, 1999, 2000, 2001) to determine the time varying demand accessing the evacuation route.

$$P(t) = \frac{1}{1 + e^{-\alpha(t-\beta)}} \tag{4.1}$$

where $P(t)$ is cumulative demand in percentage to be loaded at t, while α and β represent the slope factor and half loading time (at which half of the demand is loaded), respectively. Parameter α signifies the speed of evacuees' behavioral response. As α increases, for a given β (e.g., 12 hours), the response of evacuees is more concentrated near the half loading time as shown in Figures 4.1 and 4.2. A small value of α leads to a low response rate and more homogeneous loading of demand onto the evacuation route, and vice versa. For a given β, the time required for evacuating the majority of demand (e.g., 90%) decreases as α increases.

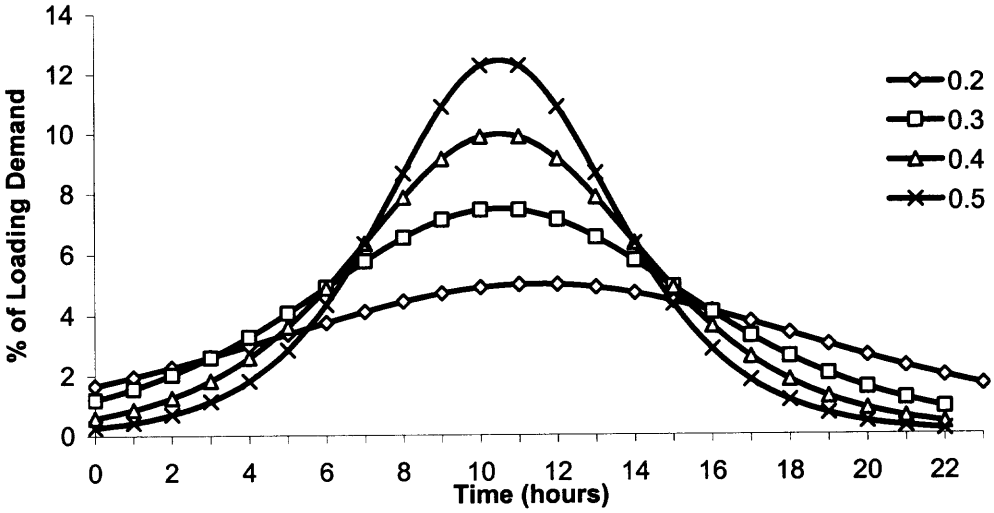

Figure 4.1 Percentage of demand loading vs. time for various α (β =12 hours).

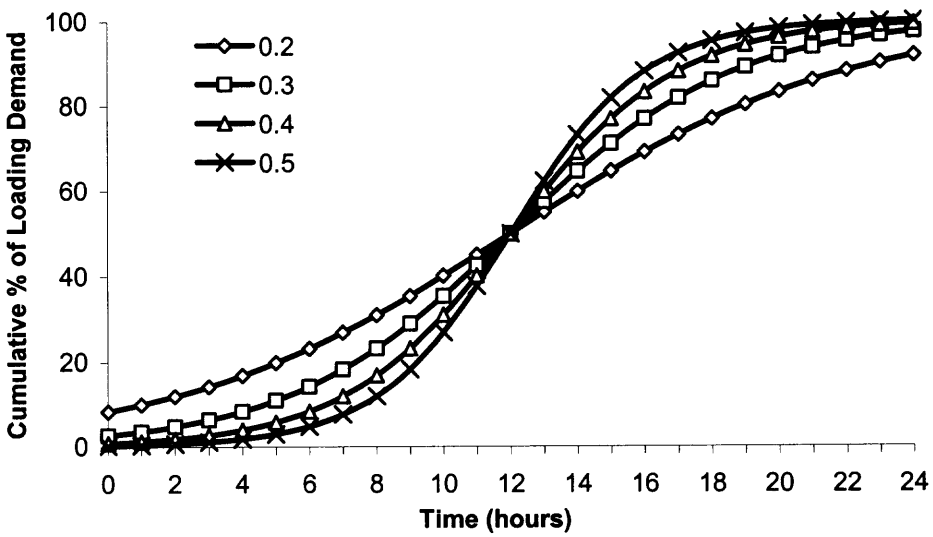

Figure 4.2 Cumulative demand vs. time for various α (β =12 hours).

In addition, as β increases for a given α, longer evacuation time should be expected due to increased demand loading time as shown in Figures 4.3 and 4.4.

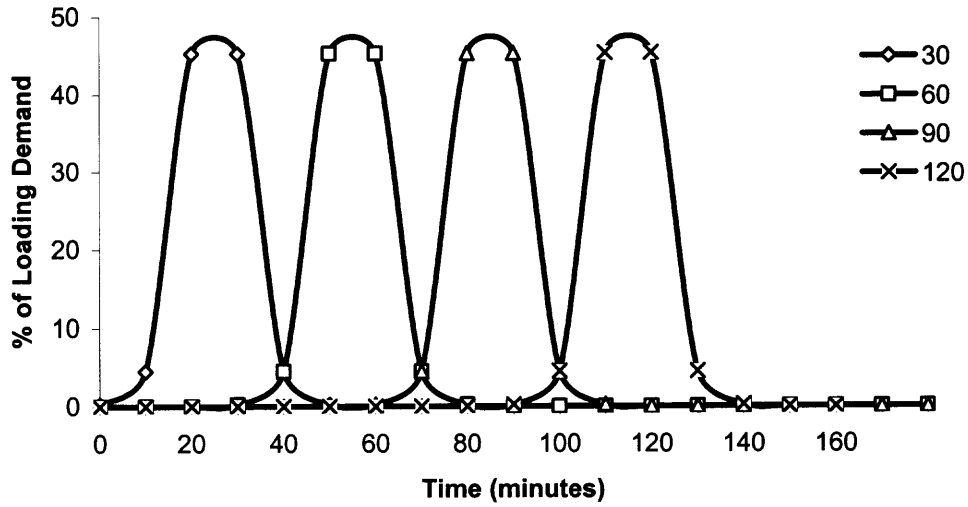

Figure 4.3 Percentage of demand loading vs. time for various β ($\alpha = 0.3$).

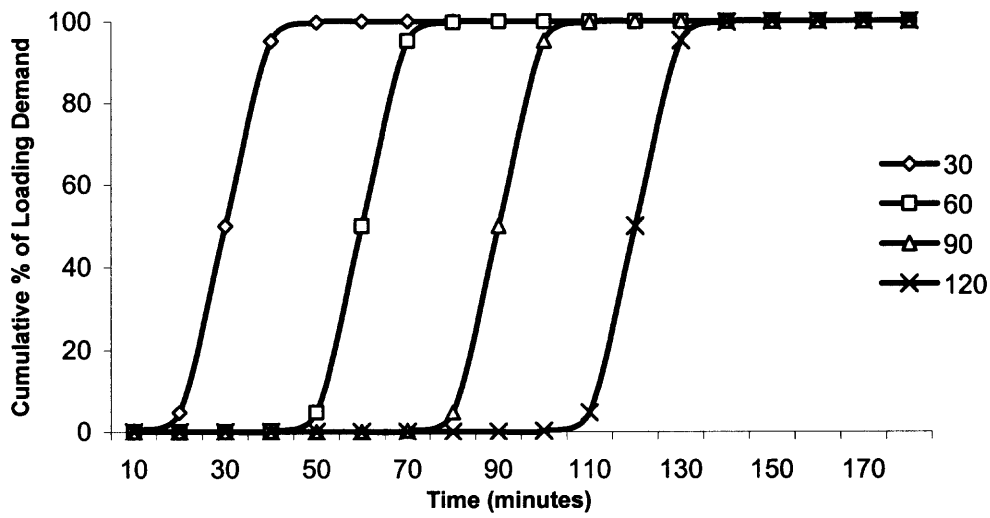

Figure 4.4 Cumulative demand vs. time for various β ($\alpha = 0.3$).

A certain proportion of demand (e.g., 10%) leaving before time 0 when evacuation orders are given, known as shadow demand denoted as Q_s, may be estimated for certain types of disasters (e.g., hurricanes) if historical data are available.

4.1.2 Spatial Demand Distribution

Similar to the temporal demand distribution, the spatial demand distribution plays a critical role in the determination of the staged zone lengths. The zone length decreases as the concentration of demand increases, and vice versa. Figure 4.5 illustrates a non-linear demand density function, denoted as $f(x)$. The total demand Q over the evacuation route from 0 to L can be derived as

$$Q = \int_0^L f(x)dx \tag{4.2}$$

where L represents the length of the evacuation route.

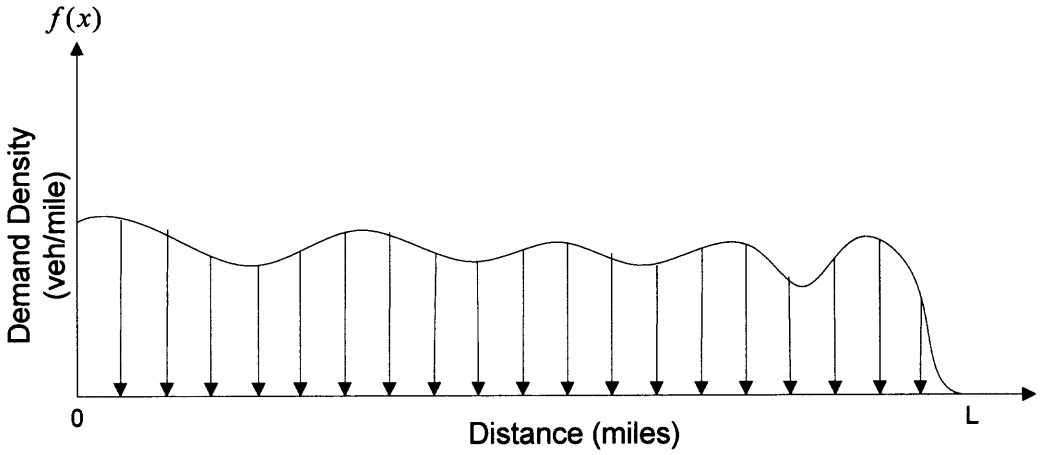

Figure 4.5 Demand density vs. distance.

4.2 Model Development

Unlike the base model discussed in Chapter 3 where the lengths of the staged zones are assumed identical, the model developed here optimizes staged zone lengths subject to the demand distribution, behavioral response of evacuees, and evolution of traffic conditions on the evacuation route. While the base model can handle uniform demand distribution

and assumes deterministic behavior of evacuees, the model developed here considers heterogeneous demand and stochastic behavioral responses (e.g., fast, medium, and slow) to evacuation orders. In addition, the access flow rate considered here is determined by the logit-based function formulated in Equation 4.1.

4.2.1 Model Formulation

The model developed here is applied to optimize the staging scheme for an evacuation, including the lengths and time-windows of staged zones based on prevailing circumstances (e.g., behavioral response, demand distribution, and evacuation route length, etc). This section discusses the formulation of evacuation time and the associated delay for a region as shown in Figure 4.6 with heterogeneous demand distribution that can be referred to Figure 4.5.

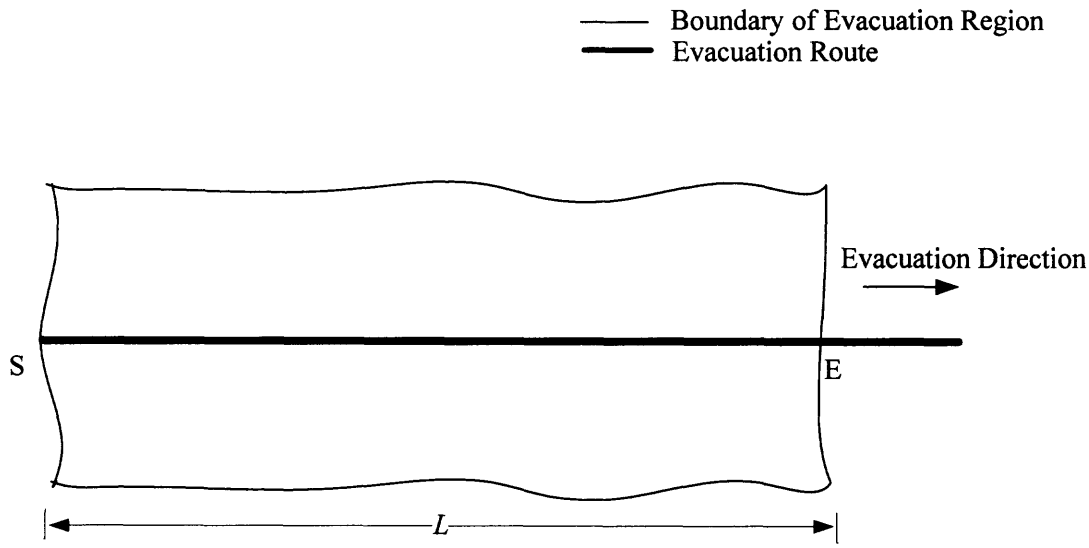

Figure 4.6 Configuration of the studied area.

4.2.2 Evacuation Time

In this section, a methodology that can minimize evacuation time through the optimization of the staging scheme is presented. A general configuration of staged zones for the evacuation region is shown in Figure 4.7, where N is the optimal number of staged zones to be determined, and L is the length of the evacuation route.

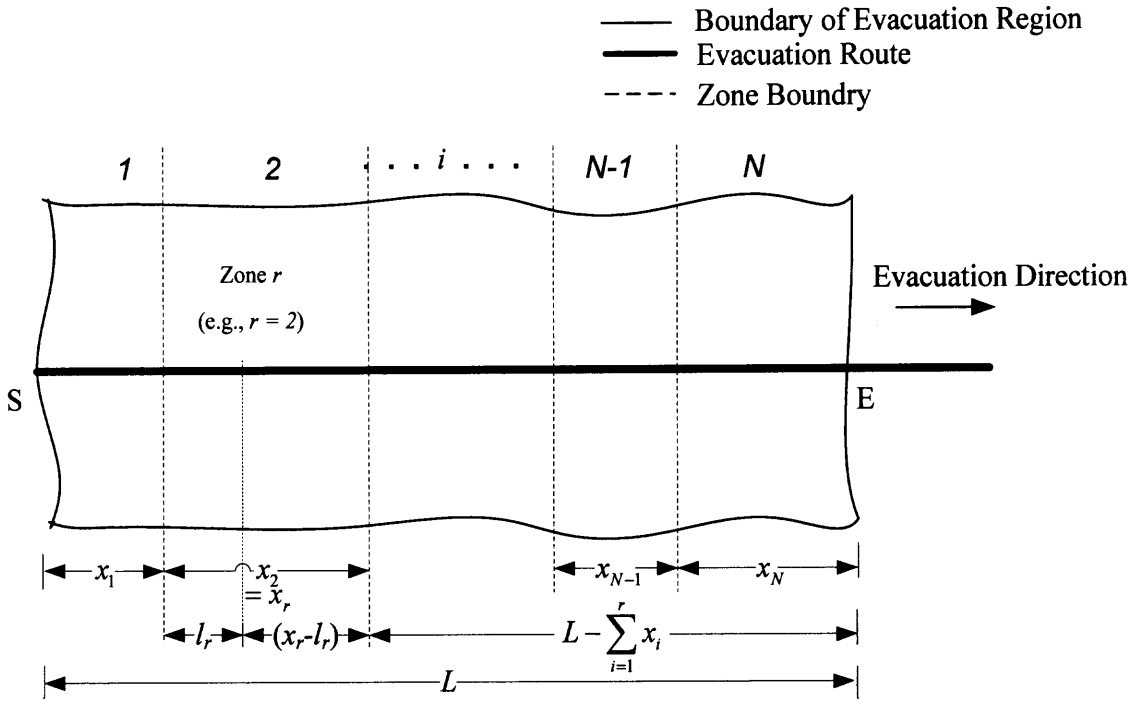

Figure 4.7 Configuration of a staged evacuation.

The methodology developed here can determine the optimal staging scheme by regulating the demand accessing the evacuation route. The time windows of staged zones may be overlapped with one another to effectively utilize available roadway capacity. The time window for a particular zone is the duration when the demand of the zone is loaded onto the evacuation route based on the loading curve defined by Equation 4.1.

Thus, the demand being evacuated while staging zone i at t may contain demand originating from previous zones.

4.2.2.1 Critical Measures for Optimal Staging Scheme. In order to determine the optimal staging scheme, several important parameters must be estimated, and are discussed below.

(1) Demand accessing the evacuation route while staging zone i at t ($Q_i^{(t)}$)

The demand accessing the evacuation route while staging zone i at t denoted as $Q_i^{(t)}$ based on the Equation 4.1, is

$$Q_i^{(t)} = \sum_{i=1}^{i} q_i^{(t)} Q_i \quad \forall i,t \tag{4.3}$$

where, $q_i^{(t)} = \left(\frac{1}{1+e^{-\alpha(t-\beta)}} - \frac{1}{1+e^{-\alpha(t-1-\beta)}} \right)$ is the percentage of demand accessing from zone i at t, $Q_i = \int_{\sum_{i=1}^{i-1} x_i}^{\sum_{i=1}^{i} x_i} f(x)dx$ is the demand of staged zone i, and x_i is the length of zone i. For example, the demand accessing the evacuation route while staging zone 1 at t is derived as $Q_1^{(t)} = q_1^{(t)} Q_1$.

(2) Demand to be evacuated while staging zone i at t ($\bar{Q}_i^{(t)}$)

The demand to be evacuated (i.e., vehicles on the evacuation route and access streets) while staging zone i at t denoted as $\bar{Q}_i^{(t)}$ is formulated as

$$\bar{Q}_i^{(t)} = Q_i^{(t)} + d_i^{(t-1)} \quad \forall i,t \tag{4.4}$$

where $d_i^{(t-1)}$ is queuing vehicles, accumulated form previous time interval $(t-1)$ while evacuating demand of zone *i* at *t*. As shown in Figure 4.8, the number of queuing vehicles at *t* denoted as $d_i^{(t)}$ is the difference between $\bar{Q}_i^{(t)}$ and the discharged volume at *t*, denoted as $Q_E^{(t)}$, while $d_i^{(t)}$ can obtained by interpolating the difference of $T_i^{(t)}$ and δ_t. Thus,

$$d_i^{(t)} = \frac{\left(T_i^{(t)} - \delta_t\right)\bar{Q}_i^{(t)}}{T_i^{(t)}} \qquad \forall i,t \tag{4.5}$$

where

$T_i^{(t)}$: evacuation time for $\bar{Q}_i^{(t)}$

δ_t: unit time interval (e.g., 1 hour)

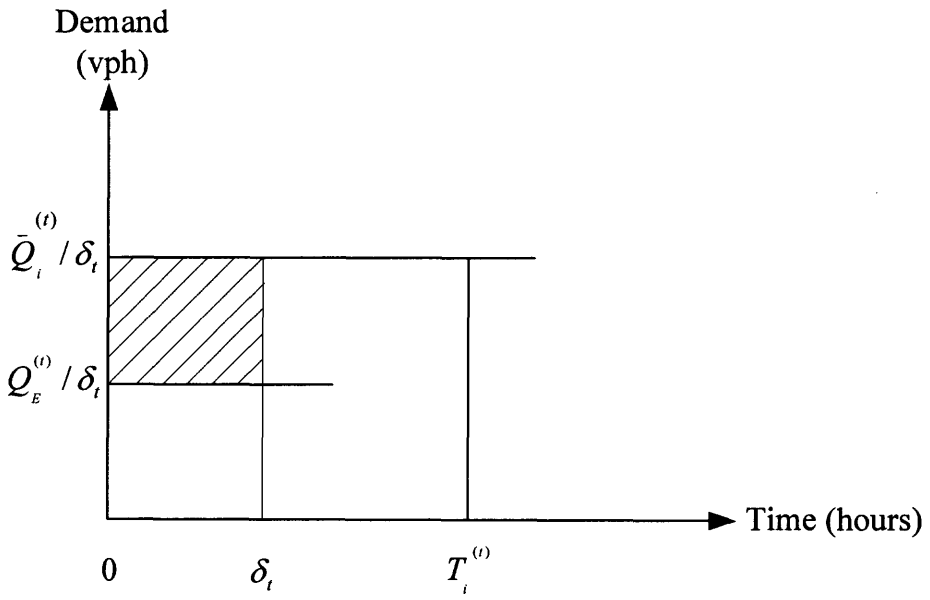

Figure 4.8 Queuing vehicles in a unit interval δ_t.

The estimation of evacuation time denoted as $T_i^{(t)}$ for $\bar{Q}_i^{(t)}$ under congested and uncongested conditions is discussed as follows. Note that the uncongested condition here refers to $\frac{\bar{Q}_i^{(t)}}{\delta_t} < c$, and congested condition refers to $\frac{\bar{Q}_i^{(t)}}{\delta_t} > c$, where $\frac{\bar{Q}_i^{(t)}}{\delta_t}$ and c are the demand at t and capacity of the evacuation route, respectively. Note that the evacuation time discussed here is used to compute the discharged volume at an interval and should not be confused with the total evacuation time discussed later.

(a) Uncongested condition ($\frac{\bar{Q}_i^{(t)}}{\delta_t} < c$)

Under uncongested condition, the evacuation time required for demand $\bar{Q}_i^{(t)}$ is denoted as $T_i^{(t)}$, which is the sum of the discharge time denoted as $t_{D_i}^{(t)}$, and the average travel time of vehicles traveling from zone r at t, denoted as $t_{R_i}^{(t)}$. Note that r is the zone closest to the beginning of the evacuation route from which demand accesses at t as shown in Figure 4.7, where r = 2 is shown as an example. In other words, when the demand of zone 1 is fully loaded onto the evacuation route, the next zone that is closest to the point S from which demand accesses the evacuation route is 2. Thus, the average travel distance is measured from zone 2. Similarly, r can vary over time from 1 to N based on the loading of the staged zones.

Note that $t_{D_i}^{(t)}$ is the ratio of the demand to be evacuated while staging zone i at t, denoted as $\bar{Q}_i^{(t)}$, and the achievable discharge rate at t, denoted as $u_i^{(t)} k_i^{(t)}$. Thus,

$$t_{D_i}^{(t)} = \frac{\bar{Q}_i^{(t)}}{u_i^{(t)} k_i^{(t)}} \tag{4.6}$$

In addition, $t_{R_i}^{(t)}$ can be formulated as the average travel time for a distance of $(x_r - l_r)$ at speed $u_r^{(t)}$, and for a distance of $L - \sum_{i=1}^{r} x_i$ at speed $u_i^{(t)}$,where

l_r is the average access distance of zone r,

$(x_r - l_r)$ is the average travel distance to pass zone r at speed $u_r^{(t)}$,

and $L - \sum_{i=1}^{r} x_i$ is the distance traveled by vehicles after passing zone r at speed $u_i^{(t)}$ while staging zone i at t.

Thus,

$$t_{R_i}^{(t)} = \frac{x_r - l_r}{u_r^{(t)}} + \frac{L - \sum_{i=1}^{r} x_i}{u_i^{(t)}} \tag{4.7}$$

Note that vehicles from zone r travel at a higher speed of $u_r^{(t)}$ for the distance of $(x_r - l_r)$, but at a lower speed of $u_i^{(t)}$ for the distance of $L - \sum_{i=1}^{r} x_i$ due to impediment from vehicles accessing the evacuation route form other zones.

The evacuation time $T_i^{(t)}$ is the sum of $t_{D_i}^{(t)}$ and $t_{R_i}^{(t)}$ and can be derived as

$$T_i^{(t)} = \frac{\bar{Q}_i^{(t)}}{u_i^{(t)} k_i^{(t)}} + \left(\frac{x_r - l_r}{u_r^{(t)}} + \frac{L - \sum_{i=1}^{r} x_i}{u_i^{(t)}} \right) \quad \forall i, t \tag{4.8}$$

Considering non-uniform demand distribution as shown in Figure 4.5 for the evacuation region shown in Figure 4.7, l_r is the total access distance divided by the demand, which can be formulated as

$$l_r = \frac{\int_{\sum_{i=1}^{r-1} x_i}^{\sum_{i=1}^{r} x_i} f(x)(x_r - x)dx}{\int_{\sum_{i=1}^{r-1} x_i}^{\sum_{i=1}^{r} x_i} f(x)dx} \tag{4.9}$$

where $f(x)$ is the demand density function, and x_r is the length of zone *r*. Note that l_r varies depending on $f(x)$ and x_r. Thus, the average distance traveled from zone *r* to the end of the evacuation route is $(x_r - l_r) + L - \sum_{i=1}^{r} x_i$.

In Equation 4.8, $u_i^{(t)}$ and $u_r^{(t)}$ can be obtained from Equation 4.11 based on $\bar{Q}_i^{(t)}$ and $Q_r^{(t)}$, respectively. As $\frac{\bar{Q}_i^{(t)}}{\delta_t} < c$, the discharge rate at *t* is $\frac{\bar{Q}_i^{(t)}}{\delta_t}$,such that

$$\frac{\bar{Q}_i^{(t)}}{\delta_t} = u_i^{(t)} k_i^{(t)} \qquad \forall i,t \tag{4.10}$$

Note that $u_i^{(t)}$ is estimated by the Edie's model for free-flow regime (also called Underwood model) defined as

$$u_i^{(t)} = u_f e^{\left(\frac{-k_i^{(t)}}{k_c}\right)} \tag{4.11}$$

where u_f is the free-flow speed (speed achieved under very low density), and k_c is the

critical density (density at maximum discharge rate). By substituting for $u_i^{(t)}$ into Equation 4.10, $\frac{\bar{Q}_i^{(t)}}{\delta_t}$ can be derived as

$$\frac{\bar{Q}_i^{(t)}}{\delta_t} = u_f e^{\left(\frac{-k_i^{(t)}}{k_c}\right)} k_i^{(t)} \qquad \forall i,t \tag{4.12}$$

where $k_i^{(t)}$, the density of the evacuation route while staging zone i at t, can be obtained from Equation 4.12. Then, $u_i^{(t)}$ can be obtained by substituting $k_i^{(t)}$ into Equation 4.11. Note that for simultaneous evacuation the following conditions sustain: $N = 1$; $r = 1$; and $x_r = L$. Thus, Equation 4.8 may be simplified as

$$T_1^{(t)} = \frac{\bar{Q}_1^{(t)}}{u_1^{(t)} k_1^{(t)}} + \frac{L - l_r}{u_1^{(t)}} \qquad \forall t \tag{4.13}$$

where l_r can be obtained from Equation 4.9.

(b) Congested Condition ($\frac{\bar{Q}_i^{(t)}}{\delta_t} > c$)

The congested flow condition may be reached when demand accessing the evacuation route exceeds the capacity. As $\frac{\bar{Q}_i^{(t)}}{\delta_t} > c$, the evacuation route is congested, the evacuation time for $\bar{Q}_i^{(t)}$ is the ratio of $\bar{Q}_i^{(t)}$ to the achievable discharge rate, $u_i^{(t)} k_i^{(t)}$. Thus,

$$T_i^{(t)} = \frac{\bar{Q}_i^{(t)}}{u_i^{(t)} k_i^{(t)}} \qquad \forall i,t \tag{4.14}$$

where $u_i^{(t)}$ and $k_i^{(t)}$ are the speed and density of the evacuation route.

In order to determine the speed-density relationship of the evacuation route for congested conditions, Akçelik's model and Edie's model for congested regime, also know as Greenberg's model, are applied. The speed of the evacuation route under this condition is first estimated by using the Akçelik's model:

$$n_i^{(t)} = n_0 + \left[0.25\delta_t \left(\left(\frac{\left(\bar{Q}_i^{(t)} / \delta_t \right)}{c} - 1 \right) + \sqrt{\left(\frac{\left(\bar{Q}_i^{(t)} / \delta_t \right)}{c} - 1 \right)^2 + \frac{8J_D}{c\delta_t} \left(\frac{\left(\bar{Q}_i^{(t)} / \delta_t \right)}{c} \right)} \right) \right] \quad \forall i,t \qquad (4.15)$$

where

$n_i^{(t)}$: Estimated travel time per mile while staging zone i at t (hours/mile)
n_0 : Free-flow travel time per mile (hours/mile),
J_D : Delay parameter (calibrated based on type of roadway)
δ_t : Time interval during which an average demand persists (e.g.,1 hour)
$\frac{\bar{Q}_i^{(t)} / \delta_t}{c}$: Ratio of the demand to be evacuated while staging zone i at t to the capacity

$u_i^{(t)}$ can be obtained from the reciprocal of travel time obtained from Equation 4.15. Thus,

$$u_i^{(t)} = \frac{1}{n_i^{(t)}} \quad \forall i,t \qquad (4.16)$$

The speed, $u_i^{(t)}$ obtained from the Akçelik's model is then used to compute the density, $k_i^{(t)}$ by using the Edie's model for congested regime (i.e., the Greenberg's model) formulated as

$$u_i^{(t)} = u_c \ln\left(\frac{k_j}{k_i^{(t)}}\right) \quad \forall i,t \tag{4.17}$$

Thus, $k_i^{(t)}$ can be derived from Equation 4.17 as

$$k_i^{(t)} = k_j e^{-\left(\frac{u_i^{(t)}}{u_c}\right)} \quad \forall i,t \tag{4.18}$$

where u_c is the critical speed (speed at maximum discharge rate, e.g., capacity), and k_j is the jam density (maximum density at which all vehicles are stopped), respectively. Finally, the achievable discharging rate while staging zone *i* at *t* is $u_i^{(t)} k_i^{(t)}$.

The delay parameter, J_D in Equation 4.15 can be calibrated if the difference between travel times of the evacuation route at capacity and free-flow conditions is known. Thus, by substituting $\frac{\bar{Q}_i^{(t)}}{\delta_t} = c$, and $n_i^{(t)} = n_c$, where n_c is the travel time per mile (hours/mile) at capacity, in Equation 4.15, J_D can be derived as

$$J_D = \frac{2c}{\delta_t}(n_c - n_0)^2 \tag{4.19}$$

For the Edie's model, if the speed at capacity $\left(\frac{1}{n_c}\right)$ is 40 mph, free-flow speed $\left(\frac{1}{n_0}\right)$ is 55 mph, the capacity of the evacuation route, *c* is 2,000 vph, and δ_t=1 hour, J_D is obtained from Equation 4.19 as 0.1859.

(3) Discharged volume at t ($Q_E^{(t)}$)

The discharged volume at t, denoted as $Q_E^{(t)}$, is defined as the number of vehicles evacuated (or successfully leaving the evacuation route).

As $\frac{\bar{Q}_i^{(t)}}{\delta_t} < c$,

$$Q_E^{(t)} = \bar{Q}_i^{(t)} - d_i^{(t)} \qquad \forall i,t \tag{4.20}$$

On the other hand, as $\frac{\bar{Q}_i^{(t)}}{\delta_t} > c$, the evacuation route is congested and $Q_E^{(t)}$ is the product of the speed, denoted as $u_i^{(t)}$, and the corresponding density, denoted as $k_i^{(t)}$.

Thus,

$$Q_E^{(t)} = u_i^{(t)} k_i^{(t)} \qquad \forall i,t \tag{4.21}$$

(4) Upper and lower bounds of flows (q_L, q_U)

The discharge rate of the evacuation route is maximized when $\frac{\bar{Q}_i^{(t)}}{\delta_t} = c$. However, this condition cannot be achieved for staged evacuation because of the time varying demand accessing the evacuation route. Therefore, in order to maintain a reasonable discharge rate of $\frac{\bar{Q}_i^{(t)}}{\delta_t}$, a criteria is set by assuming two parameters namely, q_L (lower flow limit) and q_U (upper flow limit) such that $q_L < c < q_U$. Note that q_L and q_U are user specified

parameters and there is no fixed procedure to approximate (e.g., q_L = 1,600 vph, q_U = 2,075 vph, if capacity, c = 2,000 vph). There are three conditions possible for $\frac{\bar{Q}_i^{(t)}}{\delta_t}$ as shown in Figure 4.9 and discussed below:

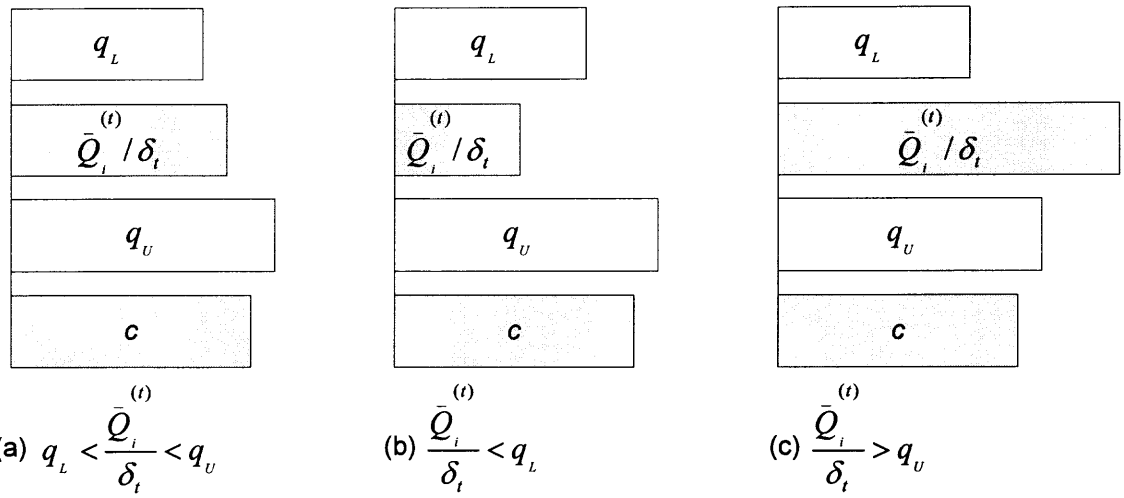

Figure 4.9 Relationships among q_L, q_U, and $\frac{\bar{Q}_i^{(t)}}{\delta_t}$.

Case (a): $q_L < \frac{\bar{Q}_i^{(t)}}{\delta_t} < q_U$

Since the discharge rate while staging zone i at t, $\frac{\bar{Q}_i^{(t)}}{\delta_t}$, is between q_L and q_U, the flow is considered to be acceptable. Also, $\frac{\bar{Q}_i^{(t)}}{\delta_t}$ is the highest when $\frac{\bar{Q}_i^{(t)}}{\delta_t} = c$. This represents the most desirable flow condition in terms of the maximum discharge rate; however, conditions (b) and (c) can also occur, based on the length of the staged zone that can decrease the discharge rate of the evacuation route and increase the evacuation time.

Case (b): $\frac{\bar{Q}_i^{(t)}}{\delta_t} < q_L$

This condition is caused by a short zone length, which results in a low, unacceptable discharge rate while staging zone *i* at *t*. However, if $\frac{\bar{Q}_i^{(t)}}{\delta_t} < q_L$ because of lighter demand loading the evacuation route based on the logit-based function defined in Equation 4.1(e.g., at the start of zone 1 and end of zone *N*), $\frac{\bar{Q}_i^{(t)}}{\delta_t}$ is considered to be acceptable.

Case (c): $\frac{\bar{Q}_i^{(t)}}{\delta_t} > q_U$

This condition is caused by a long zone length, which results in a congested flow that significantly reduces the effective discharge rate (e.g., effective discharge rate $< q_L$). Thus, this condition is undesirable. Note that although q_U is theoretically greater than *c* due to congested condition, the effective discharge rate as $q_U > c$ is less than *c*. Therefore q_U is set such that the effective discharge rate when $\frac{\bar{Q}_i^{(t)}}{\delta_t} = q_U$ is q_L under congested conditions. (i.e., q_L = Effective (q_U)). For example, a demand of 2,075 vph ($= q_U$) results in an effective discharge rate of 1,600 vph ($= q_L$).

The application of q_L and q_U is elucidated in the following sections.

4.2.2.2 Length of a Staged Zone. An iterative searching process to determine the length of zone 1 is discussed first. Subsequently, the method to determine the length of zone *i*, and the subtle difference between the estimation of the length of zone 1 and zone *i*, is discussed.

Note that staging is commenced at time 0 at which an evacuation order is issued. Initially, the length of zone 1 denoted as, x_1 is set to 1 mile and the corresponding demand loading profile is determined based on the demand of zone 1 as shown in Figure 4.10 and the logit-based function formulated in Equation 4.1.

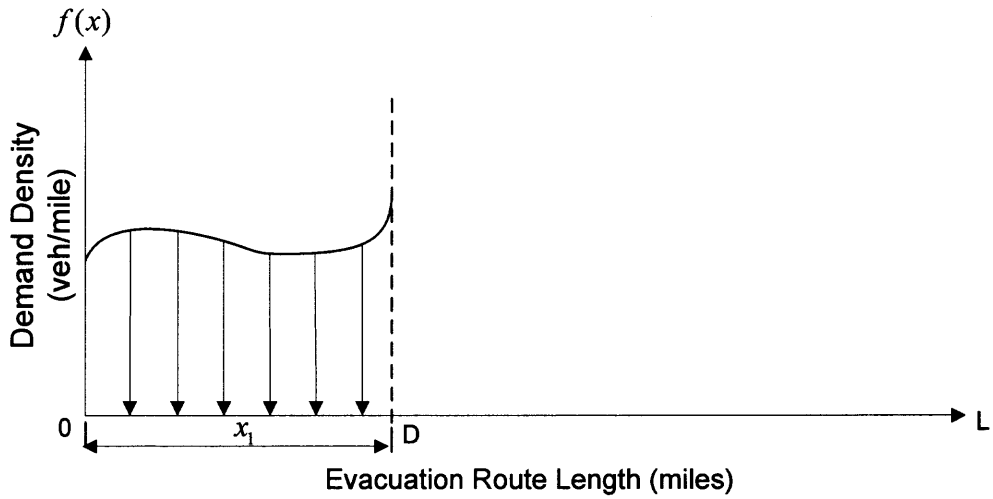

Figure 4.10 Demand density of zone 1 vs. distance.

The method to obtain the demand loading profile was discussed in Section 4.2.2.1(1). The bell shaped nature of the demand loading profile influences the demand to be evacuated by zone 1 at *t*, $\bar{Q}_1^{(t)}$. In other words, $\bar{Q}_1^{(t)}$ is expected to follow the pattern of the demand loading curve. Note that $\bar{Q}_1^{(t)}$ varies with the evolution of traffic conditions on the evacuation route (i.e., the number of vehicles queued at the end of the previous

interval and demand loaded in the current interval). $\bar{Q}_1^{(t)}$ is estimated using Equation 4.4. Note that at $t=0$, $d_i^{(t-1)} = d_S$ (queued shadow demand) and can be obtained from Equation 4.5.

If the resulting $\frac{\bar{Q}_1^{(t)}}{\delta_t}$ based on the current x_1 is less than q_L at all intervals while staging zone 1 (i.e., $\frac{\bar{Q}_1^{(t)}}{\delta_t} < q_L$, $\forall t$), x_1 is incremented such that $\frac{\bar{Q}_1^{(t)}}{\delta_t} > q_L$ for any t (e.g., $x_1 = x_1 + 0.1$). This condition ensures that the demand to be evacuated at t is not too low. On the other hand, if the resulting $\frac{\bar{Q}_1^{(t)}}{\delta_t}$ is greater than q_U at interval 0, x_1 is reduced until $\frac{\bar{Q}_1^{(0)}}{\delta_t} \le q_U$ (e.g., $x_1 = x_1 - 0.1$). This condition ensures that the demand to be evacuated at t is not too high that it decreases the effective discharge rate in the very beginning. Note that $\frac{\bar{Q}_1^{(t)}}{\delta_t}$ can be greater than q_U at later intervals while staging zone 1 (i.e., at t >0), but under this situation, the discharged volume due to zone 1 decreases due to the reduced speed of the evacuation route making x_1 inefficient. Figure 4.11 shows the conditions of feasibility of x_1 based on $\bar{Q}_1^{(t)}$.

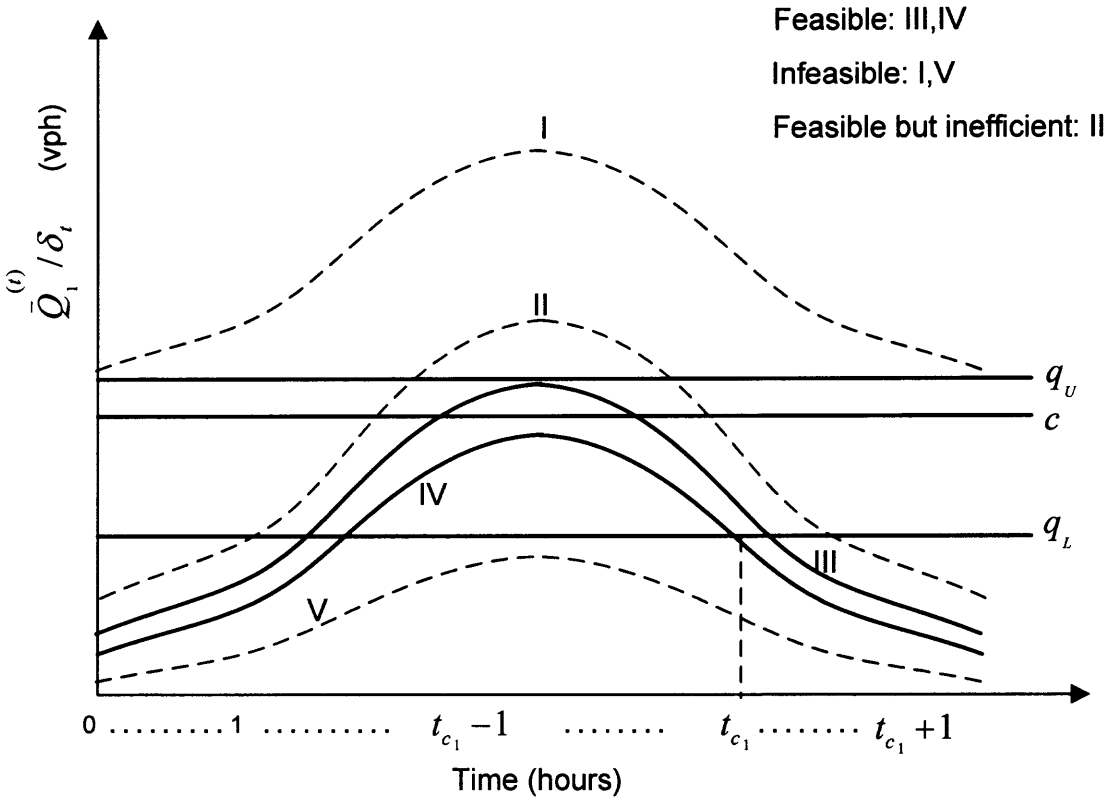

Figure 4.11 Demand distribution for various lengths of x_1.

Feasible: Based on the relationship (a) shown in the Figure 4.9(a), $\frac{\bar{Q}_1^{(t)}}{\delta_t}$ under cases III and IV is considered to be feasible as $q_L < \frac{\bar{Q}_i^{(t)}}{\delta_t} < q_U$.

Infeasible: On the other hand, cases V and I are considered to be infeasible as $\frac{\bar{Q}_1^{(t)}}{\delta_t}$ is low as discussed in relationships (b) and (c), respectively.

Feasible but Inefficient: Case II is feasible for certain duration while staging zone 1, also shown in Figure 4.9(a). However, for some duration, $\frac{\bar{Q}_i^{(t)}}{\delta_t} > q_U$, as shown in Figure 4.9 (c), which causes a reduction in discharge rate and an increase in evacuation time.

It is worth noting that Zone 2 is commenced at t_{c_1} when $\frac{\bar{Q}_1^{(t_{c_1})}}{\delta_t} < q_L$ if case IV is applied. The optimal x_1 is determined by enumerating all feasible values that can meet the condition of feasibility described above, and maximize the total discharged volume from 0 to t_{c_1} (e.g., $\text{Max} \sum_{t=0}^{t_{c_1}-1} Q_E^{(t)}$). An example that demonstrates the determination of the optimal x_1 is discussed in Section 4.4.

The determination of the length of zone i is similar to that of zone 1. Figure 4.12 shows an overlapping arrangement of time windows of staged zones that regulates the demand accessing the evacuation route so that available roadway capacity may be effectively utilized. The time window for a particular zone is the time period during which demand of the zone is loaded. Thus, as shown in the figure, demands from multiple zones can be loaded in a particular time.

The duration between $-t_S$ and 0 represents the time period for shadow evacuation. As the demand to be evacuated while staging zone i-1 at $t_{c_{i-1}}$ denoted as $\frac{\bar{Q}_{i-1}^{(t_{c_{i-1}})}}{\delta_t} < q_L$, the next staged zone i is commenced at $t_{c_{i-1}}$ while zone i-1 is still in operation (or loading demand). Thus, $\bar{Q}_i^{(t)}$ may contain demands of zones 1 to i-1.

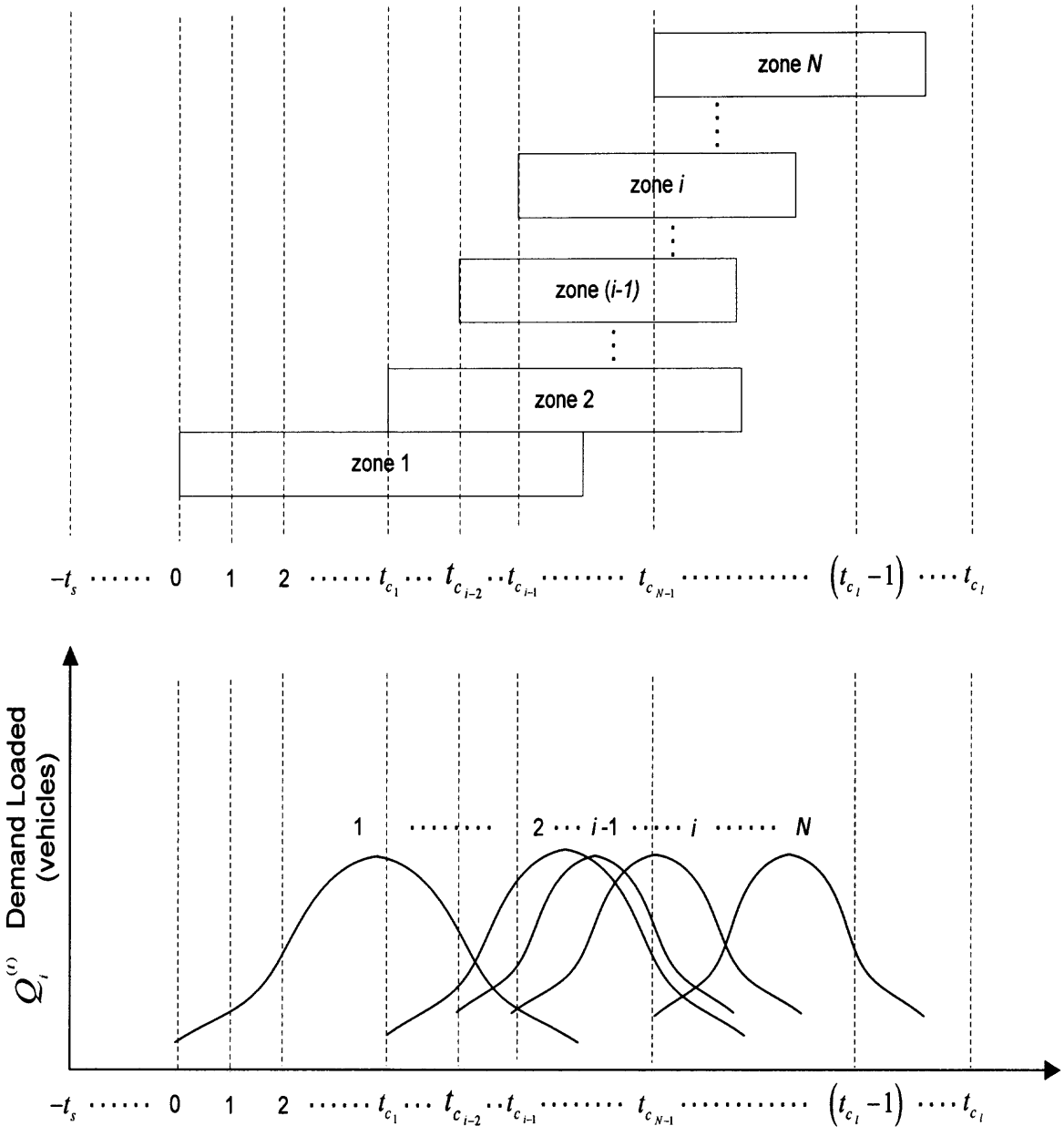

Figure 4.12 Configuration of time windows for staged zones.

Thus, when $\frac{\bar{Q}_{i-1}^{(t_{c_{i-1}})}}{\delta_t} < q_L$, the length of zone i is determined such that

$$q_L < \frac{\bar{Q}_{i-1}^{(t_{c_{i-1}})}}{\delta_t} + \frac{q_i^{(t_{c_{i-1}})} Q_i}{\delta_t} < q_U \qquad \forall i,t \tag{4.22}$$

where $\frac{q_i^{(t_{c_{i-1}})} Q_i}{\delta_t}$ is the demand accessing the evacuation route from zone i at $t_{c_{i-1}}$.

Once the length of zone i that satisfies the condition of Equation 4.22 is found, the discharged volume at t, $Q_E^{(t)}$ is determined by Equations 4.20 and 4.21 until t_{c_i} at which, $\frac{\bar{Q}_i^{t_{c_i}}}{\delta_t} < q_L$. The total discharged volume between $t_{c_{i-1}}$ and t_{c_i} (i.e., $\sum_{t=t_{c_{i-1}}}^{t_{c_i}-1} Q_E^{(t)}$) is compared for all feasible values of x_i that satisfy the condition of Equation 4.22, and the x_i that maximizes $\sum_{t=t_{c_{i-1}}}^{t_{c_i}-1} Q_E^{(t)}$ is deemed optimal.

4.2.2.3Total evacuation time (T). As shown in Figure 4.12, t_{c_l} is the time point at which the last vehicle exits the evacuation route. Usually, the time at which 90% of the total demand (i.e., 0.9Q) evacuates is used as a measure of effectiveness (MOE) to determine the efficiency of evacuation. Thus, if t_Z is the time point at which 90% of the demand evacuates, then the evacuation time for 90% of the demand denoted as T, is formulated as

$$T = \sum_{t=-t_s}^{t_Z} \delta_t \tag{4.23}$$

and

$$\sum_{t=-t_s}^{t_Z} Q_E^{(t)} = 0.9Q \tag{4.24}$$

where $-t_s$ is the time point at which shadow evacuation begins. Note that although the 90% of demand includes shadow demand, the evacuation time consumed by the shadow demand, t_s is excluded from T.

Thus,

$$T = \sum_{t=0}^{t_Z} \delta_t \tag{4.25}$$

4.2.2.5 Step Procedure to Determine the Optimal Staging Scheme.

Step 1: Determine the demand of the evacuation region based on the demand density function, $f(x)$ from Equation 4.2.

Step 2: Set zone counter i =1, time index t = 0, capacity c, upper and lower flow bounds q_L and q_U, respectively.

Step 3: Determine the shadow demand queued at t = 0 denoted as d_S from Equation 4.5.

Step 4: Set the length of zone i, x_i = 1 mile.

Step 5: Determine the demand loading profile of zone i from Equation 4.3.

Step 6: If i =1, determine x_i based on the procedure discussed in Section 4.2.2.2, else if $i > 1$, determine x_i by Equation 4.22.

Step 7: Determine the discharged volume $Q_E^{(t)}$ while staging zone i at t, from Equations 4.20 and 4.21.

Step 8: Increment the time count $t = t + 1$.

Step 9: Determine the total discharged volume while staging zone i at t until $\frac{\bar{Q}_i^{(t)}}{\delta_t} < q_L$.

Step 10: Determine the total discharged volume for other feasible x_i by setting $x_i = x_i \pm 0.1$ depending on the current x_i, and following steps 5 to 9. Note that x_i is increased or decreased based on Step 6.

Step 11: Determine the optimal length of zone i based on the maximum total discharged volume by zone i among all feasible alternatives.

Step 12: Check if 90% of the demand has been evacuated by Equation 4.24. If $\sum_{t=-t_s}^{t_Z} Q_E^{(t)} < 0.9Q$, determine the length of the next zone by incrementing the zone counter $(i = i + 1)$ and following steps 4 to 11, else goto step 13.

Step 13: The optimal number of staged zones is the current value of i. The evacuation time for 90% of the demand is determined through Equation 4.25.

Figure 4.13 shows the flow chart to search the optimal staging scheme.

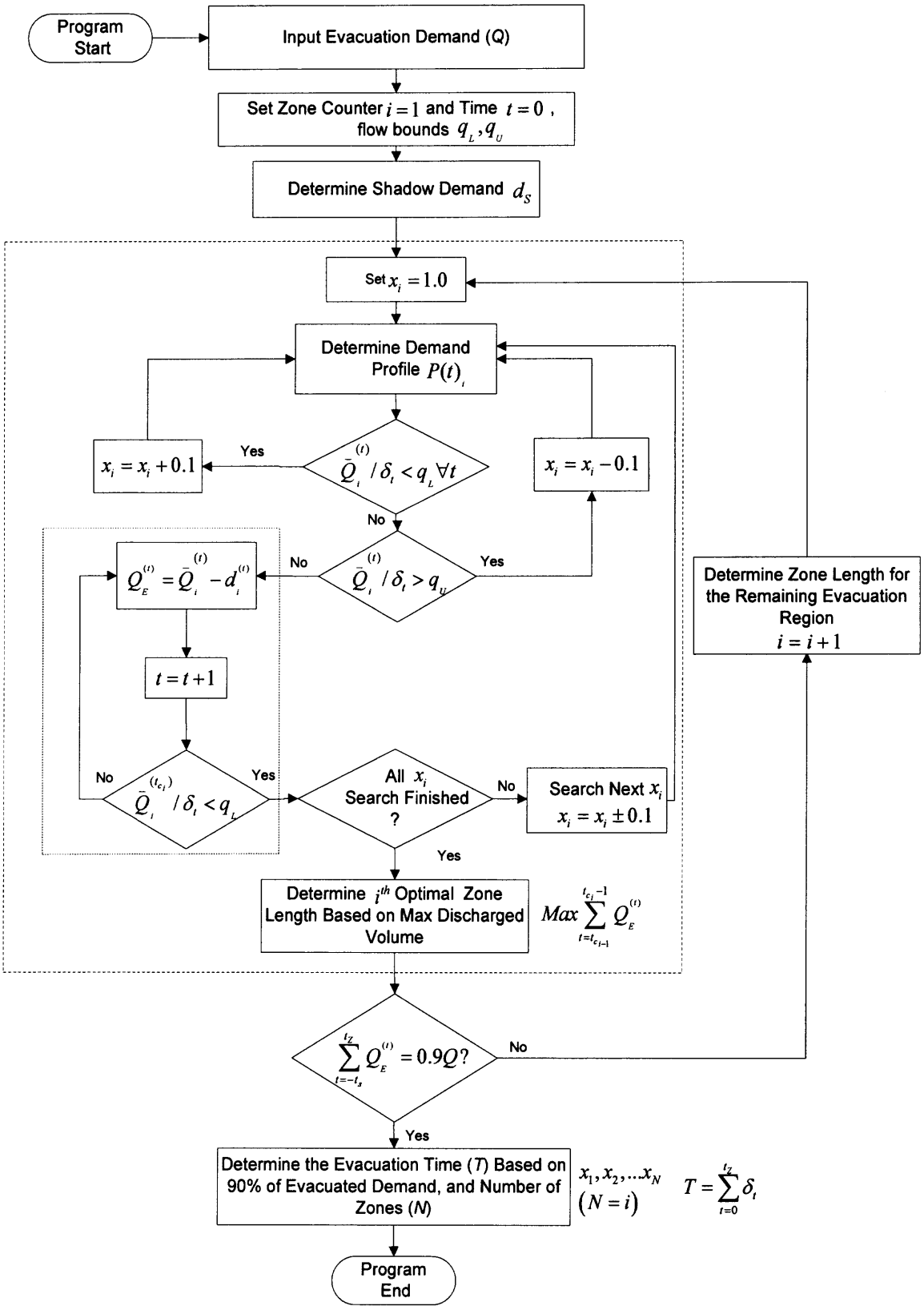

Figure 4.13 Flowchart to search the optimal staging scheme.

4.2.3 Delay

Unlike the delay discussed in Chapter 3, the model developed here considers demand heterogeneity and evacuees' behavioral response to evacuation order while formulating both queuing and moving delays. Thus, the delay incurred by evacuees while staging zone i at t varies over time.

Queuing Delay (D_Q)

The number of queuing vehicles in the network while staging zone i at t denoted as $d_i^{(t)}$ can be estimated using Equation 4.5, which was discussed in Section 4.2.2.1 and shown in Figure 4.8. The queuing delay experienced during the evacuation denoted as D_Q while staging zones 1 through N, between time points 0 and t_{c_l}, at which the last vehicle exits the evacuation route, is formulated as

$$D_Q = \sum_{i=1}^{N} \sum_{t=0}^{t_{c_l}} d_i^{(t)} \tag{4.26}$$

Thus, for staged evacuation,

$$D_Q = \sum_{i=1}^{N} \sum_{t=0}^{t_{c_l}} \frac{\left(T_i^{(t)} - \delta_t\right) \bar{Q}_i^{(t)}}{T_i^{(t)}} \tag{4.27}$$

Note that for simultaneous evacuation, $N = 1$.

Moving Delay (D_M)

The moving delay at *t*, denoted as $d_{M_i}^{(t)}$ is defined as the difference between average travel times of vehicles traveling from zone *r* while staging zone *i* at *t*, at speed $u_i^{(t)}$ denoted as $t_{R_i}^{(t)}$, and at free-flow speed u_f denoted as $t_{f_i}^{(t)}$. Note that $t_{R_i}^{(t)}$ is obtained from Equation 4.7, while $t_{f_i}^{(t)}$ is formulated as Equation 4.28. Refer Figure 4.7.

$$t_{f_i}^{(t)} = \frac{(x_r - l_r) + \left(L - \sum_{i=1}^{r} x_i\right)}{u_f} \tag{4.28}$$

Where *r* is the zone closest to the beginning of the evacuation route from which demand accesses the evacuation route at *t*, l_r is the average access distance of zone *r*, which can be obtained from Equation 4.9, and $(x_r - l_r)$ is the average travel distance to pass zone *r*. Note that $L - \sum_{i=1}^{r} x_i$ is the distance traveled by vehicles after passing zone *r*. Thus, the moving delay incurred by the discharged volume at $t, Q_E^{(t)}$, is

$$d_{M_i}^{(t)} = \left(t_{R_i}^{(t)} - t_{f_i}^{(t)}\right) Q_E^{(t)} \quad \forall i,t \tag{4.29}$$

By substituting for $t_{R_i}^{(t)}$ and $t_{f_i}^{(t)}$ obtained from Equations 4.7 and 4.28, respectively, into Equation 4.29, for staged evacuation, $d_{M_i}^{(t)}$ is derived as

$$d_{M_i}^{(t)} = \left(\left[\frac{x_r - l_r}{u_r^{(t)}} + \frac{L - \sum_{i=1}^{r} x_i}{u_i^{(t)}} \right] - \left[\frac{x_r - l_r + \left(L - \sum_{i=1}^{r} x_i\right)}{u_f} \right] \right) Q_E^{(t)} \quad \forall i,t \tag{4.30}$$

Note that for simultaneous evacuation, $(N = 1, x_r = L)$

Thus, the moving delay for staging zones 1 through N between time point 0 and t_{c_l}, D_M is formulated as

$$D_M = \sum_{i=1}^{N}\sum_{t=0}^{t_{c_l}}\left(\left[\frac{x_r - l_r}{u_r^{(t)}} + \frac{L - \sum_{i=1}^{r} x_i}{u_i^{(t)}}\right] - \left[\frac{x_r - l_r + \left(L - \sum_{i=1}^{r} x_i\right)}{u_f}\right]\right) Q_E^{(t)} \tag{4.31}$$

Note that for simultaneous evacuation, ($N=1, x_r = L$)

Total Delay (D_T)

The total delay while staging zone i at t denoted as $d_{T_i}^{(t)}$, is the sum of the queuing delay at t denoted as $d_i^{(t)}$ and the moving delay at t denoted as $d_{M_1}^{(t)}$, which are obtained from Equations 4.5 and 4.30, respectively. Thus

$$d_{T_i}^{(t)} = d_i^{(t)} + d_{M_i}^{(t)} \tag{4.32}$$

The total evacuation delay denoted as D_T is the sum of the queuing delay, D_Q and the moving delay, D_M. Thus, D_T can be derived as Equation 4.33.

$$D_T = \sum_{i=1}^{N}\sum_{t=0}^{t_{c_l}}\left\{\frac{\left(T_i^{(t)} - \delta_t\right)\bar{Q}_i^{(t)}}{T_i^{(t)}} + \left(\left[\frac{x_r - l_r}{u_r^{(t)}} + \frac{L - \sum_{i=1}^{r} x_i}{u_i^{(t)}}\right] - \left[\frac{x_r - l_r + \left(L - \sum_{i=1}^{r} x_i\right)}{u_f}\right]\right) Q_E^{(t)}\right\} \tag{4.33}$$

Note that for simultaneous evacuation, ($N=1, x_r = L$)

4.3 Numerical Example

The model developed in Section 4.2 is applied to optimize the staging scheme that minimizes evacuation time and the associated delays. The evacuation region, which can be referred to Figure 4.7 consists of a single evacuation route with one lane per direction. Unlike the example discussed in Chapter 3 where a uniform demand distribution over the evacuation route was assumed, the demand discussed here is linearly decreasing as shown in Figure 4.14.

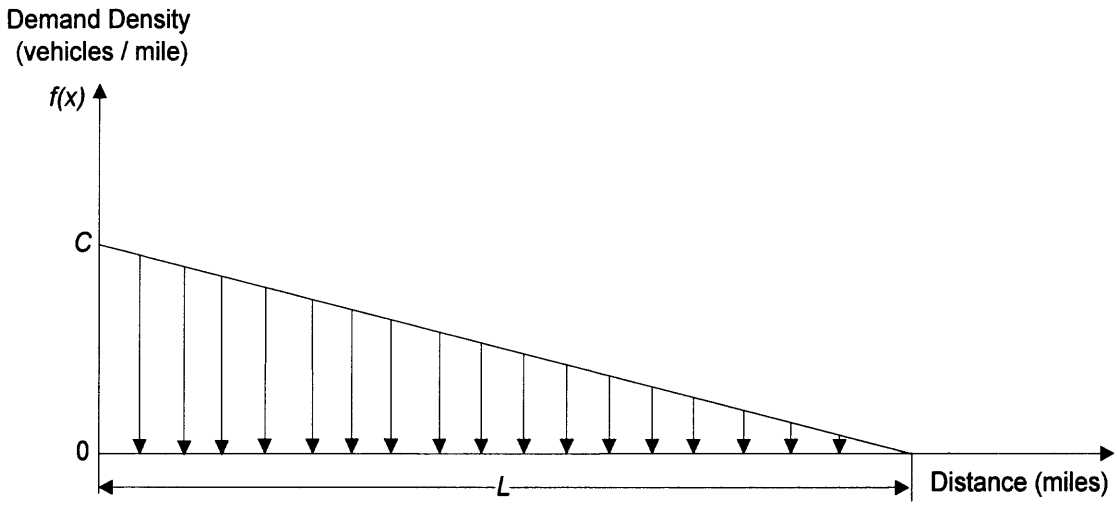

Figure 4.14 Demand density distribution of the evacuation route.

The length of the evacuation route is L miles. Assume that the demand density function over the evacuation route is $f(x)$ and formulated below.

$$f(x) = \left(\frac{-C}{L}\right)x + C \tag{4.34}$$

where C represents the highest demand density at location 0, while the lowest demand density is 0 at L. The total demand to be evacuated is denoted as Q, which can be obtained from Equation 4.35:

$$Q = \int_0^L \left[\left(\frac{-C}{L}\right)x + C\right]dx \tag{4.35}$$

In this example, L= 15 miles and C= 2,500 vehicles/mile. Thus, Q from Equation 4.35 is 20,000 vehicles. The above situation might indicate that the most vulnerable demand to be evacuated is concentrated near one end of the evacuation route. The parameters of the logit-based function formulated in Equation 4.1, namely, response rate, called α, and the half loading time, called β, are 0.6 and 2.5 hours, respectively, for a fast response scenario. Also, the duration of shadow evacuation time, (t_S), capacity of the evacuation route, (c), the lower flow limit, (q_L), and the upper flow limit, (q_U), are 2 hours, 2,000 vph, 1,600 vph, and 2,075 vph, respectively. The resulting shadow demand from Equation 4.1 is 10.9 % of the total demand (i.e, Q_S = 2,180 vehicles).

4.3.1 Model Results

In this section, the application of the models to estimate evacuation time and the associated delays for the numerical example discussed above is presented for both simultaneous and staged evacuations.

Simultaneous Evacuation

Figure 4.15 shows the demand loading profile over time for simultaneous evacuation. Since demand loading rates are above the capacity of the evacuation route (c =2,000 vph), congestion can be expected. Table 4.1 presents the evacuation demand distribution over time. Since simultaneous evacuation is also a single stage evacuation, N=1.

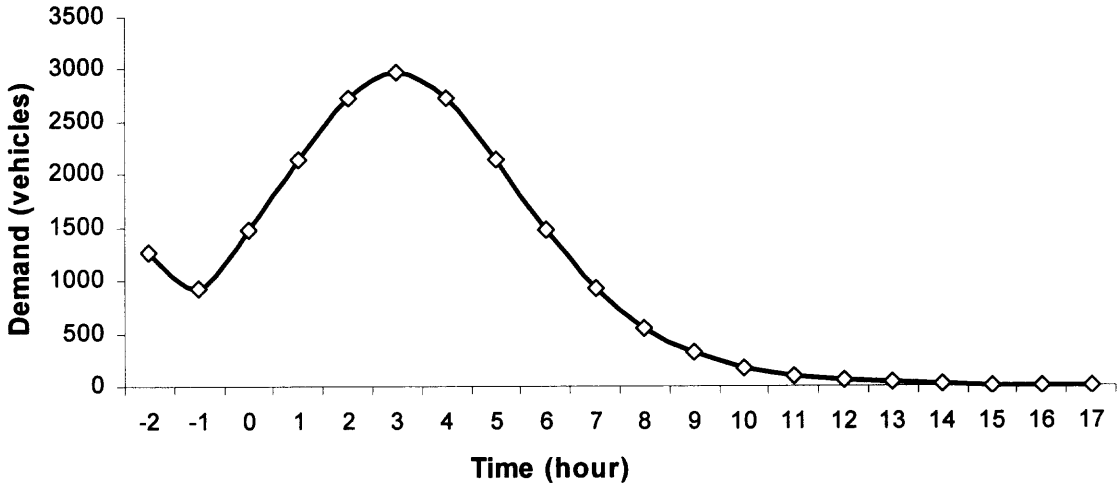

Figure 4.15 Demand loading profile over time for simultaneous evacuation.

The definitions of the variables used in Table 4.1 are listed below.

$Q_1^{(t)}$: demand accessing the evacuation route at t based on the loading profile shown in Figure 4.15,

$\bar{Q}_1^{(t)}$: demand to evacuated at t (i.e., demand present on the evacuation route and access streets),

$u_1^{(t)}$: speed of the evacuation route at t,

$k_1^{(t)}$: density of the evacuation route at t,

$T_1^{(t)}$: evacuation time for $\bar{Q}_1^{(t)}$ at t,

$d_1^{(t)}$: vehicles queued at t, and

$Q_E^{(t)}$: discharged volume or number of vehicles successfully leaving the evacuation route at t.

Table 4.1 Evacuation Demand Distribution of Simultaneous Evacuation (N=1).

(t) (hour)	$Q_1^{(t)}$ (vehicles)	$\bar{Q}_1^{(t)}$ (vehicles)	$u_1^{(t)}$ (mph)	$k_1^{(t)}$ (vpm)	$T_1^{(t)}$ (hour)	$d_1^{(t)}$ (vehicles)	$Q_E^{(t)}$ (vehicles)
-2	1259	1259	47.0	27	1.23	232	**1028**
-1	922	1154	47.0	25	1.23	213	**942**
0	1467	1679	43.0	39	1.25	332	**1347**
1	2132	2465	7.5	123	4.09	1862	**603**
2	2730	4592	6.0	130	5.89	3804	**788**
3	2978	6782	6.0	130	8.69	5994	**788**
4	2730	8724	6.0	130	11.18	7936	**788**
5	2132	10068	6.0	130	12.91	9280	**788**
6	1467	10747	6.0	130	13.78	9959	**788**
7	922	10881	6.0	130	13.95	10093	**788**
8	548	10641	6.0	130	13.64	9853	**788**
9	315	10168	6.0	130	13.04	9380	**788**
10	177	9557	6.0	130	12.25	8769	**788**
11	99	8867	6.0	130	11.37	8079	**788**
12	54	8134	6.0	130	10.43	7346	**788**
13	30	7376	6.0	130	9.46	6588	**788**
14	17	6605	6.0	130	8.47	5817	**788**
15	9	5826	6.0	130	7.47	5038	**788**
16	5	5043	6.0	130	6.46	4255	**788**
17	0	4255	6.0	130	5.45	3467	**788**
18	-	3467	6.0	130	4.44	2679	**788**
19	-	2679	6.0	130	3.43	1891	**788**
20	-	1891	42.0	45	1.00	0	**1891**
21	-	0	-	-	-	-	**0**

$Q_1^{(t)}$ is determined by using Equation 4.3. For example, demand accessing at $t = 0$, $Q_1^{(0)}$ is the product of the percentage of demand loaded at $t = 0$, 7.34%, and the total demand $Q = 20{,}000$ vehicles, which is 1,467 vehicles.

$T_1^{(t)}$ under uncongested and congested conditions is determined using Equations 4.13 and 4.14, respectively. Also, $u_1^{(t)}$ under uncongested and congested conditions is determined using Equations 4.11 and 4.16, respectively. $T_1^{(0)}$ is determined using Equation 4.13 as the sum of the discharge time and transit time. As $\frac{\bar{Q}_1^{(0)}}{\delta_t} < c$, the

discharge time is 1 hour. The average vehicle access distance denoted as l_r is obtained as 4.39 miles form Equation 4.9, and the average travel distance to exit the evacuation route, $(L - l_r)$ is 10.61 miles. The speed $u_1^{(0)}$ determined by Equation 4.11 is 43 mph. The transit time is 0.25 hours. Thus, $T_1^{(0)}$ is 1.25 hours.

$d_1^{(t)}$ can be estimated by Equation 4.5, and $Q_E^{(t)}$ under uncongested and congested conditions is determined from Equations 4.20 and 4.21, respectively. Thus, as $\bar{Q}_1^{(0)}$ = 1,679 vehicles, and the unit interval, δ_t = 1 hour, the number of queuing vehicles at $t = 0$, $d_1^{(0)}$ is determined as 332 vehicles. Therefore, the discharged volume $Q_E^{(0)}$ is obtained from Equation 4.20 as the difference of $\bar{Q}_1^{(0)}$ (= 1,679 vehicles) and $d_1^{(0)}$ (= 332 vehicles) and is 1,347 vehicles.

The demand to be evacuated at time t, $\bar{Q}_1^{(t)}$ is determined by Equation 4.4. For example, the demand to be evacuated at $t = 1$, $\bar{Q}_1^{(1)}$ is the sum of the queuing vehicles cumulated from the previous interval, which is 332 vehicles, and the access demand at t = 1, which is 2,132 vehicles. Thus, $\bar{Q}_1^{(1)}$ = 2,465 vehicles.

The congested condition is reached as $\frac{\bar{Q}_1^{(1)}}{\delta_t} > c$. In this example, for the evacuation route length of 15 miles, and an average vehicle spacing of 30 ft/ vehicle, the number of vehicles that are required to flood the evacuation route is determined as 2,640.

Thus, the maximum demand to capacity ratio, $\frac{\left(\bar{Q}_i^{(t)} / \delta_t\right)}{c}$ is 1.32. The discharged volume under congested condition is determined by Equation 4.21. As speed, $u_1^{(2)}$ = 6 mph, and density, $k_1^{(2)}$ = 130 vpmpl, the discharge volume, $Q_E^{(2)}$ is obtained as 778 vehicles. Note that, $u_1^{(2)}$ and $k_1^{(2)}$ are obtained from Equations 4.16 and 4.18, respectively.

As shown in Table 4.2, the speeds in the initial period of evacuation (e.g., t = -2 to t = 0) are higher as $\frac{\bar{Q}_1^{(0)}}{\delta_t} < c$. However, as $\frac{\bar{Q}_1^{(0)}}{\delta_t} > c$ (e.g., $\frac{\bar{Q}_1^{(2)}}{\delta_t} = 4{,}592$ vph), the speed of the evacuation route and the discharged volume at t = 2, decrease significantly (e.g., 6 mph, and 788 vehicles). This situation persists until $\frac{\bar{Q}_1^{(t)}}{\delta_t} < c$ at t = 20, after which the speed and the discharged volume increase.

Table 4.2 presents the delays under simultaneous evacuation at various intervals. As shown in table, the queuing delay at t denoted as $d_1^{(t)}$ increases quickly after the start of evacuation at t = 2, while the moving delay denoted as $d_{M_1}^{(t)}$ in general is considerably less than $d_1^{(t)}$. Note that $d_i^{(t)}$ is estimated by Equation 4.5. For example, the queuing delay at t = 2, $d_i^{(2)}$ is determined as 3,804 veh-hour, where the evacuation time for $\bar{Q}_1^{(2)}$ (= 4,592 vehicles) denoted as $T_i^{(2)}$ is 5.89 hours (See Table 4.1).

Table 4.2 Delays Under Simultaneous Evacuation

(t) (hour)	$d_1^{(t)}$ Queuing delay (veh -hour)	$d_{M_1}^{(t)}$ Moving delay (veh - hour)	$d_{T_1}^{(t)}$ Total delay (veh-hour)
-2	232	34	266
-1	213	31	244
0	332	73	405
1	1862	737	2599
2	3804	1241	5045
3	5994	1241	7235
4	7936	1241	9177
5	9280	1241	10522
6	9959	1241	11200
7	10093	1241	11335
8	9853	1241	11095
9	9380	1241	10621
10	8769	1241	10010
11	8079	1241	9321
12	7346	1241	8587
13	6588	1241	7829
14	5817	1241	7058
15	5038	1241	6279
16	4255	1241	5496
17	3467	1241	4708
18	2679	1241	3920
19	1891	1241	3132
20	0	113	113
21	0	0	0

$d_{M_1}^{(t)}$ is estimated by Equation 4.30, where the average vehicle access distance denoted as l_r is obtained as 4.39 miles from Equation 4.9, and the average travel distance to exit the evacuation route, $(L - l_r)$ is 10.61 miles, the demand accessing the evacuation route at t = 2, $Q_i^{(2)}$ is 2,730 vehicles, the speed, $u_1^{(2)}$ obtained from Equation 4.16 is 6 mph, and the free-flow speed, u_f is 55 mph. Thus, the moving delay at t = 2, $d_{M_1}^{(2)}$ is determined as 1,241 veh-hour.

The total delay at $t = 2$ denoted as $d_{T_1}^{(2)}$ is obtained form Equation 4.32 as the sum of $d_1^{(2)}$ (=3,804 veh-hour) and $d_{M_1}^{(2)}$ (= 1,241 veh-hour) and is 5,045 veh-hour.

The total evacuation delay denoted as D_T is obtained from Equation 4.33 as 145,687 veh-hour.

Staged Evacuation

In this section, the procedure to determine the lengths of the staged zones for the example is discussed. Table 4.3 presents the demand distribution of the staged evacuation over time. Since the optimal number of stages required for the evacuation is determined as 3, i can vary from 1 to 3. The definitions of the variables used in Table 4.3 are listed below.

$Q_i^{(t)}$: demand accessing the evacuation route at t while staging zone i based on Equation 4.3

$\bar{Q}_i^{(t)}$: demand to evacuated while staging zone i at t,

$u_i^{(t)}$: speed of the evacuation route while staging zone i at t,

$T_i^{(t)}$: evacuation time for $\bar{Q}_i^{(t)}$ while staging zone i at t,

$d_i^{(t)}$: vehicles queued while staging zone i at t, and

$Q_E^{(t)}$: discharged volume at t.

As shown in Table 4.3, $\frac{\bar{Q}_i^{(t)}}{\delta_t} < c$, because of which, congestion is significantly lower as compared to simultaneous evacuation.

The density of the evacuation route while staging zone i at t, $k_i^{(t)}$ can be obtained by Equation 4.12. For example, as the demand to be evacuated while staging zone 2 at t = 6 ($\bar{Q}_2^{(6)}$) is 1,865 vehicles, the free-flow speed, u_f, is 55 mph, the density of the evacuation route ($k_2^{(6)}$) is 44.5 vpmpl. Note that the density values are excluded from Table 4.3. The speed $u_2^{(6)}$ is obtained from Equation 4.11 as 42 mph.

$T_i^{(t)}$ is determined by Equation 4.8. The computation of evacuation time of zone 2 at t = 6 ($T_2^{(6)}$) shown in Table 4.3 is discussed below:

Since $\frac{\bar{Q}_2^{(6)}}{\delta_t} < c$ where c = 2,000 vph, the discharge time is 1 hour. Meanwhile, at t = 6, zone 1 is closest to the beginning of the evacuation route from which demand accesses the evacuation route (i.e., r =1). The length of zone 1, x_1 whose determination is explained in the next section, is 4.9 miles. The average access distance of zone 1, l_1 is determined by Equation 4.9 as 2.21 miles. Thus, the average vehicle travel distance to pass zone 1, l_1 is 2.69 miles.

Based on the number of vehicles accessing the evacuation route from zone 1 only at t = 6, which is 781 vehicles, the speed of vehicles passing from zone 1 at t = 6 denoted as $u_1^{(6)}$ determined by Equation 4.11 is 50 mph. The average travel distance from zone 1 to the end of the evacuation route is 12.79 miles. The speed of the evacuation route while staging zone 2 at t = 6 ($u_2^{(6)}$) determined by Equation 4.11 is 42 mph. Thus, the evacuation time $T_2^{(6)}$ for demand $\bar{Q}_2^{(6)}$ is 1.32 hours.

Table 4.3 Evacuation Demand Distribution of Staged Evacuation

	Zone 1 (x_1 = 4.9 miles)					Zone 2 (x_2 = 3.8 miles)					Zone 3 (x_3 = 6.3 miles)					
(t) (hr)	$Q_1^{(t)}$ (veh)	$u_1^{(t)}$ (mph)	$\bar{Q}_1^{(t)}$ (veh)	$T_1^{(t)}$ (hr)	$d_1^{(t)}$ (veh)	$Q_2^{(t)}$ (veh)	$u_2^{(t)}$ (mph)	$\bar{Q}_2^{(t)}$ (veh)	$T_2^{(t)}$ (hr)	$d_2^{(t)}$ (veh)	$Q_3^{(t)}$ (veh)	$u_3^{(t)}$ (mph)	$\bar{Q}_3^{(t)}$ (veh)	$T_3^{(t)}$ (hr)	$d_3^{(t)}$ (veh)	$Q_E^{(t)}$ (veh)
-2	**1259**	47	1259	1.23	232	-	-	-	-	-	-	-	-	-	-	**1028**
-1	**922**	47	1154	1.23	213	-	-	-	-	-	-	-	-	-	-	**942**
0	**781**	48	994	1.31	209	-	-	-	-	-	-	-	-	-	-	**785**
1	**1136**	46	1345	1.33	293	-	-	-	-	-	-	-	-	-	-	**1052**
2	**1454**	43	1747	1.35	400	-	-	-	-	-	-	-	-	-	-	**1346**
3	**1586**	41	1987	1.37	472	-	-	-	-	-	-	-	-	-	-	**1514**
4	**1454**	41	1927	1.37	458	-	-	-	-	-	-	-	-	-	-	**1469**
5	-	-	1594	-	-	**1539**	41	1997	1.33	498	-	-	-	-	-	**1500**
6	-		-			**1368**	42	1865	1.32	450	-	-	-	-	-	**1415**
7	-					**1242**	52	1692	1.27	365	-	-	-	-	-	**1328**
8	-					-	-	1475	-	-	**1393**	42	1758	1.32	428	**1330**
9	-					-		-			**1329**	43	1756	1.31	415	**1342**
10	-					-					**1206**	44	1621	1.30	377	**1244**
11	-					-					**1029**	47	1406	1.30	322	**1084**
12	-					-					**808**	49	1131	1.29	252	**878**
13	-					-					**577**	51	829	1.28	180	**649**
14	-					-					**378**	53	558	1.27	118	**440**
15	-					-					**231**	54	349	1.26	72	**277**
16	-					-					**135**	55	207	1.26	42	**165**
17	-					-					**76**	55	118	1.25	24	**94**
18	-					-					**42**	55	66	1.25	13	**53**
19	-					-					**24**	55	37	1.25	7	**29**
20	-					-					**13**	55	20	1.25	4	**16**
21	-					-					**7**	55	11	1.25	2	**9**
22	-					-					**3**	55	5	1.25	1	**4**
23	-					-					**2**	55	3	1.00	0	**3**

Note that the other parameters, such as $Q_i^{(t)}$, $\bar{Q}_i^{(t)}$, $d_i^{(t)}$, and $Q_E^{(t)}$, can refer to the discussion of simultaneous evacuation.

Optimal Zone Lengths

Note that the staged evacuation is commenced at $t = 0$ and continues until all the demand is evacuated. The evacuation from $t = -2$ to -1 pertains to shadow evacuation. The optimal length of the first zone was determined as 4.9 miles by enumerating all feasible values of the evacuation route from 0 to 15 miles with increments of 0.1 miles such that the total number of vehicles evacuated from time 0 to $(t_{c_1} - 1)$ is maximum, where t_{c_1} is the time at which the demand to be evacuated while staging zone 1 at t, $\frac{\bar{Q}_1^{(t)}}{\delta_t}$, is less than q_L.

As shown in Table 4.4, as $x_1 = 4.9$ miles, $\bar{Q}_1^{(t)}$ starts increasing from 994 vehicles at $t = 0$, peaks at $t = 3$ (1987 vehicles), and then starts to decline at $t = 4$. At $t = 5$, $\frac{\bar{Q}_1^{(5)}}{\delta_t} < q_L$ (i.e., $t_{c_1} = 5$). Note that $\bar{Q}_1^{(0)} = 994$ vehicles is the sum of the shadow demand queued at $t = 0$ (213 vehicles), and demand accessing from zone1 at $t = 0$, $Q_1^{(0)} = 781$ vph.

Table 4.4 Determination of x_1 (test with x_1 = 4.9 miles)

Time (t) (hr)	$Q_1^{(t)}$ (vehicles)	$u_1^{(t)}$ (mph)	$k_1^{(t)}$ (vpm)	$\bar{Q}_1^{(t)}$ (vehicles)	$T_1^{(t)}$ (hr)	$d_1^{(t)}$ (vehicles)	$Q_E^{(t)}$ (vehicles)
-2	1259	47	27	1259	1.23	232	**1028**
-1	922	47	25	1154	1.23	213	**942**
0	781	48	21	994	1.27	209	**785**
1	1136	46	30	1345	1.28	293	**1052**
2	1454	43	41	1747	1.30	400	**1346**
3	1586	41	49	1987	1.31	472	**1515**
4	1454	41	47	1927	1.31	458	**1469**
5	1136	-	-	1594	-	-	

If x_1 is less than 4.9 miles (say, 4.0 miles), it reduces the discharged volume between $t = 0$ and 4 (Table 4.5).

Table 4.5 Determination of x_1 (test with x_1 = 4.0 miles)

Time (t) (hr)	$Q_1^{(t)}$ (vehicles)	$u^{(t)}$ (mph)	$k_1^{(t)}$ (vpm)	$\bar{Q}_1^{(t)}$ (vehicles)	$T_1^{(t)}$ (hr)	$d_1^{(t)}$ (vehicles)	$Q_E^{(t)}$ (vehicles)
-2	1259	47	27	1259	1.23	232	**1028**
-1	922	47	25	1154	1.23	213	**942**
0	660	49	18	873	1.27	185	**688**
1	960	47	24	1145	1.28	250	**894**
2	1229	45	33	1479	1.29	335	**1145**
3	1340	43	39	1675	1.31	392	**1283**
4	1229	44	37	1621	1.30	373	**1248**
5	960	-	-	1333	-	-	

On the other hand, if x_1 is greater than 4.9 miles (say, 5.3 miles) it leads to a congested condition on the evacuation route which reduces the discharged volume between $t = 0$ and 4 (Table 4.6).

Table 4.6 Determination of x_1 (test with x_1 = 5.3 miles)

Time (t) (hr)	$Q_1^{(t)}$ (vehicles)	$u^{(t)}$ (mph)	$k_1^{(t)}$ (vpm)	$\bar{Q}_1^{(t)}$ (vehicles)	$T_1^{(t)}$ (hr)	$d_1^{(t)}$ (vehicles)	$Q_E^{(t)}$ (vehicles)
-2	1259	47	27	1259	1.23	232	**1028**
-1	922	47	25	1154	1.23	213	**942**
0	831	48	22	1044	1.26	217	**826**
1	1209	45	32	1426	1.28	313	**1114**
2	1548	42	44	1860	1.30	430	**1430**
3	1688	20	77	2118	1.99	1054	**1064**
4	1548	6	130	2601	3.30	1813	**788**
5	1209	-	-	3022	-	-	

As shown in Figure 4.16, the total discharged volume between t = 0 and $(t_{c_i} - 1) = 4$ denoted as $\sum_{t=0}^{4} Q_E^{(t)}$ for $x_1 = 4.0$, 5.3, and 4.9 miles are 5258 vehicles, 5222 vehicles, and 6167 vehicles, respectively. Thus, as $x_1 = 4.9$ miles, the discharged volume between 0 and $(t_{c_i} - 1) = 4$, $\sum_{t=0}^{4} Q_E^{(t)}$ is maximized.

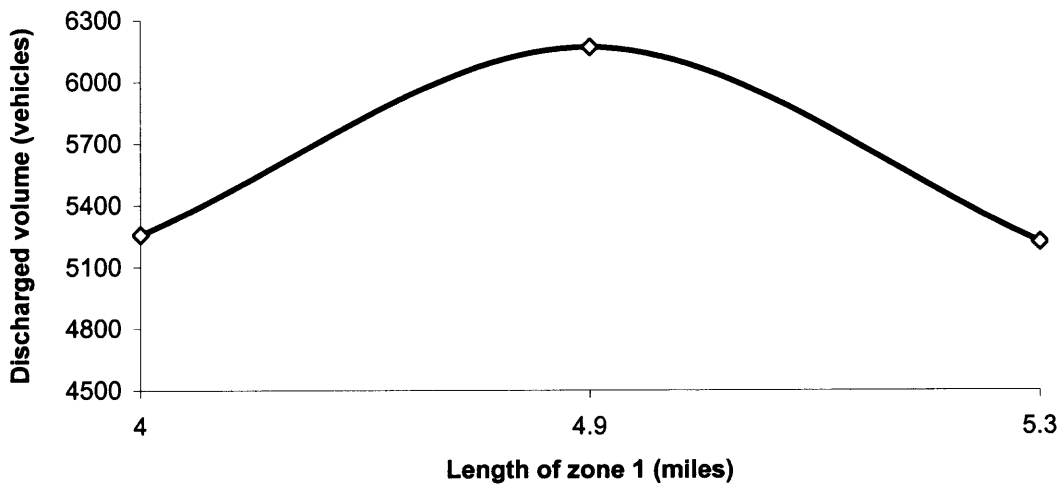

Figure 4.16 Length of zone 1 vs. discharged volume between t = 0 and 4.

Since the demand to be evacuated while staging zone 1 at $t = 5$, $\frac{\bar{Q}_1^{(5)}}{\delta_t}$, reduces to 1594 vehicles, which is less than q_L (1600 vph), the second zone length x_2 is determined based on the condition in Equation 4.22 for the remaining evacuation route length of 10.1 miles (i.e., 15- 4.9) using the same procedure described for zone 1. The optimal length of zone 2 denoted as x_2 is 3.8 miles. A similar procedure is followed to determine the optimal length of staged zone 3, denoted as x_3 as 6.3 miles. x_3 is longer than x_1 and x_2 due to a lower demand concentration (linearly decreasing demand) at the end of the evacuation route.

The optimal staging scheme for evacuating 90% of the demand (18,000 vehicles) used as a measure of effectiveness (MOE) is illustrated in Table 4.7 and Figure 4.17. The time taken for evacuating 90% of the total demand through simultaneous and staged evacuations obtained from Equation 4.25 are 18.87 hours and 11.7 hours, respectively. Thus, the total evacuation time can be reduced by 7.17 hours by implementing the optimal staged plan. Note that although the 90% of demand includes shadow demand, the evacuation time (2 hours) consumed by the shadow demand is excluded from the evacuation time results.

Table 4.7 Optimal Staging Scheme

Zone (i)	Length (miles)	Time of staging zone i (hours)	Dischrarged volume while staging zone i (vehicles)
Shadow Evacuation	-	-2 to -1	1969
1	$x_1 = 4.9$	0 to 4	6166
2	$x_2 = 3.8$	5 to 7	4243
3	$x_3 = 6.3$	8 to11.7	5622

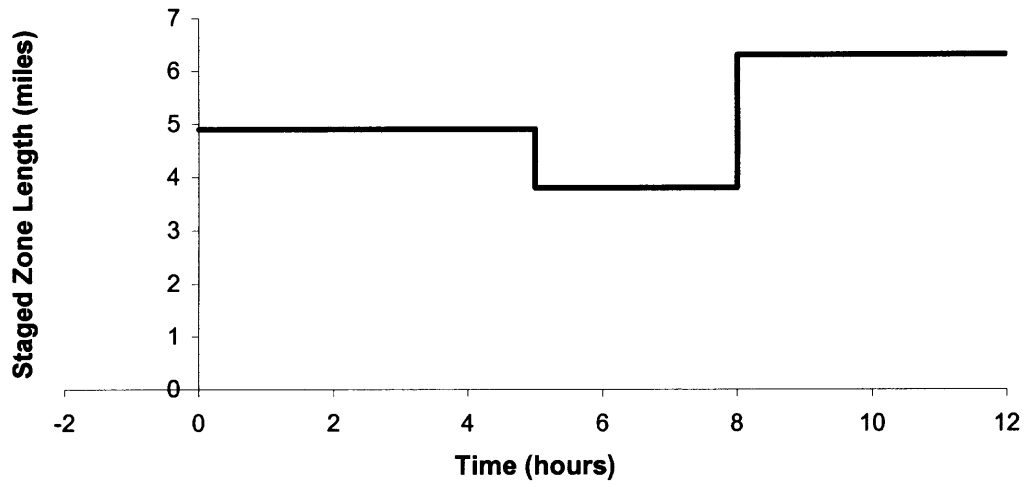

Figure 4.17 Optimal staging scheme.

Table 4.8 presents the delays under staged evacuation at various intervals. The queuing delay at t denoted as $d_i^{(t)}$, moving delay at t denoted as $d_{M_i}^{(t)}$ are obtained from Equations 4.5 and 4.30, respectively. Also, the total delay at t denoted as $d_{T_i}^{(t)}$ can be obtained from Equation 4.32. The total delay for the evacuation denoted as D_T is obtained from equation 4.33 as 6,321 veh-hour. Note that $d_i^{(t)}, d_{M_i}^{(t)}$, and D_T can refer to the discussion of simultaneous evacuation.

Table 4.8 Delays Under Staged Evacuation

(t) (hour)	$d_i^{(t)}$ Queuing delay (veh -hour)	$d_{M_i}^{(t)}$ Moving delay (veh - hour)	$d_{T_i}^{(t)}$ Total delay (veh-hour)
-2	232	34	266
-1	213	31	244
0	209	27	236
1	293	48	340
2	400	87	488
3	472	120	593
4	458	117	575
5	498	107	604
6	450	87	538
7	365	18	382
8	428	86	513
9	415	70	485
10	377	57	434
11	322	44	367
12	252	27	280
13	180	15	195
14	118	6	124
15	72	2	74
16	42	1	43
17	24	0	24
18	13	0	13
19	7	0	7
20	4	0	4
21	2	0	2
22	1	0	1

4.3.2 Comparison of Evacuation Time and Delays

Figure 4.18 shows the demand accessing the evacuation route, $Q_i^{(t)}$, and the demand to be evacuated, $\bar{Q}_i^{(t)}$ over time, for simultaneous and staged evacuations. The aggregate demand accessing the evacuation route for staged evacuation at *t* refers to the sum of the access demands of the staged zones due to the temporal zone overlapping arrangement.

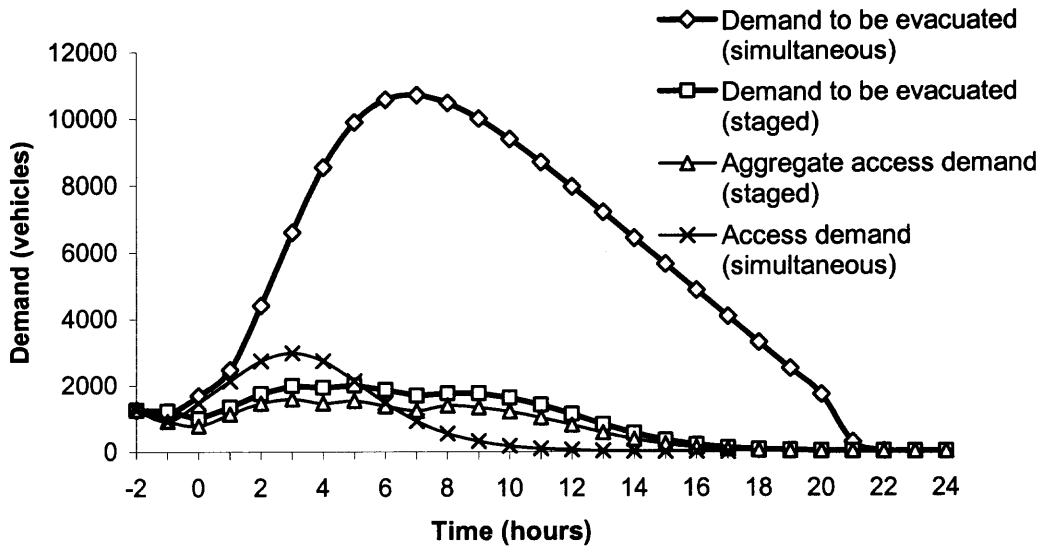

Figure 4.18 Demand distribution vs. time.

The demand to be evacuated during each hour under simultaneous evacuation is substantially higher than that of the staged evacuation. Also, the demand to be evacuated under simultaneous evacuation is greater than the capacity of the evacuation route (2,000 vph) during most of the evacuation, resulting in congestion and reduction in the discharged volume. On the other hand, under staged evacuation, the demand accessing the evacuation route is regulated, which leads to less congestion that shortens the evacuation time.

Figure 4.19 shows the discharged volume for simultaneous and staged evacuation at over time. The discharged volume during the shadow evacuation period (t = -2 to hour -1) are the same for both simultaneous and staged evacuation. But after t = 0, the discharged volume of staged evacuation is generally higher than that of simultaneous evacuation until t = 12 at which 90% of the total demand is discharged under staged evacuation. The discharged volume for staged evacuation decreases at later periods due

to light demand. The discharged volume at $t = 1$ is low due to light demand reacting to evacuation orders. Relatively low reduction in discharged volume is also observed at time periods before the commencement of evacuation of the next stage (e.g., $t = 4$ and 7), due to lighter demand loaded on the evacuation route.

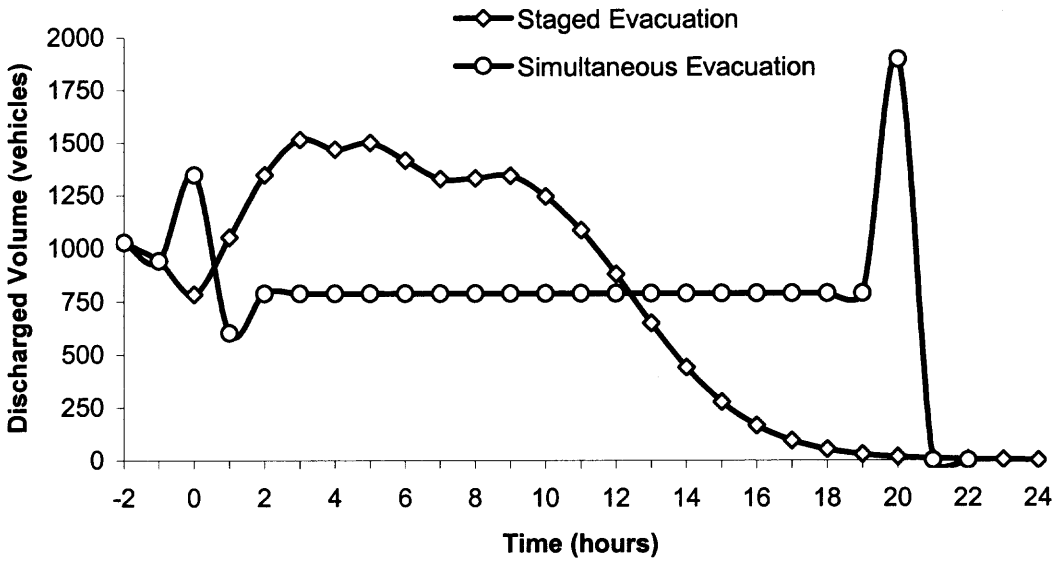

Figure 4.19 Discharged volume vs. time for simultaneous and staged evacuations.

On the other hand, the discharged volume of simultaneous evacuation is significantly low between $t = 2$ to19 due to the congestion on the evacuation route. Since the demand to be evacuated under simultaneous evacuation increases, peaks and then decreases as shown in Figure 4.18, the discharged volume is higher at $t = 0$ (1347 vehicles) before the demand exceeds capacity. Also, at the end of evacuation, a higher discharged volume is observed at $t = 20$ as congestion is cleared. Figure 4.20 shows the cumulative discharged volume by simultaneous and staged evacuations.

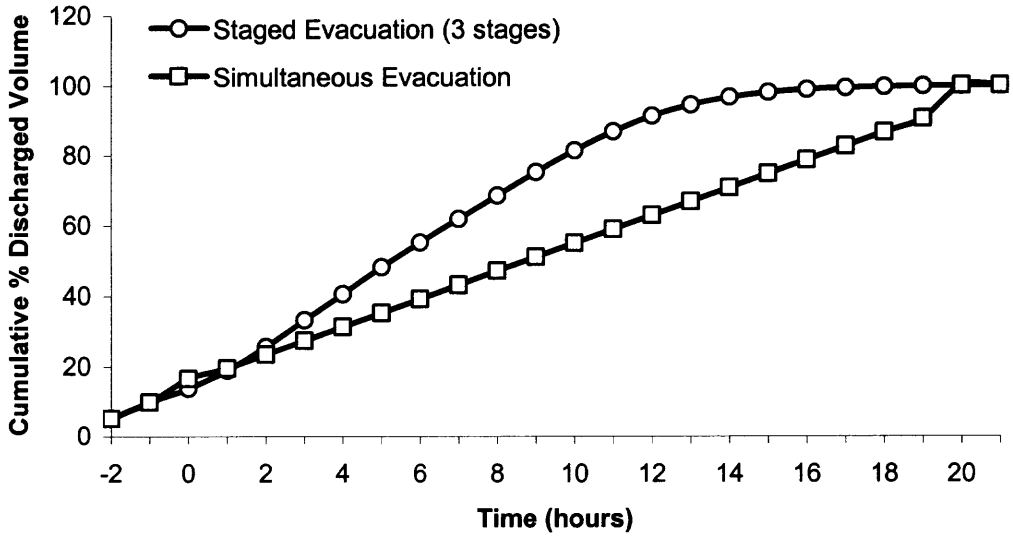

Figure 4.20 Cumulative discharged volume (%) vs. time.

Figures 4.21 and 4.22 show the delays for simultaneous and staged evacuations respectively, over time. The total delays of simultaneous and staged evacuations are 145,687 veh-hour and 6,321 veh-hour respectively. The total delay of staged evacuation when compared with simultaneous evacuation is considerably lower, mainly due to higher speed being achieved on the evacuation route due to lower congestion. Also, for staged evacuation, reduction in delay at certain intervals is observed before a new zone is commenced due to increase in the speed of the evacuation route caused by a reduction in the demand to be evacuated (e.g., $t =$ 4 and 7).

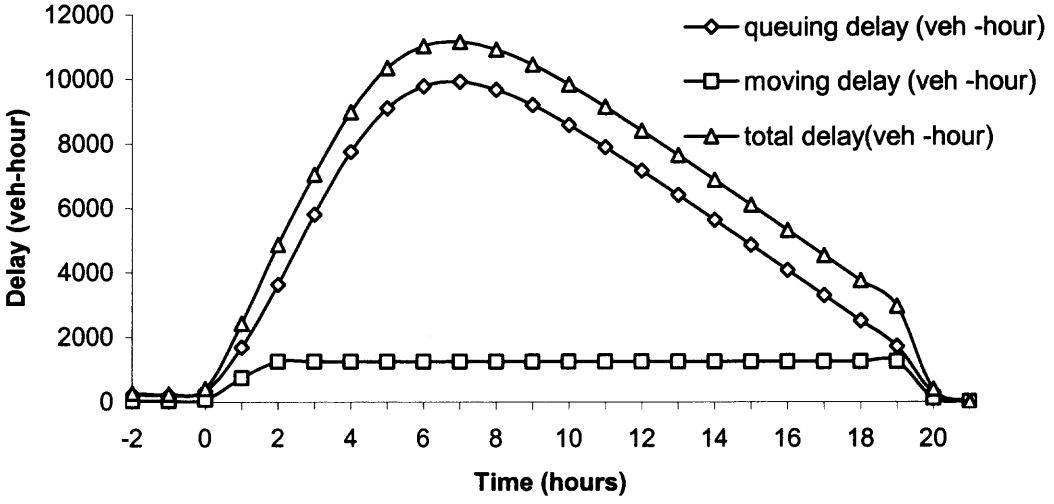

Figure 4.21 Delays under simultaneous evacuation vs. time.

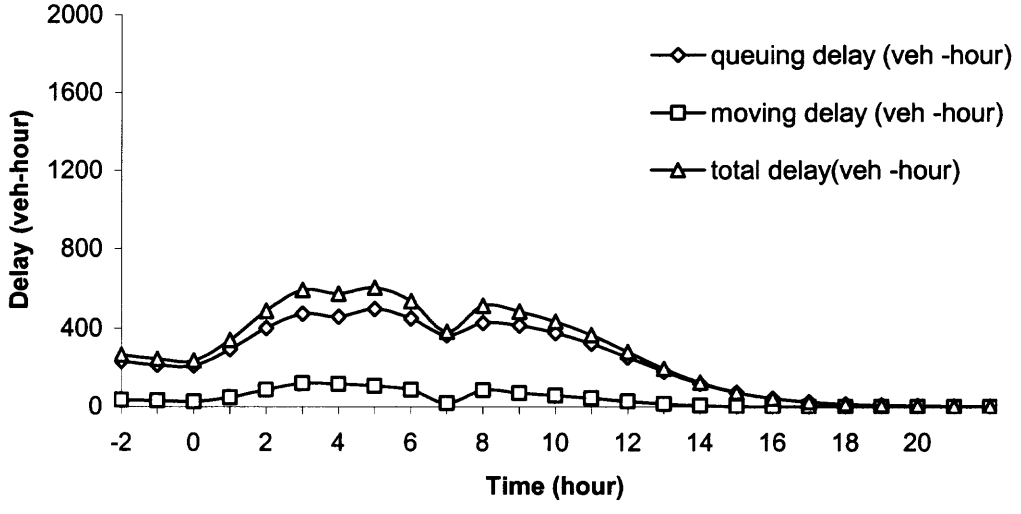

Figure 4.22 Delays under staged evacuation vs. time.

4.4 Sensitivity Analysis

In this section the impacts of variation in demand of the evacuation region and capacity of the evacuation route on evacuation time and a delay is analyzed.

In order to study the effects of variation in demand of the evacuation region, four cases of demand (Q) of 10,000 vehicles, 20,000 vehicles, 30,000 vehicles, and 40,000 vehicles are considered for the evacuation region discussed in the numerical example, Section 4.3. All other parameters are assumed to be identical as that of the numerical example and are summarized in Table 4.9.

Table 4.9 Baseline Values

Parameter	Value
L	15 miles
α	0.6
β	2.5 hours
t_S	2 hours
c	2,000 vph
q_L	1,600 vph
q_U	2,075 vph

Table 4.10 shows the evacuation time for 90% of the demand, reduction in evacuation time by staged evacuation, and the optimal staging scheme for the four cases of demand discussed above. As seen from the table, evacuation time for both simultaneous and staged evacuations increase with increase in demand. Also, reduction in evacuation time is higher at greater demand. No saving in evacuation time is observed for the demand of 10,000 vehicles due to negligible congestion during simultaneous evacuation, which obviates staging. While the number of staged zones required increases with demand, the lengths of the zones become shorter. In addition, the length of the first zone, x_1 is the

shortest for the highest demand (e.g., 40,000 vehicles), due to a high demand density at the beginning of the evacuation route and early congestion.

Table 4.10 Evacuation Time and Optimal Staging Scheme Under Varying Demand (Q)

Demand (Vehicles)	Simultaneous Evacuation Time (hours)	Staged Evacuation Time (hours)	Reduced Evacuation Time (hours)	Optimal Staging Scheme (miles)
10,000	6.51	6.51	0	$x_1 = 15.0$
20,000	18.87	11.70	7.17	$x_1 = 4.9,\ x_2 = 3.8,\ x_3 = 6.3$
30,000	28.87	15.72	13.15	$x_1 = 3.0,\ x_2 = 1.9,\ x_3 = 2.4,$ $x_4 = 4.9,\ x_5 = 2.8$
40,000	41.96	23.68	18.28	$x_1 = 1.3,\ x_2 = 0.9,\ x_3 = 2.0,$ $x_4 = 2.3,\ x_5 = 3.6,\ x_6 = 4.9$

Figures 4.23 and 4.24 show the total delays of simultaneous and staged evacuations over time for varying demands. As seen from Figure 4.23, the total delay for simultaneous evacuation is higher for greater demand, mainly due to a high queuing delay. While the total delay of staged evacuation is higher for greater demand, the total delay at Q = 40,000 vehicles is significantly higher than that of the others in the initial durations of evacuation, due to early congestion that causes an increase in queuing and moving delays. As a result, staged evacuation at Q = 40,000 vehicles is commenced only after congestion clears at t = 2. Table 4.11 shows the comparison of the total delays of simultaneous and staged evacuations for various demands.

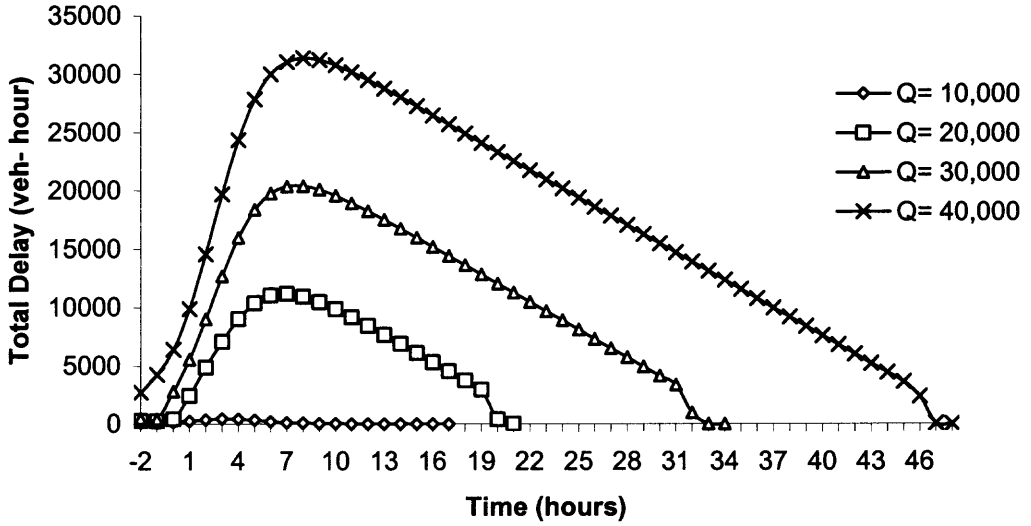

Figure 4.23 Total delay vs. time for simultaneous evacuation.

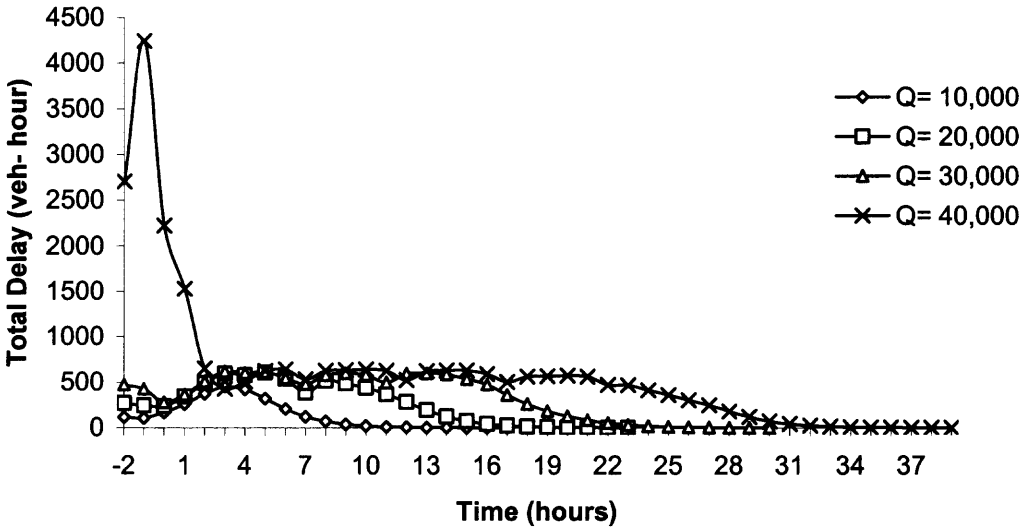

Figure 4.24 Total delay vs. time for staged evacuation.

Table 4.11 Total Delay for Evacuation Under Varying Demand

Demand (Vehicles)	Staged Evacuation Total Delay (veh-hour)	Simultaneous Evacuation Total Delay (veh-hour)
10,000	2,447	2,447
20,000	6,321	142,450
30,000	10,164	400,703
40,000	18,131	854,582

In order to study the impact of variation in capacity of the evacuation route on evacuation time and delay, lane reversal or contraflow is utilized. The use of a contraflow lane here is assumed to double the capacity of the evacuation route (i.e. net capacity = 4,000 vph) with capacity per lane being 2,000 vph. Four cases of demand, Q of 20,000 vehicles, 30,000 vehicles, 40,000 vehicles, and 50,000 vehicles are considered for the evacuation region discussed in the numerical example in section 4.3. All other parameters are assumed to be identical as that of the numerical example and are summarized in Table 4.9.

Table 4.12 shows the evacuation time for 90% of the demand, reduction in evacuation time by staged evacuation, and the optimal staging scheme for the four cases of demand discussed above under enhanced capacity. No reduction in evacuation time is observed from staged evacuation at Q= 20,000 as congestion under simultaneous evacuation in the presence of excess capacity is negligible, which makes staged evacuation redundant. However, reduction in evacuation time by staged evacuation is greater for higher demand (e.g., Q= 30,000 vehicles to Q= 50,000 vehicles) due to higher congestion during simultaneous evacuation. Also, the number of staged zones is

greater with higher demand but, the lengths of zones shorten. For instance, 4 zones of sizes $x_1 = 3.9$, $x_2 = 2.7$, $x_3 = 3.6, x_4 = 4.8$, miles are required for Q = 50,000 vehicles.

Table 4.12 Evacuation Time and Optimal Staging Scheme Under Varying Demand (c = 4,000 vph)

Demand (Vehicles)	Simultaneous Evacuation Time (hours)	Staged Evacuation Time (hours)	Reduced Evacuation Time (hours)	Optimal Staging Scheme (miles)
20,000	6.51	6.51	0	$x_1 = 15.0$
30,000	13.18	9.10	4.09	$x_1 = 7.5,\ x_2 = 7.5$
40,000	19.05	11.35	7.70	$x_1 = 5.1,\ x_2 = 4.3,\ x_3 = 5.6$
50,000	24.94	14.11	10.83	$x_1 = 3.9,\ x_2 = 2.7,\ x_3 = 3.6,$ $x_4 = 4.8$

Figures 4.25 and 4.26 show the total delays of simultaneous and staged evacuations over time for varying demands at enhanced evacuation route capacity. The total delay for both evacuations is higher at greater demand, mainly due to a high queuing delay. Table 4.13 shows the comparison of the total delays of simultaneous and staged evacuations for various demands at enhanced route capacity.

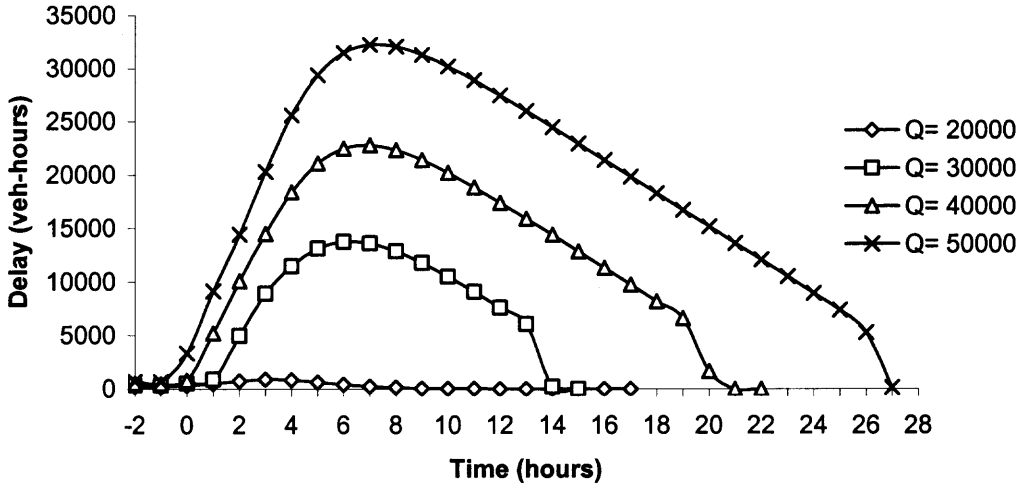

Figure 4.25 Total delay vs. time for simultaneous evacuation (c = 4,000 vph).

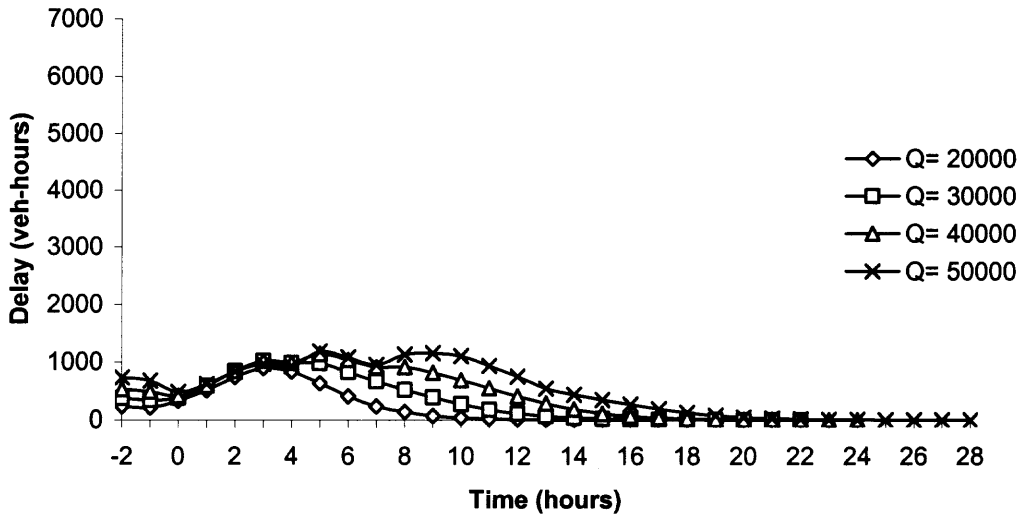

Figure 4.26 Total delay vs. time for staged evacuation (c = 4,000 vph).

Table 4.13 Total Delay for Evacuation Under Varying Demand (c = 4,000 vph)

Demand (Vehicles)	Simultaneous Evacuation Total Delay (veh-hour)	Staged Evacuation Total Delay (veh-hour)
20,000	4,890	4,890
30,000	125,184	7,921
40,000	295,796	11,059
50,000	537,705	14,220

4.5 Summary

In this chapter, a more realistic model was developed by enhancing the base model in Chapter 3 by considering the heterogeneous demand distribution over an evacuation region and evacuees' behavior responses to evacuation order (e.g., fast, medium, and slow. While the model developed in Chapter 3 assumed the access flow rate constant during evacuation, the behavioral model employs the S-shaped logit-based function to determine the access flow. The enhanced model determines the optimal lengths and time windows of staged zones based on the demand distribution, behavioral response of evacuees, and predicted evolution of traffic conditions on the evacuation route by an iterative searching procedure. The significance of temporal overlapping of time windows of staged zones to maximize the discharged volume was illustrated.

The applicability of the model was demonstrated with a numerical example. Results showed that the evacuation time of staged evacuation for evacuating 90% of the demand, which is used a measure of effectiveness, is considerably less than that of simultaneous evacuation. Sensitivity analysis of demand and capacity on evacuation time and delay was conducted. Results indicate that reduction in evacuation time and delay by

staged evacuation as compared to simultaneous evacuation is higher for greater demands. While similar results are observed when the capacity of the evacuation route is doubled by contraflow, no reduction in evacuation time and delay by staged evacuation is seen for low demand when contraflow is utilized.

While this chapter presented the applicability of staged evacuation under varying behavioral response and demand distribution scenarios, the feasibility of implementing staged evacuation is a critical issue, and is discussed in the next chapter.

CHAPTER 5

ENHANCEMENT OF STAGED EVACUATION MODELS

The model developed in Chapter 4 determined the optimal staging scheme that minimizes evacuation time and delay. However, non-compliance behavior of evacuees to evacuation order was not considered. For example, variation in level of compliance can further increase the complexity for estimating the demand accessing the evacuation route over time and the evacuation time and delays may be underestimated. In this chapter, the practicability of a staged evacuation scheme considering various compliance levels is investigated. In addition, a method that revises the optimal staging scheme obtained in Chapter 4 is developed. The model discussed here is called Enhanced Model II, which is an extension of the Enhanced Model I by considering the compliance effect.

This chapter is organized into the following sections: Section 5.1 discusses the effectiveness of staged evacuation based on the level of compliance of zones and the deviation from scheduled demand access time; Section 5.2 illustrates a method to revise the optimal staging scheme; Section 5.3 presents a numerical example, which shows the impacts of levels of compliance on evacuation time and delay, and the improvement in the effectiveness of staging with the revised scheme; and finally Section 5.4 presents a summary of Chapter 5.

5.1 Level of Compliance

The level of evacuees' compliance to an evacuation order may significantly influence evacuation time and the associated delay. In this section, the impact of the compliance on the evacuation time and delays are analyzed. Compliance here is defined as the conformity of a staged zone to its demand loading pattern and the corresponding scheduled demand access time. The effectiveness of a staged evacuation considering level of compliance is the efficacy of the staging scheme in comparison to the optimal staging scheme obtained in Chapter 4 considering full (e.g., 100%) compliance.

Assume that the level of compliance for demand of zone i denoted as P_i may be different from that of other zones. The average compliance level of an evacuation region denoted as P may be formulated as

$$P = \frac{\sum_{i=1}^{N} P_i Q_i}{Q} \tag{5.1}$$

where Q is the total demand to be evacuated from the region, Q_i is the demand of zone i, and N is the number of staged zones. Note that P represents the overall level of compliance for an evacuation region.

Assume that the reduction in evacuation time achieved through staged evacuation by evacuating the majority of the demand (e.g., 90% of the total demand) is ΔT, which is equal to the evacuation time of simultaneous evacuation minus that of staged evacuation as formulated in Equation 5.2.

$$\Delta T = T_{sim} - T_n \tag{5.2}$$

where T_{sim} and T_n are evacuation times of simultaneous and staged evacuations, respectively. The effectiveness of a staged evacuation scheme considering compliance

level denoted as η is the ratio of the reduction in evacuation time achieved by the staging scheme to that of the optimal staging scheme denoted as ΔT_{opt}. Thus,

$$\eta = \frac{\Delta T}{\Delta T_{opt}} = \frac{T_{sim} - T_n}{T_{sim} - T_{opt}} \quad \forall T_{sim} > T_n \tag{5.3}$$

where T_{opt} is the estimated evacuation time for the optimal staging scheme that minimizes evacuation time and delay. For the condition that $T_{sim} = T_{opt}$, the optimal evacuation scheme is a simultaneous evacuation, where $N = 1$.

Parameter η is primarily dependent on the evacuation time of a staged scheme, T_n, which is affected by P_i and the deviation of the scheduled access time for the demand of zone *i*, denoted as s_i. In this study, s_i is a user specified parameter, which is the difference between the scheduled demand access time point of zone *i*, $t_{c_{i-1}}$ and *t*.

$$s_i = t_{c_{i-1}} - t \tag{5.4}$$

Thus, s_i affects the demand to be evacuated while staging zone *i* at *t* and may have significant impact on congestion that influences T_n.

Since the level of compliance for demand of zone *i* is denoted as P_i, the level of non-compliance for demand of zone *i* may be denoted as $(1 - P_i)$. Thus, the compliance demand of zone *i* ($P_i Q_i$) is defined as one that begins to access the evacuation route at a planned time *t*, whereas, non-compliance demand of zone *i* ($(1 - P_i) Q_i$) is one that should access at $t + s_i$, but begins to accesses at *t*. Note that the demand distributions of both compliance and non-compliance demands are based on the loading curve formulated in Equation 4.1.

The model developed in Chapter 4 was demonstrated as an effective way to search the optimal staging scheme that maximizes the discharged volume of an evacuation route. Therefore, the time windows of staged zones may be overlapped with one another, so that the available capacity can be efficiently utilized. When level of compliance is considered while staging zone *i* at *t*, the demand accessing the evacuation route may contain the compliance (scheduled) and non-compliance demands of zones 1 through *i*, and the non-compliance demand of zones *i*+1 through *N*. This is because, at time *t*, zones 1 to *i* are already staged, but zones *i*+1 through *N* await staging. Figure 5.1 shows a general configuration of time-windows for all staged zones considering non-compliance effect.

As shown in Figure 5.1, $t_{c_{i-1}}$ represents the scheduled demand access time point of zone *i*, while s_i represents the deviation of the scheduled demand access time of zone *i*. Thus, the non-compliance demand of zone *i* $(=(1-P_i)Q_i)$ begins to access the evacuation route at $\left(t_{c_{i-1}}-s_i\right)$, while the scheduled demand $(=P_iQ_i)$ accesses the evacuation route at $t_{c_{i-1}}$. The last vehicle exits the evacuation route at t_{c_I}.

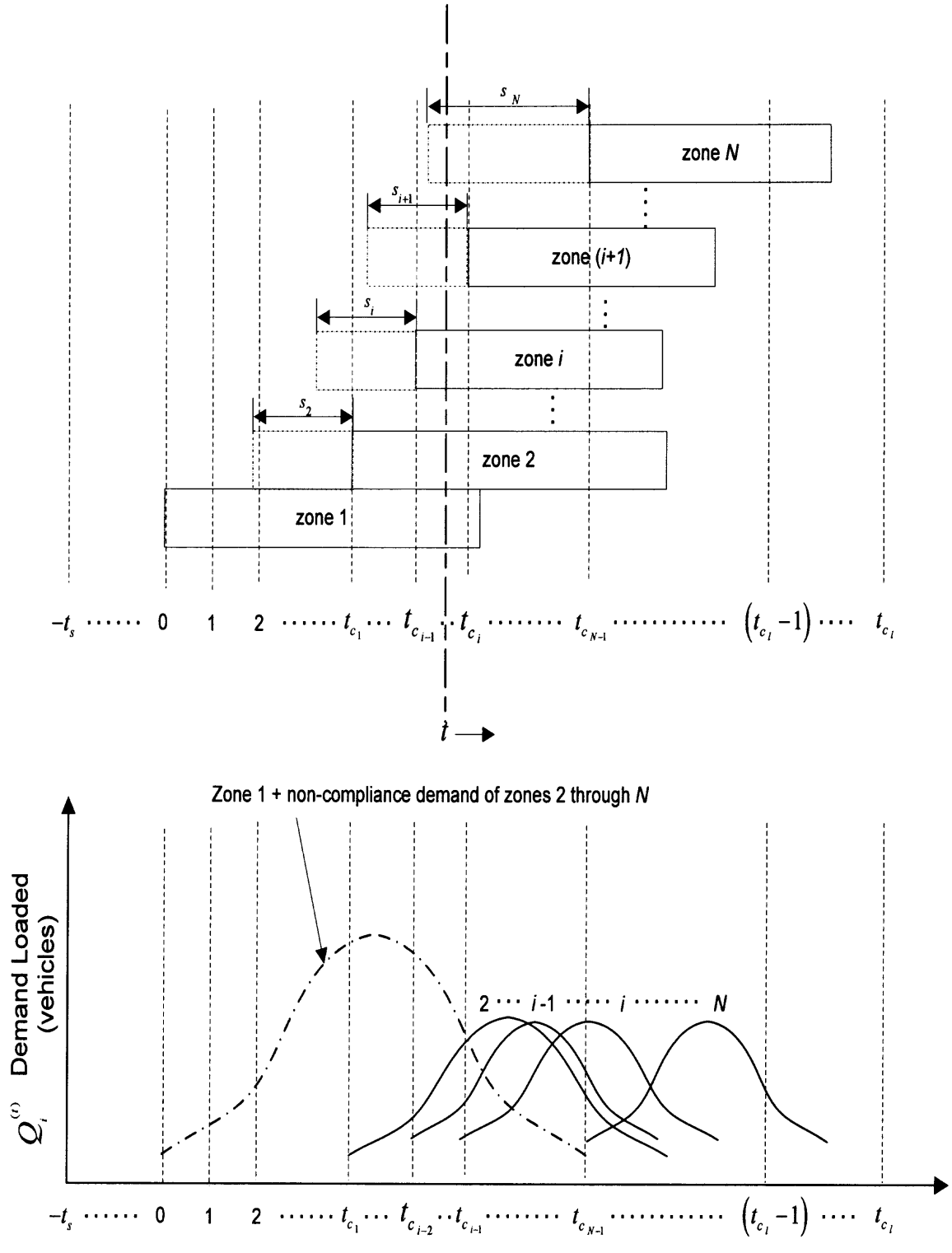

Figure 5.1 Time-windows of staged zones considering non-compliance effect.

Figure 5.2(a) shows the demand distribution considering 100% compliance, and it has been studied in the example discussed in Chapter 4. Figure 5.2(b) demonstrates that as the compliance demand of zones 2 through N reduces, the demand accessing the evacuation route while staging zone 1 at t increases. Similar situation may be found while staging later zones.

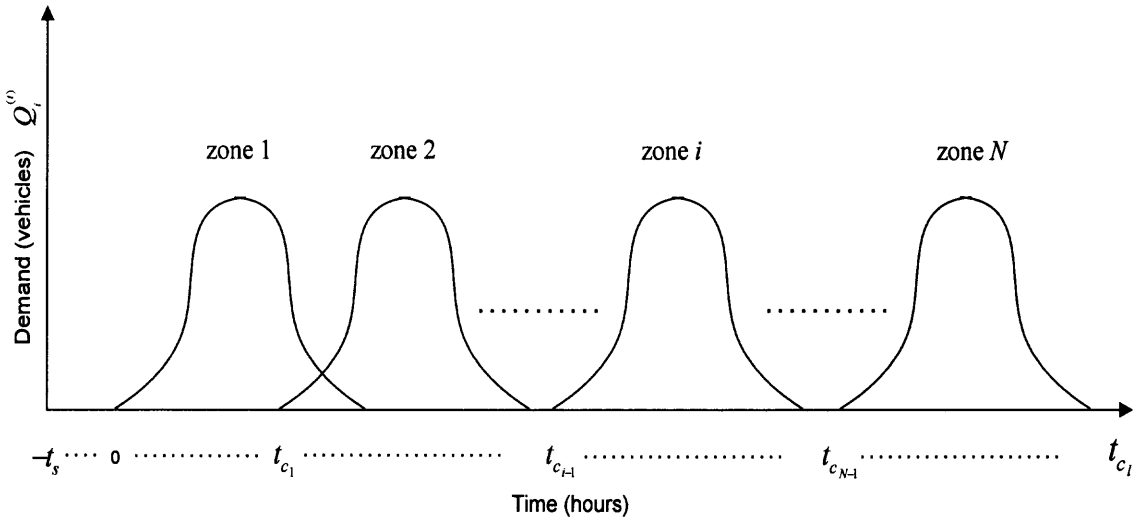

Figure 5.2(a) Demand distribution considering 100% compliance.

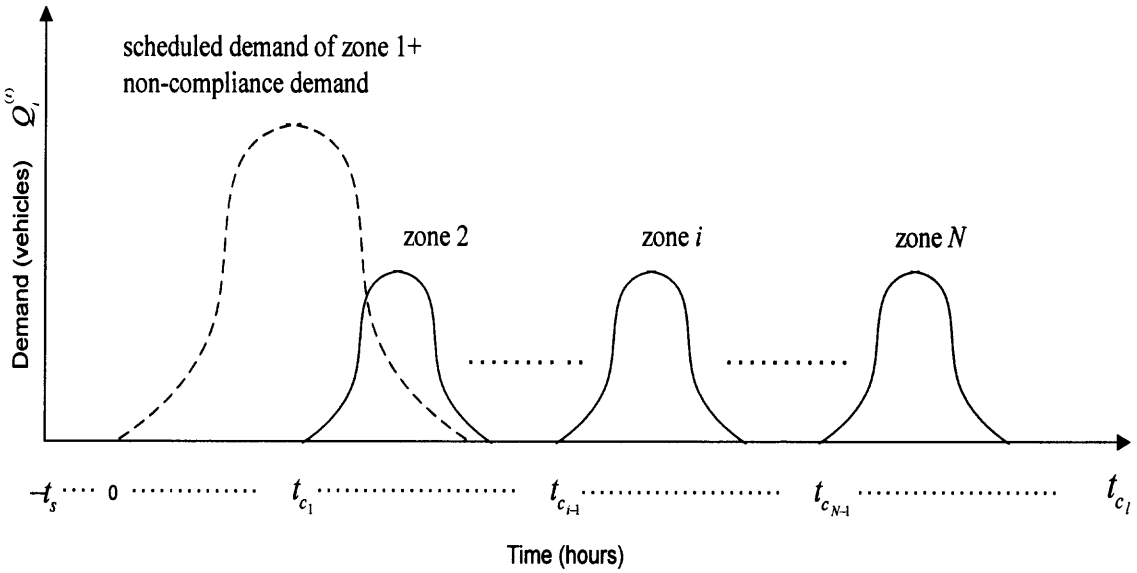

Figure 5.2(b) Demand distribution considering non-compliance effect.

Based on the discussion in Section 4.2.2.1(1), the percentage of compliance demand accessing from zone i at t ($q_{C_i}^{(t)}$) is

$$q_{C_i}^{(t)} = \left(\frac{1}{1+e^{-\alpha(t-\beta)}} - \frac{1}{1+e^{-\alpha(t-1-\beta)}} \right) \tag{5.5}$$

while the percentage of non-compliance demand accessing form zone i at t ($q_{N_i}^{(t)}$) is

$$q_{N_i}^{(t)} = \left(\frac{1}{1+e^{-\alpha(t+s_i-\beta)}} - \frac{1}{1+e^{-\alpha(t-1+s_i-\beta)}} \right) \tag{5.6}$$

Thus, by considering the non-compliance effect, the total demand accessing the evacuation route while staging zone i at t, denoted as $Q_{T_i}^{(t)}$, is the sum of the compliance demands of zones 1 through i accessing at t

$$Q_{C_i}^{(t)} = \sum_{i=1}^{i} \left(q_{C_i}^{(t)} P_i Q_i \right) \quad \forall i,t \tag{5.7}$$

and the non-compliance demand of zones 1 through N accessing at t

$$Q_{n_i}^{(t)} = \sum_{i=1}^{N} \left(q_{N_i}^{(t)} (1-P_i) Q_i \right) \quad \forall i,t \tag{5.8}$$

where $q_{C_i}^{(t)} P_i Q_i$ and $q_{N_i}^{(t)} (1-P_i) Q_i$ are the compliance and non-compliance demands of zone i accessing the evacuation route at t, respectively. Thus, $Q_{T_i}^{(t)}$ can be derived as

$$Q_{T_i}^{(t)} = \sum_{i=1}^{i} \left(q_{C_i}^{(t)} P_i Q_i \right) + \sum_{i=1}^{N} \left(q_{N_i}^{(t)} (1-P_i) Q_i \right) \quad \forall i,t \tag{5.9}$$

5.2 Revision of the Optimal Staging Scheme to Consider Non-compliance Effect

If the levels of compliance and the deviations of scheduled demand access times for all zones are known, the optimal staging scheme developed in Chapter 4 can be revised to accommodate the non-compliance demand. The revised staging scheme is determined by applying the staging model developed in Chapter 4 by considering the non-compliance demand in addition. Thus, in order to accommodate the non-compliance demand and effectively utilize capacity at *t*, the scheduled access demand is reduced by decreasing the length of a staged zone as discussed in Section 4.1.2.

Since the loading profile of non-compliance demand accessing the evacuation route at *t* ($Q_{n_i}^{(t)}$) is known, the length of staged zone *i* may be determined such that the loading profile of the total demand accessing the evacuation route while staging zone *i* at *t* ($Q_{T_i}^{(t)}$), results in a profile of the demand to be evacuated while staging zone *i* at *t* ($\bar{Q}_i^{(t)}$) that maximizes the total discharged volume between $t_{c_{i-1}}$ and t_{c_i}, which are the time points of staging zone *i*. Note that the determination of the optimal length of zone *i* is discussed in Section 4.2.2.2. $Q_{c_i}^{(t)}$, $Q_{n_i}^{(t)}$, and $Q_{T_i}^{(t)}$ are determined by Equations 5.7, 5.8, and 5.9, respectively.

Figure 5.3 shows the resulting profile of $\bar{Q}_i^{(t)}$ due to non-compliance effect. As shown in the figure, the discharge rate $\frac{\bar{Q}_i^{(t)}}{\delta_t}$ does not exceed (*c*) and (q_U) and thus maximizes the total discharged volume between $t_{c_{i-1}}$ and t_{c_i}. Note that *c*, q_L, and q_U are capacity, lower flow limit and upper flow limit, respectively. Thus, the revised length of

zone i restricts the compliance demand accessing the evacuation route over time and allows the inevitable non-compliance demand to discharge, thereby reducing congestion, and decreasing the evacuation time.

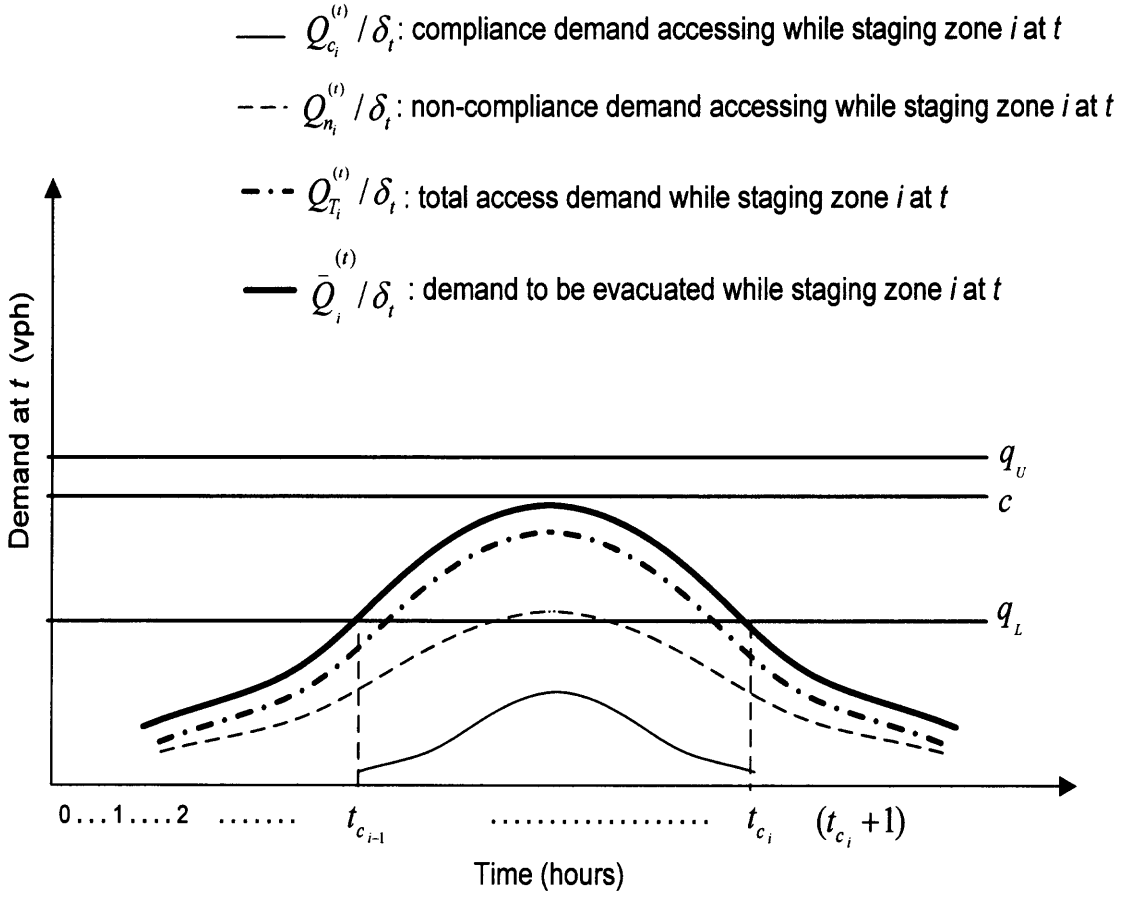

Figure 5.3 Selection of revised length of zone i.

The revision of the optimal staging scheme to accommodate the non-compliance demand is demonstrated using a numerical example discussed next.

5.3 Numerical Example

In this section, the level of compliance affecting the optimal staging scheme shown in Figure 4.17 is examined, while the background of this example is identical to the example presented in Chapter 4.

The length of the evacuation route L is assumed to be 15 miles. The evacuation region can be referred to Figure 4.7, which consists of a single evacuation route with one lane and the demand is linearly decreasing as shown in Figure 4.14. The demand density function $f(x)$ over the evacuation route can be referred to Equation 4.38. The highest demand density at the beginning of the evacuation route C is 2,500 vehicles/mile. By using Equation 4.38, the demand of the evacuation region Q is 20,000 vehicles. The parameters of the logit-based function formulated in Equation 4.1, namely response rate α and the half loading time β are 0.6 and 2.5 hours, respectively, for a fast response scenario. Also, the duration of shadow evacuation time t_S, capacity of the evacuation route c, the lower flow limit q_L, and the upper flow limit q_U, are 2 hours, 2,000 vph, 1,600 vph, and 2,075 vph, respectively.

By applying the model developed in Chapter 4, the optimal zone lengths for the example were 4.9, 3.8, and 6.3 miles as shown in Figure 4.17 and Table 4.8. The time needed for evacuating 90% of the total demand through simultaneous and the optimal staged evacuations were 18.87 hours and 11.7 hours, respectively. The reduction in evacuation time was 7.17 hours.

By considering different levels of compliance and deviations of scheduled demand access time for staged zones discussed in the optimal scheme shown in Figure 4.17 and Table 4.8, two scenarios are evaluated and results are used for demonstrating the

impacts of compliance levels on evacuation time and delay. If the optimal staging scheme is applied under varying levels of compliance, it is termed as the non-compliance scheme; on the other hand, if the optimal staging scheme is revised according to the level of compliance, it is termed as the revised scheme.

5.3.1 Scenario 1: Variable P_i with Fixed s_i

In Scenario 1, the effects of various levels of compliance with a constant deviation of scheduled demand access time of staged zones are considered. Thus, P_i may vary but s_i is fixed for all staged zones, over different cases. The levels of compliance of zones 2 and 3 denoted as P_2 and P_3, respectively, are identical for each case. s_i for the zones 2 and 3 is assumed to be 1 hour. Note that the non-compliance demand from zone 1 is considered in the estimation of shadow demand, and hence P_1 is 100% (i.e., $s_1 = 0$). The average compliance denoted as P for various combinations of P_2 and P_3 can be obtained by Equation 5.1 and summarized in Table 5.1.

Table 5.1 Level of Compliance

Case	P_2 (%)	P_3 (%)	P (%)
1	10	10	58
2	20	20	63
3	30	30	67
4	40	40	72
5	50	50	77

The resulting staged evacuation time (T_n) determined by Equation 4.25, reduced evacuation time (compared to simultaneous evacuation) (ΔT) determined by Equation 5.2, and effectiveness of staged evacuation (η) determined by Equation 5.3, for the 5

cases, are shown in Table 5.2. As shown in the table, generally, as P increases both ΔT and η increase.

Table 5.2 Effects of Levels of Compliance (P) (s_i = 1 hour)

Case	Average Compliance P (%)	Evacuation Time for 90% of Demand (hours) T_n	Reduced Evacuation Time (hours) ΔT	Effectiveness of Staged Evacuation, η (%)
1	58	17.23	1.64	22.93
2	63	17.23	1.64	22.85
3	67	17.16	1.71	23.85
4	72	17.09	1.78	24.81
5	77	17.03	1.84	25.71

Figure 5.4 shows the total delay over time for various P while s_i = 1 hour.

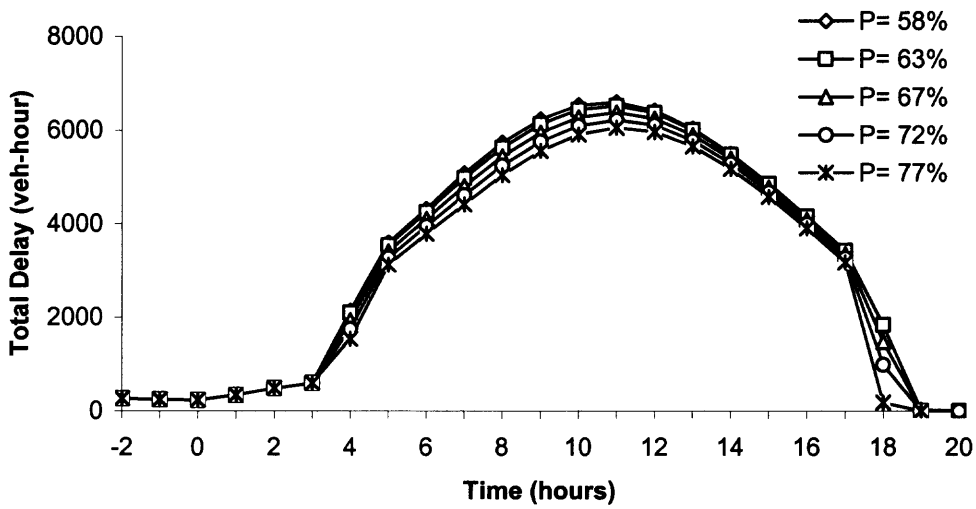

Figure 5.4 Total delay vs. time for various P (s_i = 1 hour).

As P increases, the total delay of evacuation (D_T) decreases due to lesser congestion due to regulated demand accessing the evacuation route that reduces congestion.

Revision of the Optimal Staging Scheme for Scenario 1

In this section, the revision of the optimal staging scheme for various P at constant s_i is analyzed. The method to revise the optimal staging scheme is discussed in Section 5.2.

Table 5.3 presents T_n, ΔT, and η of the revised scheme for Scenario 1. Note that although the evacuation times for Cases 3, 4, and 5 are less than that of the optimal staging scheme (11.7 hours), the demand evacuated from the most densely populated regions in the 90% of total demand used as a measure of effectiveness, MOE, for these cases, is not as high as that of the optimal staging scheme. In other words, it is possible to reduce the evacuation time further than that of the optimal staging scheme (T_{opt}) by evacuating sparsely populated zones in conjunction with the densely populated zones, but is not desirable. Thus, $\eta > 100\%$ for Cases 3, 4, and 5 as T_n is less than the evacuation time of the optimal staging scheme.

Table 5.3 Revised Staging Scheme for Various P ($s_i = 1$ hour)

Case	Average Compliance P (%)	Evacuation Time for 90% of Demand (hours) T_n	Reduced Evacuation Time (hours) ΔT	Effectiveness of Staged Evacuation η (%)
1	58	12.26	6.61	92.14
2	63	11.99	6.88	95.98
3	67	11.64	7.23	100.83
4	72	11.66	7.21	100.60
5	77	11.41	7.46	103.98

Figure 5.5 shows the improvement of η with the revised staging scheme over the non-compliance scheme for various P.

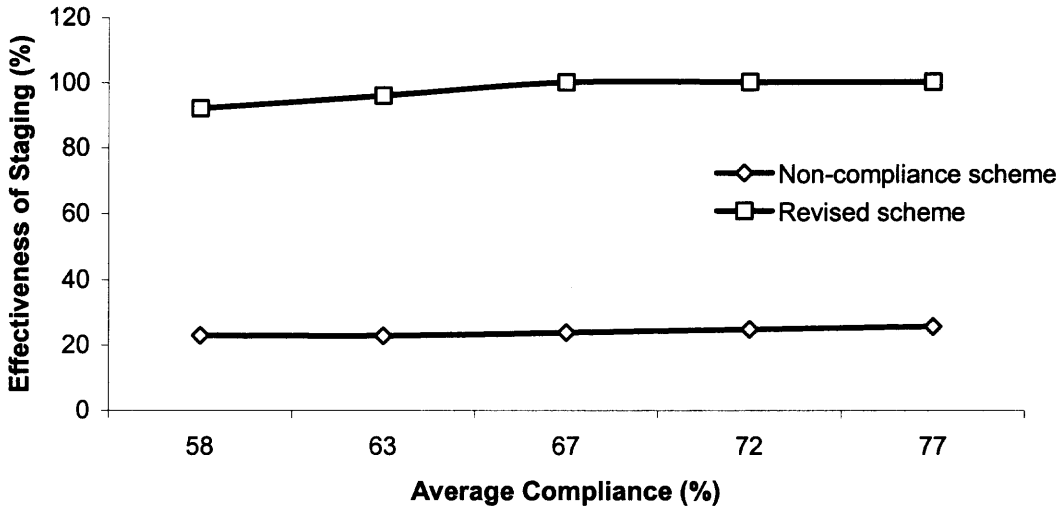

Figure 5.5 Effectiveness of staging vs. average compliance (η vs. P).

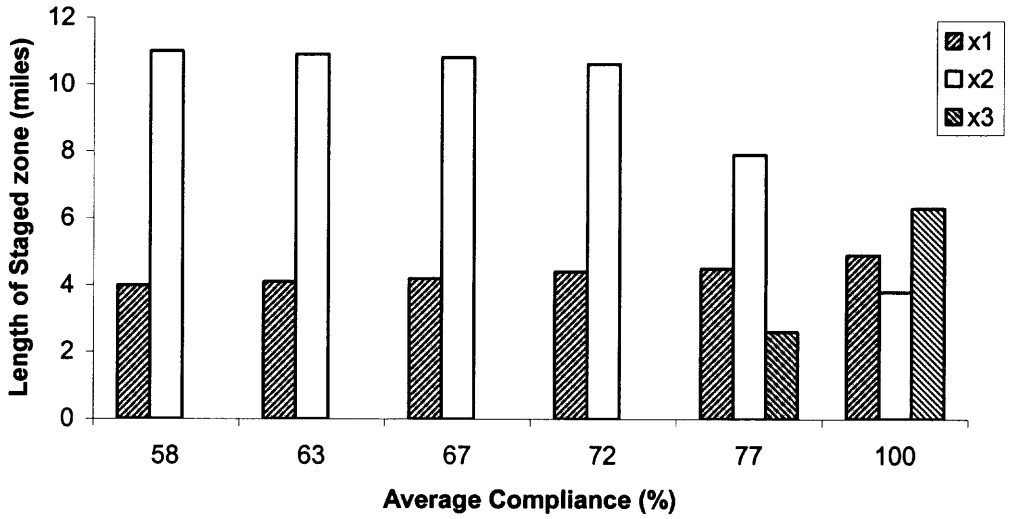

Figure 5.6 Staged zone lengths for various P for revised scheme.

Figure 5.6 shows the lengths of the staged zones for the revised scheme for various P. As shown in the figure, the length of zone 1 of the revised scheme is less than that of the optimal scheme that considers 100% compliance due to increase in the demand to be

evacuated while staging zone 1 at t ($\bar{Q}_1^{(t)}$), caused by the non-compliance demand. But, the duration of staging zone 1 increases for the revised scheme in order to discharge a large non-compliance demand. Also, the revised zone 1 is longer at greater P due to a lower non-compliance demand, which reduces $\bar{Q}_1^{(t)}$. To this end, a longer zone length is required to discharge a greater volume.

Table 5.4 shows the demand distribution for the revised scheme for Case 1 (P =58 %). The definitions of the variables used in the table are as below.

$Q_{c_i}^{(t)}$: compliance demand of zones 1 through i accessing at t,

$Q_{n_i}^{(t)}$: non-compliance demand of zones 1 through N accessing at t,

$Q_{T_i}^{(t)}$: Total demand accessing while staging zone i at t,

$\bar{Q}_i^{(t)}$: demand to evacuated while staging zone i at t,

$u_i^{(t)}$: speed of the evacuation route at while staging zone i at t,

$T_i^{(t)}$: evacuation time for $\bar{Q}_i^{(t)}$ while staging zone i at t,

$d_i^{(t)}$: vehicles queued while staging zone i at t,, and

$Q_E^{(t)}$: discharged volume at t.

As shown in the table, the compliance demand accessing the evacuation route while staging zone 1 (x_1 = 4 miles) at t ($Q_{c_1}^{(t)}$), results in $\bar{Q}_1^{(t)}$, which causes negligible congestion, and maximizes the discharge rate between t = 0 to 8, by considering non-compliance effect.

Table 5.4 Demand Distribution of Revised Scheme for Case 1: P = 58% (s_i = 1 hour)

		Zone 1 (x_1 = 4.0 miles)						Zone 2 (x_2 = 11.0 miles)						
(t) (hr)	$Q_{n_i}^{(t)}$ (veh)	$Q_{c_1}^{(t)}$ (veh)	$Q_{T_1}^{(t)}$ (veh)	$u_1^{(t)}$ (mph)	$T_1^{(t)}$ (hr)	$\bar{Q}_1^{(t)}$ (veh)	$d_1^{(t)}$ (veh)	$Q_{c_2}^{(t)}$ (veh)	$Q_{T_2}^{(t)}$ (veh)	$u_2^{(t)}$ (mph)	$T_2^{(t)}$ (hr)	$\bar{Q}_2^{(t)}$ (veh)	$d_2^{(t)}$ (veh)	$Q_E^{(t)}$ (veh)
-2	-	1259	**1259**	47	1.23	1259	232	-	-	-	-	-	-	**1028**
-1	-	922	**922**	47	1.23	1154	213	-	-	-	-	-	-	**942**
0	-	660	**660**	49	1.27	873	185	-	-	-	-	-	-	**688**
1	-	960	**960**	47	1.28	1145	250	-	-	-	-	-	-	**894**
2	-	1229	**1229**	45	1.29	1479	335	-	-	-	-	-	-	**1145**
3	-	1340	**1340**	43	1.31	1675	392	-	-	-	-	-	-	**1283**
4	**363**	1229	**1592**	41	1.32	1984	482	-	-	-	-	-	-	**1502**
5	**528**	960	**1488**	41	1.32	1970	478	-	-	-	-	-	-	**1491**
6	**676**	660	**1336**	43	1.31	1814	425	-	-	-	-	-	-	**1389**
7	**991**	415	**1406**	42	1.31	1831	437	-	-	-	-	-	-	**1395**
8	**1045**	247	**1292**	44	1.30	1729	398	-	-	-	-	-	-	**1331**
9	**1001**					1540		190	**1190**	43	1.30	1730	395	**1335**
10	**879**							276	**1154**	44	1.29	1629	365	**1264**
11	**701**							353	**1054**	45	1.28	1464	323	**1140**
12	**505**							385	**890**	47	1.27	1238	266	**972**
13	**332**							353	**685**	49	1.26	964	201	**763**
14	**204**							276	**479**	51	1.25	688	140	**548**
15	**119**							190	**309**	52	1.25	453	91	**362**
16	**68**							119	**187**	53	1.25	280	55	**225**
17	**38**							71	**109**	54	1.24	164	32	**132**
18	**21**							41	**62**	55	1.00	94	18	**76**
19	**12**							23	**35**	55	1.00	53	10	**43**
20	**6**							13	**19**	55	1.00	29	6	**24**
21	**3**							7	**10**	55	1.00	16	3	**13**
22	**2**							4	**5**	55	1.00	8	2	**7**
23	**1**							2	**3**	55	1.00	5	1	**4**
24	**0**							1	**1**	55	1.00	2	0	**2**
25								1	**1**	55	1.00	1	0	**1**

As compared to the optimal staging scheme shown in Figure 4.17 where $x_1 = 4.9$ miles for t = 0 to 4, x_1 for the revised scheme decreases, but the duration of staging of zone 1 increases (i.e., t = 0 to 8) in order to discharge the non-compliance demand, which begins to access the evacuation route at t = 4. Note that $Q_{c_i}^{(t)}, Q_{n_i}^{(t)}$, and $Q_{T_i}^{(t)}$ are determined by Equations 5.7, 5.8, and 5.9, respectively. The determination of parameters $\bar{Q}_i^{(t)}, u_i^{(t)}, T_i^{(t)}, d_i^{(t)}$ and $Q_E^{(t)}$ can be referred to Section 4.3.1.

Figure 5.7 and Table 5.5 show the total delay for the revised scheme over time for various P while s_i = 1 hour. As show in the table, the total delay of the revised scheme as compared to that of the non-compliance scheme is significantly lower for all cases.

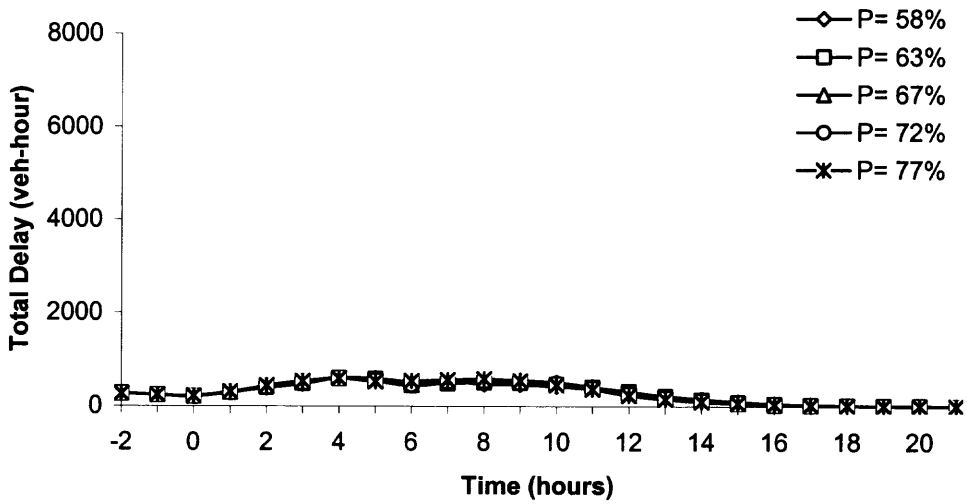

Figure 5.7 Total delay vs. time for various P (s_i = 1 hour) for the revised scheme.

Table 5.5 Total Delay for Various P ($s_i = 1$ hour)

Case	Average Compliance P (%)	Non-compliance Scheme D_T (veh-hour)	Revised Scheme D_T (veh-hour)
1	58	74,115	6,268
2	63	73,345	6,301
3	67	71,185	6,298
4	72	68,668	6,238
5	77	65,689	6,333

5.3.2 Scenario 2: Variable s_i with Fixed P

In Scenario 2, the effects of variation of deviation of scheduled demand access times of zones at a constant average level of compliance are studied. Thus, s_i may vary but P are fixed (77%) for the demand of zones 2 and 3, for different cases. Note that P_1 is assumed 100% ($s_1 = 0$), and s_i for the various cases are shown in Table 5.6.

Table 5.6 Deviation of Scheduled Demand Access Time

Case	s_2 (hour)	s_3 (hour)
1	1.0	1.0
2	2.0	2.0
3	3.0	3.0
4	4.0	4.0
5	5.0	5.0

The resulting staged evacuation time (T_n) determined by Equation 4.25, reduced evacuation time (compared to simultaneous evacuation) (ΔT) determined by Equation 5.2, and effectiveness of staged evacuation (η) determined by Equation 5.3, for the above cases, are shown in Table 5.7. As shown in the table, η is lower at higher s_i and is the lowest at as s_i = 4, 5, because congestion occurs early causing the demand buildup to

last longer, i.e., a high demand accessing the evacuation route in early periods of staging takes a longer time to discharge due to a low discharge rate.

Table 5.7 Effects of Various s_i for $(P = 77\%)$

Case	Deviation of Scheduled Access Time (hours) s_i	Evacuation Time for 90% of Demand (hours) T_n	Reduced Evacuation Time (hours) ΔT	Effectiveness of Staged Evacuation η (%)
1	1.0	17.03	1.84	25.71
2	2.0	18.08	0.79	10.99
3	3.0	18.14	0.73	10.24
4	4.0	18.29	0.58	8.11
5	5.0	18.29	0.58	8.10

The demand loading profile of the optimal staging scheme discussed in Chapter 4, (Table 4.8), and Scenario 2 (Case-5) can be observed from Figures 5.8 and 5.9, respectively. Figure 5.8 shows the demand distribution of individual zones, and aggregate demand of zones over time.

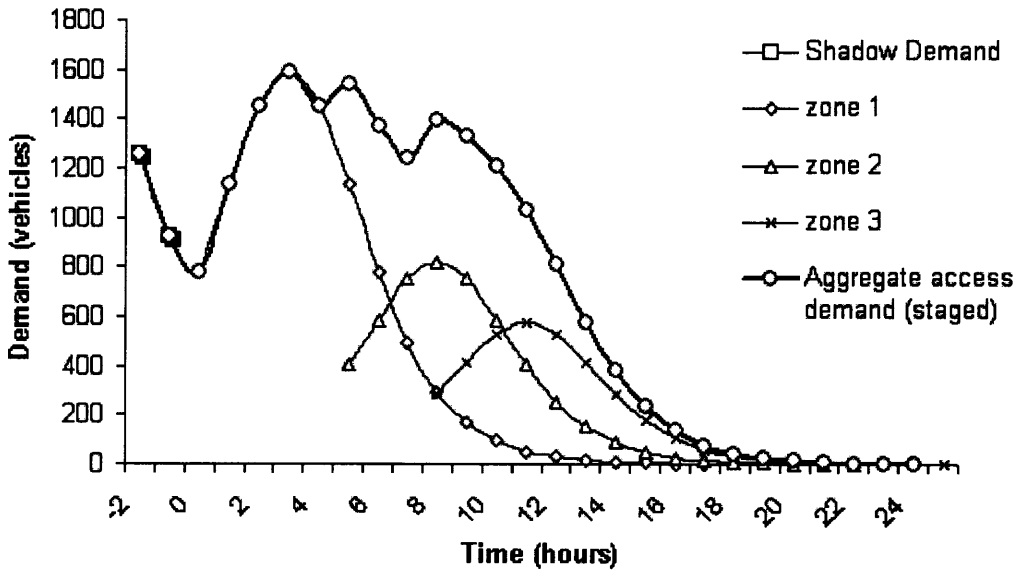

Figure 5.8 Demand distribution for all staged zones (optimal staging scheme).

As shown in Figure 5.9, for the case $s_2 = s_3 =$ 5 hours, the demand accessing the evacuation route while staging zone 1 increases, which results in significant congestion at t = 2, 3 and 4, as shown in Table 5.8. The definitions of the variables can be referred to Table 5.5.

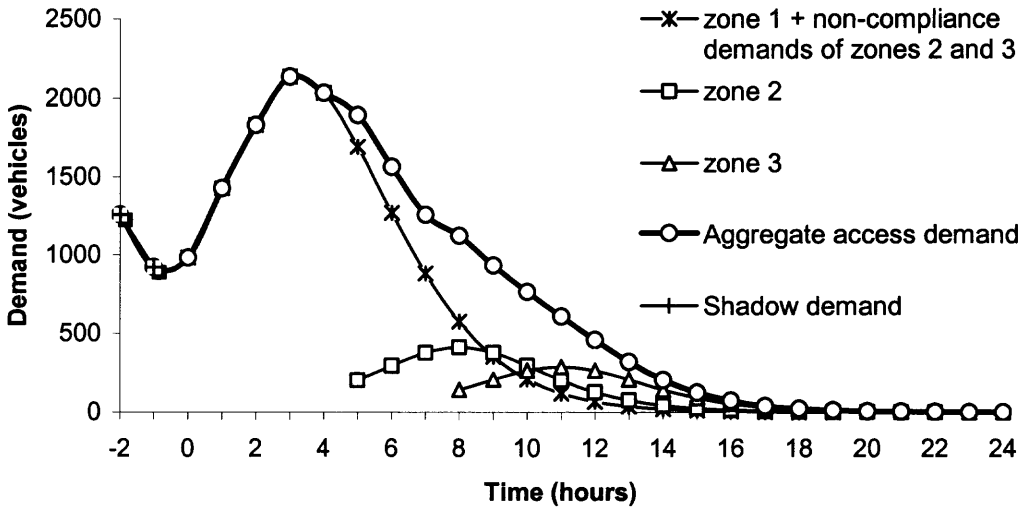

Figure 5.9 Demand loading profile with $s_2 = s_3 = 5$ hours (P = 77 %).

Table 5.8 Demand Distribution ($s_2 = s_3 = 5$ hours and $P = 77\%$)

(t) (hr)	$Q_{n_1}^{(t)}$ (veh)	$Q_{c_1}^{(t)}$ (veh)	$Q_{T_i}^{(t)}$ (veh)	$u_1^{(t)}$ (mph)	$k_1^{(t)}$ (vpmpl)	$\bar{Q}_1^{(t)}$ (veh)	$T_1^{(t)}$ (hr)	$d_1^{(t)}$ (veh)	$Q_E^{(t)}$ (veh)
-2	-	-	-	47	27	1259	1.23	232	**1028**
-1	-	-	-	47	25	1154	1.23	213	**942**
0	**202**	781	983	47	21	1195	1.27	1195	**940**
1	**293**	1136	1429	43	30	1685	1.30	1685	**1299**
2	**375**	1454	1830	14	41	2216	2.59	2216	**854**
3	**551**	1586	2137	6	130	3499	6.63	3499	**788**
4	**581**	1454	2035	6	130	4746	8.23	4746	**788**
5	**556**	1136	1692			5649		5649	

Figure 5.10 shows the total delay over time for various s_i for $P = 77\%$. As s_i increases, the total delay of evacuation (D_T) increases due to greater congestion as shown in Table 5.9 (e.g., $s_2 = s_3 = 5$).

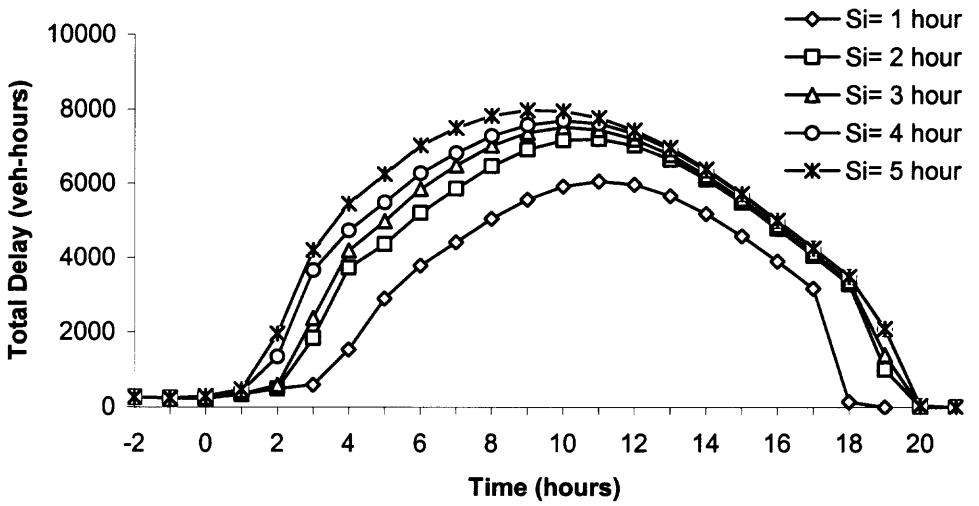

Figure 5.10 Total delay vs. time for various s_i at $P = 77\%$.

Revision of the Optimal Staging Scheme for Scenario 2

In this section, the revision of the optimal staged scheme developed in Chapter 4 for varying s_i at constant P is analyzed. Table 5.10 presents T_n, ΔT, and η of the revised scheme for Scenario 2. As shown in the table η is significantly higher than that of the non-compliance scheme for various cases shown in Table 5.8.

Table 5.9 Revised Staging Scheme for Various s_i ($P = 77\%$)

Case	Deviation of Scheduled Access Time (hours) s_i	Evacuation Time for 90% of Demand (hours) T_n	Reduced Evacuation Time (hours) ΔT	Effectiveness of Staged Evacuation η (%)
1	1.0	11.41	7.46	100.00
2	2.0	11.71	7.16	99.90
3	3.0	11.70	7.17	100.00
4	4.0	12.07	6.80	94.83
5	5.0	11.73	7.14	99.59

Figure 5.11 shows the improvement of η with the revised staging scheme over the non-compliance scheme for various s_i.

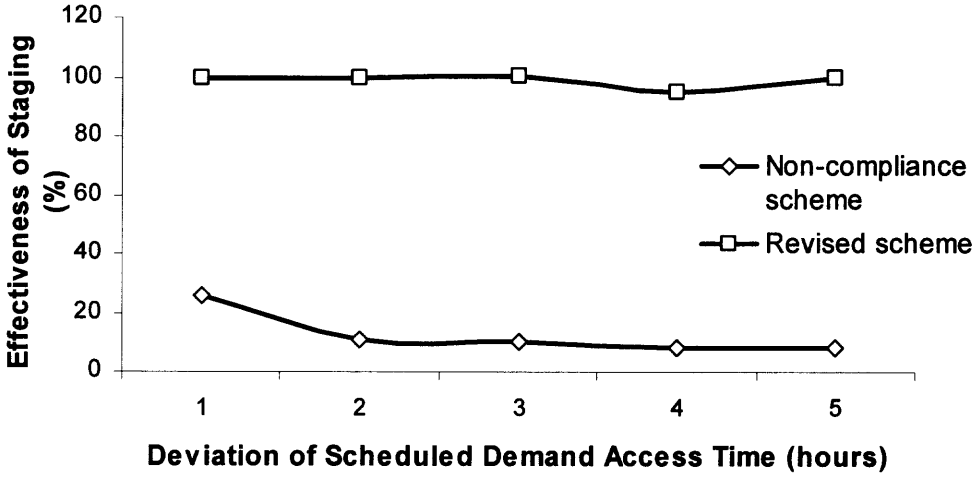

Figure 5.11 Effectiveness of staging vs. deviation of scheduled demand access time.

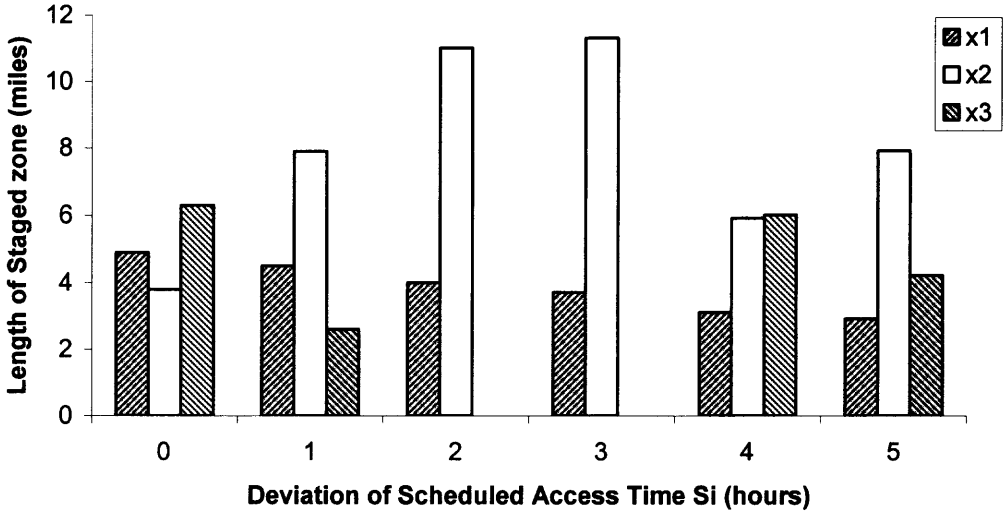

Figure 5.12 Staged zone lengths for various s_i for revised scheme.

Figure 5.12 shows the lengths of the staged zones for the revised scheme for various s_i. As shown in the figure, the length of zone 1 of the revised scheme is less than that of the optimal scheme that considers 100% compliance ($s_i = 0$) due to increase in the demand to be evacuated at t while staging zone 1, $\bar{Q}_1^{(t)}$, caused by the non-compliance demand. Also, the revised zone 1 is shorter at greater s_i due to a higher non-compliance demand, which enhances $\bar{Q}_1^{(t)}$. Evidently, a shorter zone length is required to discharge a greater non-compliance demand.

Figure 5.13 and Table 5.10 show the total delay for the revised scheme over time for various s_i for $P = 77\%$. As shown in the table, the total delay of the revised scheme as compared to that of the non-compliance scheme is significantly lower for all cases of s_i.

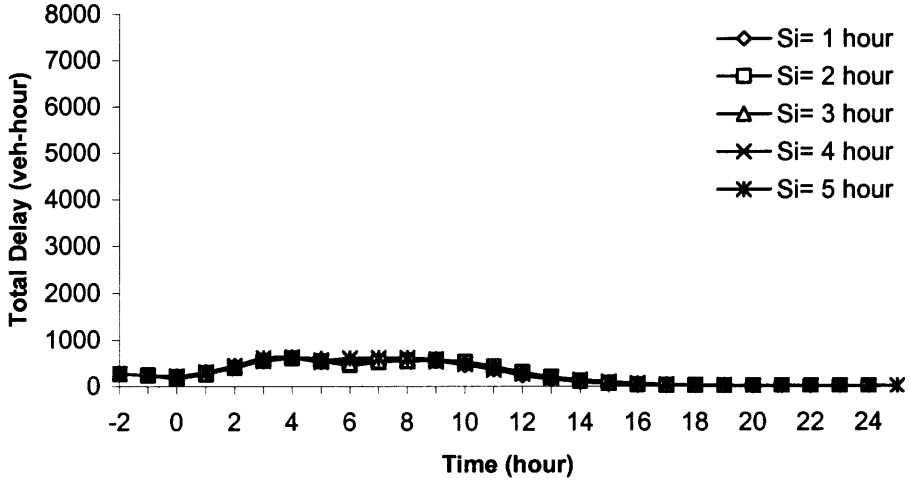

Figure 5.13 Total delay vs. time for various s_i as $P = 77\%$ for the revised scheme.

Table 5.10 Total Delay for Various s_i ($P = 77\%$)

Case	Average Compliance P (%)	Non-compliance Scheme D_T (veh-hour)	Revised Scheme D_T (veh-hour)
1	1	65,426	6,333
2	2	88,120	6,383
3	3	93,817	6,512
4	4	100,272	6,543
5	5	106,011	6,761

5.4 Summary

In this chapter the practicability of staged evacuation due to the effects of various compliance levels of staged zones to evacuation order was investigated. Compliance here is defined as the conformity of a staged zone to its demand loading pattern and the corresponding scheduled demand access time, according to the optimal staged scheme developed in Chapter 4. The effectiveness of a staged evacuation scheme due to variation in compliance levels was also investigated. The factors that primarily influence the

effectiveness of staged evacuation are the level of compliance of zones denoted as P_i, and deviation of scheduled demand access time of zones denoted as s_i.

For a given s_i for all zones, the reduced evacuation time by staged evacuation as compared to simultaneous evacuation, and effectiveness of staging were found to increase with increase in levels of average compliance denoted as P. Also, for a given P_i for all zones, the reduced evacuation time, and effectiveness of staging, were found to decrease with increase in s_i.

In order to account for the non-compliance of the zones, the optimal staged scheme was revised. It was found that the length of zone 1 of the revised scheme for various P_i at constant s_i is less than that of the optimal scheme. Also, the revised zone 1 is longer at greater P due to a lower non-compliance demand. While the length of zone 1 of the revised scheme for various s_i at constant P is less than that of the optimal scheme, the revised zone 1 is shorter at higher s_i due to a greater non-compliance demand that causes congestion in early periods of staging.

CHAPTER 6

CONCLUSIONS

In this study analytical models were developed to optimize the evacuation scheme by minimizing evacuation time and the associated delays. In this chapter the results and findings are summarized and recommendations for future work are presented. This chapter is organized into the following sections: Section 6.1 presents the important results and findings of this study; Section 6.2 discusses the research contributions; and finally Section 6.3 identifies critical areas of interest for future research and makes valuable recommendations.

6.1 Results and Findings

Analytical models were developed for estimating evacuation time and the associated delays, and the impacts of a simultaneous and a staged evacuation were analyzed. Evacuation time was defined as the time required for evacuating all vehicles from a designated region, while the delay included queuing and moving delays. A comprehensive literature review was conducted of various evacuation models to determine their advantages and limitations. Some previous studies dealt with staged evacuation, but the quantitative analysis between the impacts of simultaneous and staged evacuations was limited. This study discussed some important issues that were not thoroughly investigated in the past, including the effects of critical parameters (e.g., speed, vehicle density, access flow, etc) on evacuation time, evacuees' behavioral

response including loading patterns, demand distribution over the evacuation route, effects of congestion on capacity of evacuation routes, etc.

The base model developed in Chapter 3 optimized the number of staged zones for a given set of conditions (e.g., uniformity of access flow, demand, and capacity, etc) under deterministic behavior. A numerical approach was developed to search the optimal number of stages that minimizes the total evacuation time while analyzing the associated delay. In the example discussed in Chapter 3, the evacuation time was a convex curve, where the minimum number of stages denoted as N was reached at 3. In addition, the delay decreased significantly with the increase of the number of stages and was the lowest at $N = 5$. It was also found that the evacuation time is primarily influenced by the discharge time, depending on the traffic volume. In addition, the delay under congested conditions is contributed by the queuing delay incurred by evacuees waiting to exit the evacuation route. A sensitivity analysis was conducted and the parameters that were considered as the most sensitive (including access flow rate, demand, and the evacuation route length) to the evacuation time and delay were identified. The findings of the analysis in Chapter 3 are summarized as follows:

- The optimal number of stages at which the evacuation time is minimum increases as the access flow rate increases. Also, lower access flow rates lead to lower delays for a given number of stages.

- The minimum evacuation time was attained at $N = 3$ for all values of demand (5,000 vehicles to 25,000 vehicles), although, the evacuation time increased with the increase of demand for any value of N. Also, the delay increased with the increase of demand for any N due to increased volume entering the route.

- The optimal number of stages at which the evacuation time is minimum, increased with increase in the length of the evacuation route, L. Also, for a given N, the delay increased with L.

An Enhanced Model I was developed in Chapter 4, considering heterogeneous demand distribution over the evacuation route and evacuees' behavioral responses (e.g., fast, medium, and slow) to evacuation orders. A review of various behavioral models was conducted and the Behavioral response curves model (Sigmoid or S-Curves) was selected for modeling evacuees' behavior in the Enhanced Model I. Based on a numerical searching process, the staging scheme including the time windows and lengths of staged zones was optimized, considering demand distribution, behavioral response of evacuees, and evolution of traffic conditions on the evacuation route. Unlike the base model, the Enhanced Model I determines the zone lengths by regulating the demand accessing the evacuation route to effectively utilize available capacity. Hence, the lengths of the staged zones are unequal. The model was tested in a numerical example. It was found that the evacuation time and delay of staged evacuation as compared to simultaneous evacuation was substantially lower than that of simultaneous evacuation. A sensitivity analysis of the effect of demand and capacity on evacuation time and delay was conducted, the findings of which are summarized below.

- The reduction in evacuation time by staged evacuation was higher at greater demand. In addition, the total delays for both simultaneous and staged evacuations were higher at greater demand.
- While similar results were observed when the capacity of the evacuation route is enhanced through contraflow, no reduction in evacuation time by staged evacuation was observed at low demand when contraflow or lane reversal is utilized.

Finally, the practicability of staged evacuation at various levels of compliance was explored in Chapter 5. An Enhanced Model II, an extension of the Enhanced Model I, was developed by considering the impact of compliance level. Compliance was defined

as the conformity of a staged zone to its demand loading pattern. The Enhanced model II was tested in a numerical example.

Results indicate that the level of compliance and deviation from the scheduled demand access time of staged zones influence the effectiveness of staging. For given deviations of the scheduled demand access times for all zones, the reduction in evacuation time by staging, and effectiveness of staging were found to increase with increase in compliance levels. Also, for given levels of compliance for all zones, the reduction in evacuation time and effectiveness of staging were found to decrease with increase in deviation of the scheduled demand access time.

To accommodate the non-compliance demand of the zones, a method to revise the optimal staged scheme was illustrated. The length of zone 1 of the revised scheme for various levels of average compliance at a constant deviation of scheduled demand access time was less than that of the optimal scheme. Also, the revised length of zone 1 was longer for greater average compliance due to a lower non-compliance demand. While the length of zone 1 of the revised scheme for various deviations of scheduled demand access time at constant average level of compliance was less than that of the optimal scheme, the revised zone 1 was shorter at higher deviation of the scheduled demand access time due to a greater non-compliance demand that causes congestion in early periods of staging.

6.2 Contributions

The objective of this research was to optimize a staged evacuation by minimizing evacuation time and the associated delays. The applicability of the model and the reduction in evacuation time achieved by staged evacuation over simultaneous evacuation were demonstrated using numerical examples.

The methodology presented in this research comprised of models that could be applied under varying demand distribution and evacuation response scenarios. Sensitivity analysis of key parameters, namely access flow rate, demand, and evacuation route length for the base model revealed the relationships among variables and identified the relative importance of factors that contribute to them. Since evacuees' behavioral response to evacuation orders (fast, medium, and slow) and demand distribution over the evacuation route affects the evacuation time, a more realistic estimation of evacuation time and delay was achieved by incorporating behavioral aspects using the S-shaped logit-based function. The Enhanced model I developed for stochastic behavioral response and heterogeneous demand distribution, defined a sequential step procedure to achieve the optimal staging scheme. The results of the model can be used to recommend the time windows and lengths of staged zones based on the prevailing evacuation circumstances (e.g., behavioral response, demand distribution, length of the evacuation route, etc).

The time taken for evacuating 90% of the demand, used as a measure of effectiveness (MOE) by staged evacuation is significantly lower than that of simultaneous evacuation. The effectiveness of staged evacuation under excess capacity was investigated and it was found that the reduction in evacuation time through staged evacuation over simultaneous evacuation is greater at higher demand and no reduction in

evacuation time is achieved for low demand when excess capacity is available. The methodology presented in this research showed that temporal regulation of demand accessing the evacuation route through the overlapping arrangement of time windows of staged zones can enhance the discharged volume and reduces evacuation time and delays significantly.

An analysis of the practicability of staged evacuation showed that the levels of compliance and deviation of scheduled demand access time of staged zones influence the effectiveness of staging. In addition, a method to revise the optimal staging scheme to accommodate the non-compliance demand was developed.

The models developed in this research can serve as useful tools to provide suitable guidelines for emergency management authorities in making critical decisions during the evacuation process.

6.3 Recommendations for Future Research

In this research, heterogeneous demand distribution over the evacuation region and evacuees' behavioral responses (e.g., fast, medium, and slow) to evacuation orders were considered. Although this research employed the Behavioral response curves (Sigmoid or S-Curves) model for loading evacuation demand onto the evacuation network, other models (e.g., sequential-logit model) can be used. Also, it is possible to model dynamic behavioral response patterns that can vary based on the traffic conditions on the evacuation routes.

The effects of various levels of compliance on evacuation time and delay of staged evacuation were demonstrated in this research. The factors that potentially affect

the effectiveness of staged evacuation include communications amongst emergency personnel and evacuees, responses to evacuation orders (fast, medium, or slow), traffic control at intersections, availability of alternative evacuation routes, demand, etc. Thus, it is possible to develop a thorough model to assess the impacts of these factors on the effectiveness of staged evacuation.

The methodology developed in this research employed Edie's and Akçelik's models to estimate the speed-density relationship and the corresponding discharge rate of the evacuation route. However, if possible, data obtained during evacuations can be used to calibrate the flow-density relationships under congested flow conditions to achieve more accurate estimates of evacuation time and delay.

The model developed in this research minimized evacuation time and delay for the most densely populated region. The 90% of demand evacuated, which is used as a measure of effectiveness, primarily includes demand from populous areas. It is also possible to develop a more complex model to globally minimize evacuation time and delay by evacuating sparsely populated regions in conjunction with dense areas.

REFERENCES

Akçelik, R., Traffic Models, August 2004, Retrieved on September 22, 2005 from http://www.aatraffic.com/TrafficModels.htm.

Akçelik, R., Travel Time Functions for Transport Planning Purposes: Davidson's Function, its Time-Dependent Form and an Alternative Travel Time Function, *Australian Road Research, Volume 21*, Number 3, pp. 49-59, 1991.

Baker, E.J., Hurricane Evacuation Behavior, *International Journal of Mass Emergencies and Disasters, Volume 9*, Number 2, pp. 287-310,1991.

Barrett, B., Bin,R., and Pillai,R., Developing a Dynamic Traffic Management Modeling Framework for Hurricane Evacuation, *Transportation Research Record 1733*, Transportation Research Board, pp. 115-121, 2000.

Batty, M., Desyllas, J., and Duxbury, E., The Discrete Dynamics of Small-Scale Spatial Events: Agent-Based Models of Mobility in Carnivals and Street Parades, *International Journal of Geographical Information Science, Volume 17*, Number 7, pp. 673-697, 2003.

Burkard, R.E., Dlaska, K., and Klinz, B., The Quickest Flow Problem, *ZOR Methods and Models of Operations Research, Volume 37*, pp. 31-58, 1993.

Cayford, R., Lin, W.H., and Daganzo, C.F., The NETCELL Simulation Package: Technical description, *California PATH Research Report UCB-ITS-PRR-97-23*, University of California, Berkeley, 1997. Retrieved on February 20, 2006 from http://citeseer.ifi.unizh.ch/cayford97netcell.html.

Church, R.L. and Sexton, R.M., Modeling Small Area Evacuation: Can Existing Transportation Infrastructure Impede Public Safety?, Final Report to the California Department of Transportation, 2002. Retrieved on Mar 1, 2005 from http://www.ncgia.ucsb.edu/vital/research/pubs/200204-Evacuation.pdf.

Chen, Y. L., and Chin, Y. H, The Quickest Path Problem, *Computers and Operations Research, Volume 17*, 1990.

Chen, X., and Zhan, B.F., Agent-Based Modeling and Simulation of Urban Evacuation: Relative Effectiveness of Simultaneous and Staged Evacuation Strategies, *Transportation Research Board*, 83rd Annual Meeting, Washington D.C., 2004.

Cova, T. J., and Johnson, J.P., Microsimulation of Neighborhood Evacuations in the Urban -Wildland Interface, *Environment and Planning A, Volume 34*, pp. 2211 - 2229, 2002.

Cova, T. J., and Johnson, J.P., A Network Flow Model for Lane-Based Evacuation Routing, *Transportation Research Part A, Volume 37*, pp. 579-604, 2003.

Chen, G. H., and Hung, Y. C., On the Quickest Path Problem, *Information Processing Letters 46*, 1993.

Church, R.L., and Cova, T. J., Mapping Evacuation Risk on Transportation Networks using a Spatial Optimization Model, *Transportation Research Part C: Emerging Technologies, Volume 8*, Number 1, pp. 321-336, 2000.

Creamer, M., and Ludwig, J., A Fast Simulation Model for Traffic Flow on the Basis of Boolean operations, *Mathematical and Computers in Simulation, Volume 28*, pp. 297-303, 1986.

Collins, R., Using ITS in Helping Florida Manage Evacuations, *Technical Presentation to the 2001 National Hurricane Conference*, Washington D.C., 2001

Davidson, K. B., The Theoretical Basis of a Flow–Travel Time Relationship for Use in Transportation Planning, *Australian Road Research, Volume* 8, pp. 32-35, 1978.

Dia, H., and Cottman, N., Evaluation of Incident Management System Using Traffic Simulation, 2003. Retrieved on Sept 5, 2005 from http://www.iasi.rm.cnr.it/ewgt/13conference/60_dia.pdf.

De Silva F, and Eglese, R., Integrating Simulation Modeling and GIS: Spatial Decision Support Systems for Evacuation Planning, *Journal of the Operational Research Society, Volume 51*, pp. 423-430, 2000.

David, K.D., and Scott, S., Ex-FEMA Chief Tells of Frustration and Chaos, The New York Times, September, 2005.

Daganzo, F.C., The Cell Transmission Model: A Dynamic Representation of Highway Traffic Consistent With the Hydrodynamic Theory, *Transportation Research. Part B, Volume 28B*, Number 4, pp. 269-287, 1994.

Dowling, R., and Skabardonis, A., Improving Average Travel Speeds Estimated by Planning Models, *Transportation Research Record 1366*, Transportation Research Board, pp. 68-74, 1992.

Dowling, R., Singh, R., and Cheng, W., The Accuracy and Performance of Improved Speed-Flow Curves, *Transportation Research Record 1646*, Transportation Research Board, pp. 9-17, 1992.

Dynasmart-P Version 1.0 User's Guide. Retrieved on January 10, 2006 from http://www.dynasmart.umd.edu/documents/DYNASMART-P Users-Guide-1.0.pdf.

Fahy, R. F., An Evacuation Model for High Rise Buildings, *Proceedings form the Intemational Symposium on Fin Safety Science*, 1991.

Federal Emergency Management Agency (FEMA), *Southeast United States Hurricane Evacuation Traffic Study*, Executive Summary, Washington D.C, 2000.

Fleischer, L., Faster Algorithms for the Quickest Transshipment Problem, *SIAM Joumal on Optimization, Volume 12*, 2001.

Fu, H.,Wilmot, C.G., A Sequential Logit Dynamic Travel Demand Model For Hurricane Evacuation, *Transportation Research Board*, 83rd Annual Meeting, Washington D.C, 2004.

Fujishige, S., Makiio, K., Takabatake, T., and Mamada, S., The Evacuation Problem and Related Topics, Presented at the Society of Instrument and Control Engineers (SICE) conference, Osaka, Fukui University, Fukui, Japan, Aug 5-7, 2002.

Hamza-Lup,G.L., Hua,K.A., Le, M., and Rui, P., Enhancing Intelligent Transportation Systems to Improve and Support Homeland Security, *2004 IEEE Intelligent Transportation Systems Conference*, Washington D.C., October 3-6, 2004.

Hamza-Lup, G.L., Hua, K.A., Peng, R., and Ho, Y.H., Real-Time Traffic Evacuation Management under Multiple Coordinated Human-Caused Threats, *12thWorld Congress on ITS*, Paper 4379, San Francisco, November 2005.

Gatrell, A, and Vincent, P., Managing Natural and Technological Hazards in Handling Geographical Information: Methodology and Potential Applications, *Longman Scientific and Technical*, New York, pp. 148-80, 1991.

Hall, L.H, Traffic Stream Characteristics, *Transportation Research Board Special Report 165*, FHWA, pp. 22-25, 1994.

Han, L.D., and Yuan, F., Evacuation Modeling and Operations Using Dynamic Traffic Assignment and Most Desirable Destination Approaches, *Transportation Research Board*, 84th Annual Meeting, Washington. D.C., 2005.

Haoqiang, F., Development of Dynamic Travel Demand Models for Hurricane Evacuation, Ph.D Dissertation, Department of Civil & Environmental Engineering, Louisiana State University, 2004

HMM Associates, Evacuation Time Estimates for Area Near Pilgrim Station, Boston Edison Company, 1980.

Highway Capacity Manual (HCM) 2000, *Chapter 31 and Special Report 209*, Transportation Research Board, National Research Council, Washington D.C., U.S.A.

Hobeika, A.G., and Jamei, B., MASSVAC: A Model for Calculating Evacuation Times Under Natural Disaster, *Conference of Computer Simulation in Emergency Planning, Volume 15*, Society of Computer Simulation, La Jolla, pp. 5-15, 1985.

Hobeika, A. G., and Kim, C., Comparison of Traffic Assignments in Evacuation Modeling, *IEEE Transactions on Engineering Management, Volume 45*, Number 2, pp. 192-98, 1998.

Hoppe, B. and Tardos, E., Polynomial Time Algorithms for Some Evacuation Problems, *Proceedings of the 5th Annual AGM-SIAM Symposium on Discrete Algorithms*, 1994.

Irwin, M.D., and Hurlbert, J.S., A Behavioral Analysis of Hurricane Preparedness and Evacuation in Southwestern Louisiana, Louisiana Population Data Center, September 1995.

Kwon, E., and Pitt, S., Evaluation of Emergency Evacuation Strategies for Downtown Event Traffic Using a Dynamic Network Model, *Transportation Research Board*, 84th Annual Meeting, Washington. D.C., 2005.

Lewis, D.C., Transportation Planning for Hurricane Evacuations, *ITE Journal, Volume 55*, Number 8, pp. 31-35, August 1985.

Lim, .Y.Y., Modeling and Evaluating Evacuation Contraflow Termination Point Designs, Master's Thesis, Department of Civil and Environmental Engineering, Louisiana State University, 2003.

Liu,Y., Lai, X., and Chang, G., A Two-Level Integrated Optimization Model for Planning of Emergency Evacuation, *Transportation Research Board*, 84th Annual Meeting, Washington. D.C., 2005

Liu, Y., Lai, X., Chang, G., A Cell-Based Network Optimization Model For Staged Evacuation Planning Under Emergencies, *Transportation Research Board* 85th Annual Meeting, Washington. D.C., 2006.

Murray-Tuite, P.M., Mahmassani, H.S, Transportation Network Evacuation Planning with Household Activity Interactions, *Transportation Research Board* 83rd Annual Meeting, Washington. D.C., 2004.

Munday, D., Remnants of Hurricane Floyd: Feelings of anger remain. Post and Courier, Sept 26, 1999.

Malone, S., Miller, C.A., and Neill, D.B., Traffic Flow Models and the Evacuation Problem, *UMAP Journal, Volume 22*, pp. 271-290, 2001.

Mei, B., Development of Trip Generation Models of Hurricane Evacuation, MS Thesis, Department of Civil and Environmental Engineering, Louisiana State University, 2002.

Nagel, K., and Schreckenberg, M., A Cellular Automaton Model for Freeway Traffic, *Journal de Physique I, Volume 2*, Number 12, pp. 2212-2229, 1992.

Franzese, O., and Sorensen, J., Fast Deployable System for Consequence Management: The Emergency Evacuation Component, National Transportation Research Center, Oak Ridge National Laboratory. Retrieved on January 12, 2006 from http://www.ornl.gov/~webworks/cppr/y2001/pres/120065.pdf

Pal, A., Graettinger, A., and J, Triche, M. H, Emergency Evacuation Modeling Based On Geographical Information System Data, *Transportation Research Board*, 83rd Annual Meeting, Washington. D.C., 2004.

Post, Buckley, Schuh and Jernigan, Inc. (PBS&J), Southeast Louisiana Hurricane Evacuation Study: Transportation Model Support Document, Final Report, Tallahassee, Florida, 1993.

Post, Buckley, Schuh and Jernigan, Inc. (PBS&J), Reverse Lane Standards and ITS Strategies Southeast United States Hurricane Study. Technical Memorandum 3, Final Report, Federal Emergency Management Agency, Post, Tallahassee, Florida, 2000.

Radwan, E., A Computer Simulation Model for Rural Network Evacuation Under Natural Disasters, *ITE Journal*, pp. 25-30, 1985.

Rahaf, A, and Stopher, P.R., A Review of the Procedures Associated with Devising Emergency Evacuation Plans, *Transportation Research Board*, 83rd Annual Meeting, Washington. D.C., 2004.

Rathi A, Santiago, A., The new NETSIM Simulation program, *Traffic Engineering and Control, Volume 31*, pp. 317-320, 1990.

Roess, R.P., William,M. R., and Prassas, E.S, Traffic Engineering, Prentice Hall, Upper Saddle River, New Jersey, pp. 121 and 285, 1998.

Sbayti, H., Mahmassani, H., Optimal Scheduling of Evacuation Operations, *Transportation Research Board*, 85th Annual Meeting, Washington. D.C., 2006.

Sheffi, Y., Mahmassani, H., and Powell, W., NETVAC: A Transportation Network Evacuation Model, Center of Transportation Studies, MIT, 1980.

Singh, Rupinder., Improved Speed-Flow Relationships: Application to Transportation Planning Models, Presented at the 7th *Transportation Research Board*, Conference on Application of Transportation Planning Methods, Boston, Massachusetts, March 1999.

Skabardonis, A., and Dowling, R., Improved Speed-Flow Relationships for Planning Applications, *Transportation Research Record 1572*, Transportation Research Board, pp. 18-23, 1997.

Stern, E., and Sinuany-Stern, Z., A Behavioral-Based Simulation Model for Urban Evacuation, *Papers of the Regional Science Association*, *Volume.66*, pp. 87-103, 1989.

Sinuany-Stern, Z., and Stern,E., Simulating the Evacuation of a Small City: The Effects of Traffic Factors. Socio-Economic Planning Sciences, *Volume 27*, Number 2, pp. 97-108, 1993.

Stamatiadis, N., and Colton, E., Use of Simulation to Improve Diversion Routes for Incident-Management Programs, *ITE Journal*, 1999. Retrieved July 23rd, 2005 from http://www.ite.org/membersonly/itejournal/pdf/jea99a90.pdf

Smith, B., Lessons Learned About Transportation Operations During Major Evacuations -South Carolina, *Technical Presentation to the FHWA Transportation Operations During Major Evacuations: Hurricane Workshop*, Atlanta, Georgia, 2000.

Southworth, F., and Chin, S., Network Evacuation Modeling for Flooding as A Result of Dam Failure, *Environment and Planning A*, *Volume 19*, pp. 1543-1558, 1987.

Tuydes, H., and Ziliaskopoulos, A., Network Re-design to Optimize Evacuation Contraflow, *Transportation Research Board*, 83rd Annual Meeting, Washington. D.C., 2004.

Tweedie, S., Rowland, J., Walsh, S., Rhoten, R., and Hagle, P., A Methodology for Estimating Emergency Evacuation Times, *The Social Science Journal*, Western Social Science Association, *Volume 21*, Number 2, pp. 189-204, 1986.

U.S. Army Corps of Engineers, *Northwest Florida Hurricane Evacuation Study Technical Data Report*, 1997.

U.S. Army Corps of Engineers, *Northwest Florida Hurricane Evacuation Study Technical Data Report*, 1999.

U.S. Army Corps of Engineers, Alabama Hurricane Evacuation Study Technical Report, 2001.

Urbanik, T., Texas Hurricane Evacuation Study, *Texas Transportation Institute*, College Station, TX, 1978.

Urbanik, T., and Desrosler, A.E., An Analysis of Evacuation Time Estimates around 52 Nuclear Power Plant sites, An Evacuation, *US Nuclear Regulatory Commission, NUREG/CR 7856, Volume 1*, 1981.

Urbanik,T., Evacuation time estimates for nuclear power plants, *Journal of Hazardous Materials, Volume 75*, pp. 165-180, 2000.

Whitehead, J.C., One Million Dollars a Mile? The Opportunity Costs of Hurricane Evacuation, *Triangle Resource and Environmental Economics Seminar*, February 2000.

Wilmot, C.G, and Meduri, N., A Methodology to Establish Hurricane Evacuation Zones, *Transportation Research Board*, 84th Annual Meeting, Washington. D.C., 2005.

Wolshon, B., Urbina, E., and Levitan, M., National Review of Hurricane Evacuation Plans and Policies, *LSU Hurricane Center Technical Report*, Louisiana State University, Baton Rouge, Louisiana, 2001.

Wolshon, B., The Emergence of Homeland Security Stresses the Importance of Evacuation Management, *Time, Volume 9*, Number 2, April 2004. Retrieved on Sep 22, 2005 from http://hurricane.lsu.edu/_in_the_news/tmemag0404.htm.

Wolshon, B., Catarella, M., and Alison., L.L., Louisiana Highway Evacuation Plan for Hurricane Katrina: Proactive Management of a Regional Evacuation, *Journal of Transportation Engineering, ASCE, Volume 1*, January 2006.

Yamsda, T., A Network Approach to a City Emergency Evacuation Planning, *International Journal of Systems Science, Volume.27*, pp. 931-936, 1996.